AD-A140 020 SURFACE AND BULK PHASE SEPARATIONS IN BLOCK COPOLYMERS AND THEIR BLENDS(U) VIRGINIA POLYTECHNIC INST AND STATE UNIV BLACKSBURG N M PATEL ET AL. MAR 84 VPI-E-84-7 1/2

UNCLASSIFIED N00014-82-K-0185 F/G 11/9 NL

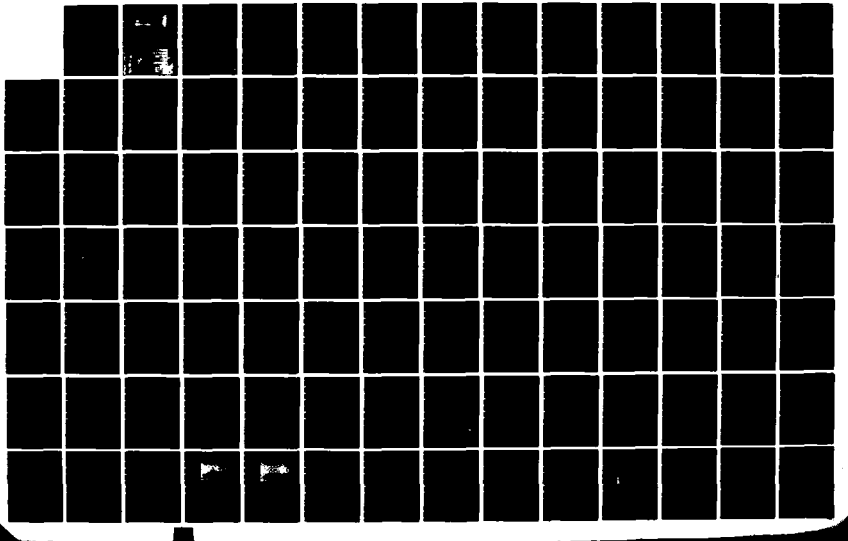

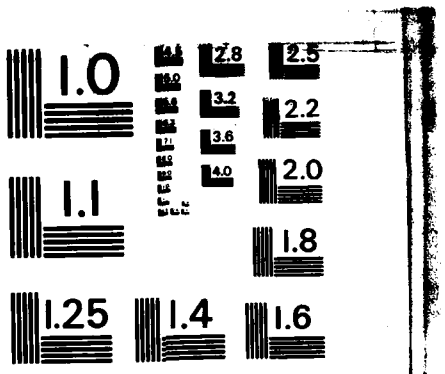

COLLEGE OF ENGINEERING

VPI-E-84-7 March 1984

SURFACE AND BULK PHASE SEPARATION IN BLOCK COPOLYMERS AND THEIR BLENDS

Niranjan M. Patel and David W. Dwight

VIRGINIA POLYTECHNIC INSTITUTE & STATE UNIVERSITY

College of Engineering
Virginia Polytechnic Institute and State University
Blacksburg, VA 24061

VPI-E-84-7 March 1984

SURFACE AND BULK PHASE SEPARATION IN BLOCK COPOLYMERS AND THEIR BLENDS

Niranjan M. Patel and David W. Dwight

Center for Adhesion Science
and
Department of Chemical and Materials Engineering
Virginia Polytechnic Institute and State University
Blacksburg, Virginia 24061

Sponsored by:

Office of Naval Research
Grant No. N00014-82-K-0185
800 N. Quincy St.
Arlington, VA 22217

Army Research Office
Grant No. DAAG29-80-K-0093
P.O.B. 12211
Research Triangle Park, NC 27709

BIBLIOGRAPHIC DATA SHEET	1. Report No.	2.	3. Recipient's Accession No.

4. Title and Subtitle
"Surface and Bulk Phase Separations in Block Copolymers and Their Blends"

5. Report Date
March 1984

6.

7. Author(s)
Niranjan M. Patel and David W. Dwight

8. Performing Organization Rept. No.

9. Performing Organization Name and Address
Center for Adhesion Science and Departments of Chemical Engineering and Materials Engineering, VPI & SU, Blacksburg, VA 24061

10. Project/Task/Work Unit No.

11. Contract/Grant No.
ONR N00014-82-K-0185
ARO DAAG29-80-K-0093

12. Sponsoring Organization Name and Address
ONR, 800 N. Quincy St., Arlington, VA 22217
ARO, POB 12211, Research Triangle Park, NC 27709

13. Type of Report & Period Covered
9/30/82 to Interim, 12/30/83

14.

15. Supplementary Notes

16. Abstracts Surface and bulk properties have been studied in terms of composition and morphology of siloxane containing block copolymers and their blends with homopolymers. X-ray Photoelectron Spectroscopy (XPS) has been used to obtain the compositional information from the top 60 angstroms or so at the surface. Transmission Electron Microscopy (TEM) was utilized to probe the bulk morphology. An attempt is made to compare the bulk and the surface and find possible mechanisms governing them. It is found that solvent-cast neat block copolymers have a uniform layer at the surface that is rich in siloxane whereas their bulk has a microphase-separated domain structure. In the case of blends, siloxane enrichment is quite pronounced even at bulk concentrations as low as 0.05% w/w siloxane. Amount of surface siloxane as a function of bulk content is studied with the help of XPS. At the same time, the bulk morphology of these blends is studied by TEM. The changes occurring in the surface and the bulk are found to have similar patterns. It is shown that the observed surface behavior may be related to the bulk morphology. Molecular weight of the blocks in the copolymers is found to be a very important parameter

(ove

17. Key Words and Document Analysis. 17a. Descriptors

Block Copolymers; Homopolymers; Multi-component; Multi-phase; Morphology; Micro-phase separation; Macro-phase Separation; Polymer Blends; Surface Properties; X-ray Photoelectron Spectroscopy (XPS); Electron Spectroscopy for Chemical Analysis (ESCA); Transmission Electron Microscopy (TEM).

17b. Identifiers/Open-Ended Terms

17c. COSATI Field/Group

18. Availability Statement	19. Security Class (This Report) UNCLASSIFIED	21. No. of Pages
Distribution Unlimited	20. Security Class (This Page) UNCLASSIFIED	22. Price

Block 16 (continued)

governing both the surface and the bulk properties in the neat copolymers as well as their blends.

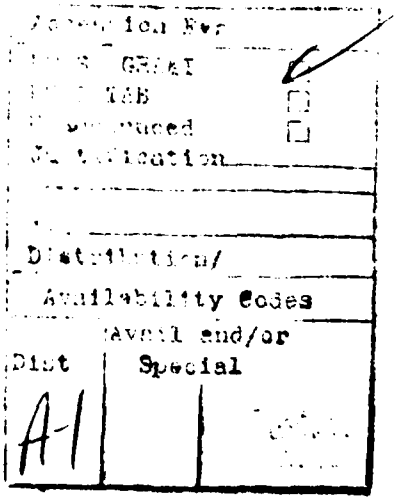

SURFACE AND BULK PHASE SEPARATIONS IN BLOCK COPOLYMERS AND THEIR BLENDS

(ABSTRACT)

Surface and bulk properties have been studied in terms of composition and morphology of siloxane containing block copolymers and their blends with homopolymers. X-ray Photoelectron Spectroscopy(XPS) has been used to obtain the compositional information from the top 60 angstroms or so at the surface. Transmission Electron Microscopy(TEM) was utilized to probe the bulk morphology. An attempt is made to compare the bulk and the surface and find possible mechanisms governing them. It is found that solvent-cast neat block copolymers have a uniform layer at the surface that is rich in siloxane whereas their bulk has a microphase-separated domain structure. In case of blends, siloxane enrichment is quite pronounced even at bulk concentrations as low as 0.05% w/w siloxane. Amount of surface siloxane as a function of bulk content is studied with the help of XPS. At the same time, the bulk morphology of these blends is studied by TEM. The changes occuring in the surface and the bulk are found to have similar patterns. It is shown that the observed surface behavior may be related to the bulk morphology. Molecular weight of the blocks in the copolymers is found to be a very important parameter governing both the surface and the bulk properties in the neat copolymers as well as their blends.

ACKNOWLEDGEMENTS

The authors wish to acknowledge the financial support provided by Office of Naval Research, Arlington, VA 22217, through the grant NOOO14-82-K-0185 and by Army Research Office, Research Triangle Park, NC 27709 through the grant DAAG29-80-K-0093 for this research project.

TABLE OF CONTENTS

LIST OF FIGURES

LIST OF TABLES

CHAPTER I

INTRODUCTION

Block copolymers have the chemical structure of long sequences(blocks) of one type of repeat unit A joined at one end or both to long sequences of an another type B. Dissimilar nature of the two blocks combined with the fact that they are chemically linked to each other are manifest in a variety of specific physical and mechanical properties quite different from the corresponding homopolymeric systems. A greater attraction of these polymers comes because of their flexible parameters which can be easily controlled to tailor systems of specific applications. Some of these parameters are the chemical nature of the blocks, architecture of the copolymer (such as diblock, triblock, perfectly alternating or random multiblock), lengths of the blocks- individually and in relation to one another, and processing conditions.

There are two classes of properties uniquely exhibited by block copolymers- the surface properties and the bulk properties. The surface properties of the block copolymers originate from the difference in the surface free energies of the components involved. More than a hundred years ago, Gibbs[1] showed that any component that has a lower energy would tend to get enriched in the surface of a condensed phase. Thus in a block copolymer, the component of lower surface free energy

would preferentially segregate at the surface. A surface that is different in character from the bulk is then obtained.

The bulk properties arise from their microheterogeneous morphology. Due to incompatibility, each block tends to make separate phases which are restricted to microscopic sizes (in hundreds of angstroms or less) by the chemical link between the blocks. Depending on the parameters mentioned above, a number of morphological configurations are possible for this "micro-phase" separation giving rise to a variety of properties. KRATON® by Shell[2] is one of the earliest commercial and most successful examples where such a structure is exploited. The bulk of this triblock copolymer is formed of spherical glassy polystyrene domains connected through flexible butadiene chains. The spherical domains act as anchor points, hence giving elastomeric properties to the polymer. The class of polymers exhibiting this pseudo-elastomeric properties are often named as *thermoplastic* elastomers due to the fact that they can still be processed like a normal thermoplastic above their softening points.

These morphological and colloidal properties of block copolymers can be further utilized by blending them with homopolymers to obtain numerous desirable properties[3]. When added in small amounts to a blend of two incompatible homopolymers corresponding to the blocks, copolymer chains can act as a polymer surfactant or an "alloying agent" providing stability between the separated phases[4]. High impact polystyrene(HIPS) and acrylonitrile-butadiene-styrene(ABS) are excellent examples where impact strengths of glassy materials are modified by incorporating rubbery dispersions stabilized with the help

of block copolymers. On the other hand, small amounts of homopolymers can be imbibed into the respective microphases of the original block copolymer[5]. Also, the addition of an adequate amount of a block copolymer to a homopolymer is known to increase the toughness of the latter by the same mechanism as above of elastomeric inclusions in the homopolymer matrix[6,7].

Surface modification of bulk polymers are also brought about by incorporation of block copolymers in them. The low surface energy block surface-segregates even at very low concentrations, thereby changing the surface without a considerable change in the bulk. This has been found useful in such practical applications as improvement of adhesive properties[8], enhancement of soil release capabilities in modern textiles[9], stabilization of urethane foams[10], reduction of the friction coefficient[11], etc.

Both the bulk and the surface of block copolymers have been active areas of research in the last decade or so. The nature of the bulk has been fairly well studied as regards to the morphology and structure and their relation to bulk properties. Relatively less systematic work has been done on the surfaces. Earlier efforts involved measurements of surface tensions in solutions or melts and contact angles in solids to understand the chemical nature of the surfaces. Unambiguous quantitative interpretations from such measurements are rare[12] especially when lateral inhomogeneities and roughness are present. Also the information comes only from the topmost layer of the surface. Vertical inhomogeneities, the knowledge of which have importance in many applications, are ignored. Recent

advances in applications of X-ray Photoelectron Spectroscopy(XPS) or ESCA(Electron Spectroscopy for Chemical Analysis), as it is popularly known, to polymeric systems[12] have made possible to obtain direct chemical information on the top few angstroms of the surface.

Studies on pure block copolymers have shown that the surface may differ from the bulk in not only the chemical composition but also in the morphology[13]. Blends of block copolymers with homopolymers corresponding to the higher surface energy block have exhibited a phenomenon of 'critical' concentration[14,15]. At this concentration of the block copolymer in the bulk, the surface composition of the low energy component seems to jump to a much higher value before approaching a value representative of the pure block copolymer surface. Much more work has to be done before mechanisms of such a behavior can be understood well. There are also questions as to whether and, if so, how the surface composition, surface morphology and the bulk morphology are related to each other in both neat block copolymers and their blends. The present work studies these surface and bulk phase separations in a number of block copolymers and their blends of varying compositions and attempts to answer some of these questions.

XPS has been utilized exclusively for obtaining the chemical composition of the surface. Transmission Electron Microscopy(TEM) on thin films of polymer elucidate the domain- micro or macro- structure in the bulk. In the following chapter, a review of the previous work done in this area is presented. Principles of XPS have been dealt with next before the report of the present research is given.

CHAPTER II

LITERATURE REVIEW

This chapter contains a review of the surface properties (in terms of chemistry and morphology) and the bulk morphology of block copolymers and their blends with homopolymers. The latter subject has been explored extensively in the past decade or so. However, in the former area, the effort is more scattered over the same period of time. In the following two major sections each of these angles have been reviewed individually with a greater emphasis being placed on the surface studies. To avoid lengthy repetitions, each polymer has been designated by a suitable abbreviated form that is used in all later referrals.

2.1 THE SURFACE.

The concept of modification of polymer surfaces without considerable change in bulk properties, using additives such as surface active agents is not new. Allan[16] reported that addition of a certain amount of oleamide, an amphipatic(polar/non-polar) substance, causes a marked lowering in the coefficient of friction between thin films of polyethylene. In a systematic study on polyethylene and a series of

halogenated derivatives of polyethylene, Zisman and co-workers[17,18] established that lowering the free energy of a solid, γ_o, or the critical surface tension of wetting, γ_c, decreases the coefficient of friction. This led them to study the addition of surface active fluorinated compounds to a number of polymers such as poly(methyl methacrylate), poly(vinyl chloride) and several poly(vinylidiene chloride) copolymers[19]. In each case it was found that a very small amount of the additive greatly reduced the critical surface tension and coefficient of friction. It was also pointed out that siloxane-containing compounds may be expected to show similar surface activity.

One of the earliest reports of the application of block copolymers is as non-ionic surfactants[20]. PLURONIC® polyols- poly(propylene oxide)(PPO)/poly(ethylene oxide)(PEO) block copolymers, introduced by BASF in the early 50's, and many other polyols, were found to have uses as surface active agents in areas ranging from cosmetics to water treatment, as reviewed by Lunsted and Schmolka[21]. Another instance of a block copolymer used as a surface active agent was the stabilization of "one shot" polyurethane foams by polysiloxane/polyether block copolymers[10]. A necessary condition in foam stabilization is lowering of the surface tension, γ_s, at the bubble surface. Measurement on aqueous solutions of these copolymers showed limiting surface tensions of 20-21 dyn/cm at 25 °C(compared to 72.6 dyn/cm for pure water) at concentrations as low as 10^{-5} mole/liter[22]. Occurance of micellization was thought to be the reason for this limiting surface tension. Due to the above practical applications, the initial research effort was concentrated on understanding of the behavior of bloc..

copolymers at liquid-air interfaces. But soon there was an interest towards their usefulness in modifying the solid polymer surfaces too. Hence the review presented here is suitably divided into these two areas of application of block copolymers to surfaces.

2.1.1 LIQUID SURFACES.

In an effort to better understand the mechanism of surface tension lowering by block copolymers, Kendrick and co-workers[23] performed a study on solutions of poly(dimethyl siloxane)(PDMS)/polyether(PETH) in polyol LG 56, similar to the one used in urethane foam manufacture. A limiting value of 20.8 dyn/cm was observed in equilibrium surface tension measurement by pendant drop method. They demonstrated that a number average degree of polymerization, $\langle X_n \rangle$, of the siloxane block of at least 20 was required to reach a surface tension of 20.3 dyn/cm- which is that of a PDMS fluid[24]. In order to achieve this value of surface tension, the siloxane portion of the copolymer must lie in the surface with methyl groups in the same orientation as that which prevails at the surface of a pure PDMS fluid. This means that the orientation of the siloxane portion must be free of long-range interaction from the ether portion. In other words, the siloxane block must be longer than a statistical segment of the freely jointed model[25]. This suggests that the ultimate surface tension is controlled not so much by the low-high surface energy balance of the copolymer as by the length of the lower surface energy component. Similar solution behavior was noted when water and tripropylene glycol were used as solvents[26].

Same conclusions were arrived at by Rastogi and St. Pierre[27] from their study on surface tensions of a series of PLURONIC® polyols. The results clearly demonstrated that block copolymers of same overall composition had different surface tensions- the lowest being of that having largest PPO chain. At $<X_n>$=56 of PPO, the surface seemed to be made entirely of PPO whose overall fraction the copolymer was only 10%. Random copolymers of PPO/PEO showed no surface segregation at all, the overall surface tension being mole fraction weighted average of individual values. Their results are summarized on the Figure(2.1).

Investigation on polystyrene(PS)/PDMS[28] revealed two other points in addition to the dependence of surface segregation on chain length of lower surface energy component and the overall composition as established earlier. The limiting value of surface tensions of the copolymer solutions also depended on the type of solvent. Styrene being a non-solvent for siloxane, the limiting value in its solutions was 23.5 dyn/cm, reached at 0.5% w/w block copolymer. On the other hand, in case of benzene, a good solvent for siloxane, the corresponding values were 25.3 dyn/cm at 1% w/w block copolymer. It was also shown by a simultaneous study of light scattering, refractive indices and surface tensions of benzene solutions, that the phenomenon of limiting surface tension is not necessarily accompanied by micellization in the solution.

Surface properties of a series of PS/polytetrahydrofuran(PTHF) were studied by Yamashita and Takahashi[29,30]. Here one component(PTHF) is crystallizable, an important fact that may affect the solid surface characteristics as discussed later. The length of PTHF

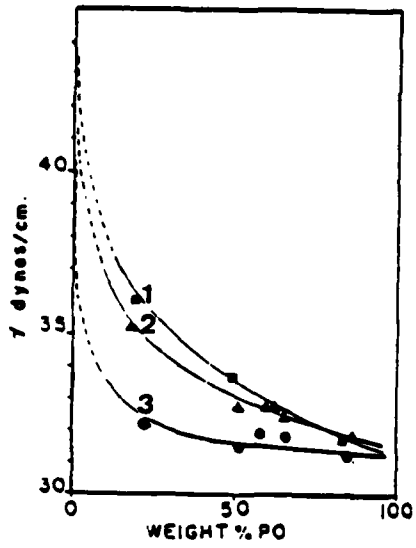

FIGURE(2.1a). Surface tension vs. weight %propylene oxide, poly(propylene oxide)/poly(ethylene oxide) block copolymers, 25 °C with degree of polymerization of the base unit: 1. 16, 2. 30, and 3. 56. [from 27]

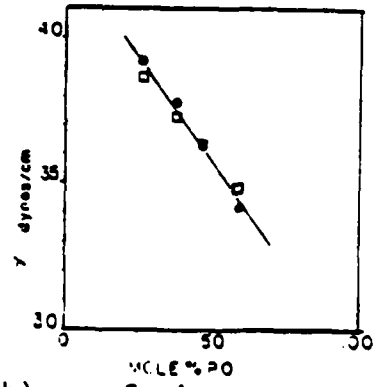

FIGURE(2.1b). Surface tension vs. mole% propylene oxide, poly(propylene oxide)/poly(ethylene oxide) random copolymers, 25 °C. [from 27]

block was kept constant and that of PS was varied. It was shown that a difference of only 3 dyn/cm between the surface tensions of PTHF and PS- much smaller than that between PS and PDMS, is sufficient for a considerable surface segregation. On addition of 0.3-1% w/w of the block copolymer to a PS homopolymer, the equilibrium surface tensions of molten blends resembled that of molten PTHF at the same temperature. The higher the temperature and the THF content, the smaller was the difference between surface tensions of the blend and PTHF and faster the time to achieve the equilibrium.

2.1.2 SOLID SURFACES.

On surveying the literature on surface studies of solid polymers, two distinct experimental approaches are conspicuous. In the first approach, indirect methods such as wettability, critical surface tensions, coefficient of friction, etc. are utilized to obtain information on the chemical nature of surfaces. In this approach the 'surface' is defined to be the outermost layer of the solid. The second approach uses more direct methods such as spectrometric techniques which probes typically the top few monolayers instead. Thus the *subsurface* is also examined along with the *surface*, analogous to the *interphase* vs. the *interface*. The latter approach has been popular only in the last few years or so on the advent of more confident interpretations of data in some techniques such as X-ray Photoelectron Spectroscopy (XPS).

2.1.1.1 Indirect Methods. Extending the idea of using low surface energy additives for polymer surface modification, as pointed out by Zisman[19], and the fact that block copolymers show surface

activity, Owen and Kendrick[28] utilized PS/PDMS block copolymers to modify the solid surface properties of PS. Contact angle measurements demonstrated that the critical surface tension of PS reduced from 32.5 dyn/cm to 22-28 dyn/cm by addition of 1% block copolymer by weight-greater reduction with polymer having higher content of siloxane. Legrand and Gaines[31] conducted similar experiments on effect of poly(bisphenol-A carbonate)(PBAC)/PDMS block copolymer on the surface of a PBAC homopolymer. Wetting characteristics of a typically siloxane surface(air side) were obtained when homopolymer was incorporated with greater than 0.1% by weight of copolymer with 60-80% w/w siloxane fraction, 20 or more units long. In these conditions, the wetting effect seemed to be independent of copolymer concentration, siloxane content or block lengths. In light of this insensitivity to the above variables, they suggested that the block copolymer formed a sort of a duplex film, in which siloxane blocks are outermost while the carbonate blocks are intermingled with the bulk homopolymer.

They also studied the effect of substrate-side polymer surface as a function of the substrate used. Three substrates were used: glass, FEP Teflon, and silicone pretreated glass. It was found that the wettability of the glass side surface was similar to that of homopolymer, while the FEP Teflon and silicone treated glass side surfaces more or less resembled pure siloxane surface. The explanation of this behavior can be given by the fact that the "clean" glass, having high surface energy would prefer the higher energy PC rather than siloxane at the interface, in order to minimize the interfacial free energy. On the other hand, both FEP Teflon and silicone treated glass being low

surface energy surfaces, siloxane will be favored at the interface.

Gaines and Bender[32] recognized one more factor that might be important in practical application of block copolymers to modify solid surfaces of organic homopolymers. They did a time-dependent study on surface tensions of molten PS after some amount of a PS/PDMS AB block copolymer has been added to it. The rate of surface tension lowering was found to be a diffusion controlled process.

Owen and Thompson[11] synthesized polyamide/PDMS AB and ABA block copolymers and used them to modify surface properties of a commercial Nylon 6 and polyethylene(PE). Samples were prepared by compression molding above their respective melting points forming homogeneous solids. Again incorporation of 1-2% block copolymers of $\langle X_n \rangle$ of 53-112 and 40-80% by weight of siloxane brought the critical surface tension of Nylon 6 from 33 down to 26 dyn/cm. Kinetic friction coefficient values also supported the segregation of siloxane at the surface. Addition of 2% of a high siloxane content block copolymer to PE produced a surface of a critical surface tension of 22 dyn/cm. This showed for the first time that block copolymer may also be used to modify surfaces of homopolymers other than the one corresponding to the higher surface energy component. However, the bulk properties may suffer, if the copolymer has no "anchoring" mechanism promoting the adhesion of its domains to the homopolymer.

In addition to their study on molten blends as discussed earlier, Yamashita and Takahashi[29,30] also investigated the solid state properties of PS/PTHF block copolymers with electron microscopy and wettability experiments. Surface and bulk morphology here depended,

in addition to incompatibility and surface energy difference, also on the tendency of PTHF to crystallize. At higher PTHF content, crystallization prevailed over microphase separation giving a fibrillar morphology. On increasing the styrene content, the morphology changed to lamellar, rod-like and finally to spherical micro-domains, with continuous phase changing from PTHF to PS. They measured the PS fraction at the surface from electron micrographs with PTHF component stained by osmium tetroxide. A very peculiar relation between surface and bulk PS fraction was obtained. On varying the block copolymer styrene content from 0 to 15% by mole, the surface content jumped to about 90%. This was explained by arguing that the PTHF fibrils, which looked white under the microscope, were covered by amorphous PS during crystallization. On the other hand, above 90% PS content in the bulk, the surface content decreased rapidly to about 20%, indicating that there was a diffusion of spherical domains of PTHF from the bulk promoted by the decrease of the surface energy. The intermediate region had a linear inverse relation showing that as more THF is added, crystallization dominates which in turn encourages PS coverage at the surface. Although this surface vs. bulk relationship was qualitatively supported by the wettability results, the validity of calculation of PS fraction on the surface from electron micrographs may be questionable. This is because osmium tetroxide may have stained both the bulk and the surface and measurement of dark areas and white areas would by no means be representative of the surface only.

An another system where one block was crystallizable was studied by O'Malley and Stauffer[33]. But difference here was that the

crystallizable component, poly(hexamethyl sebacate)(PHMS), was of higher surface energy(γ_c=28 dyn/cm) than the other block PDMS. Critical surface tensions from Zisman plots of block copolymers containing 27 to 70% w/w PDMS were found to be about 22 dyn/cm. In the bulk, evidence of both spherulitic crystal structure of PHMS phase and microphase separation were found. This showed that contrary to results of Yamashita and co-workers, here the crystallization process did not interfere with the surface properties. The basis of this PDMS-like surface structure was attributed to migration of siloxane domains from the phase separated bulk and orienting themselves at the polymer-air interface. It was also found here that blending 27% w/w siloxane copolymer to PHMS homopolymer with overall siloxane varying from 1 to 10% produced surfaces with γ_c≈22 dyn/cm.

Litt and Herz[34] examined the block copolymers of poly(N-lauroyl ethylenimine)(PLI) and poly(N-acetyl trimethyleimine)(PAI). Critical surface tensions on several polymers, each having different composition and degree of polymerization, were found to be 22 dyn/cm corresponding to that of the low surface energy crystallizable component PLI. Litt and Matsuda[35] studied a similar system of PLI/poly(N-propionyl ethylenimine)(PPI) block copolymers. Zisman plots of solvent cast copolymer films gave γ_c's of 22 dyn/cm, independent of the composition. This value is same as that for a surface of closed packed methyl groups indicating that backbone methyl groups and tertiary amide groups are not exposed at the surface. Attenuated total reflection-infrared(ATR-IR) spectroscopy further confirmed that the surface was covered by the long hydrocarbon side chains of PLI with

methyl groups. The limiting areas of the segments adsorbed at the interface from surface tension vs. concentration plot using the approximate Gibbs adsorption isotherm were calculated to be 14-16 Å/monomer unit. These results, in conjunction with their previous study on crystal structure[36] of PLI, helped them to propose a model for molecular arrangement at the surface as depicted in the Figure(2.2). It shows that the surface is composed of a two dimensional crystalline film with PLI segments lifted out of the interface, closely packed hydrocarbon chains forming the outermost layer.

Yamashita et al.[37] have studied "macromer" type graft copolymers for surface activity. Surface modification, as measured by water and dodecane contact angle measurements, of poly(methyl methacrylate(PMMA) was achieved by incorporation of small amounts of graft copolymers of PMMA/poly(perfluoroalkyl acrylate)(PPFA). Only 0.2% w/w of the graft copolymer containing 50% w/w of PPFA was sufficient to modify the homopolymer to fluoropolymer like surfaces. For comparison, a random copolymer of the same composition was used. Here, the contact angles decreased linearly as a function of log wt% copolymer- in contrast to the phase-separated graft copolymer where it dropped drastically in the initial stage and then leveled off. This indicates that the in the statistical or random copolymer modified polymer, the surface represents the average composition without preferential segregation of the PFA segments. Further demonstration of the surface segregation in systems containing graft copolymers was given by Ito and co-workers[38]. The two blocks involved were PS and poly(2-hydroxy methacrylate)(PHEMA) with PS serving as the graft.

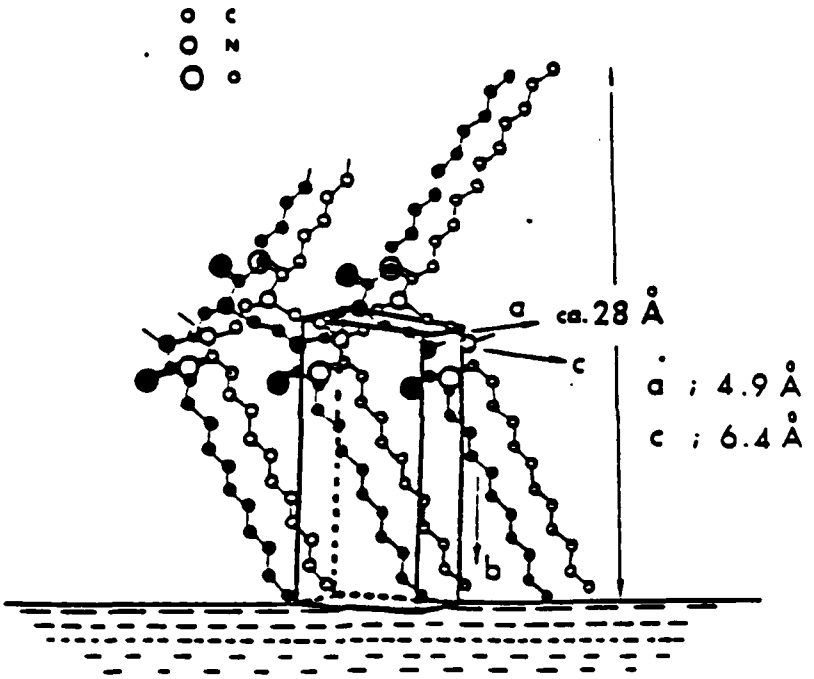

FIGURE(2.2). Schematic representation of packing of poly(N-lauroyl ethylenimine) molecule at the solution/air interface of poly(N-lauroyl ethylenimine)/poly(n-propionyl ethylenimine) block copolymer. [from 35]

Comparisons were also made with random copolymers. Two variables were tested: the casting solvent and the thermal history. Random copolymers, as expected, showed smooth change in water contact angle with composition, becoming more wettable with increasing PHEMA (hydrophilic) content, independent of the two variables mentioned above. The graft copolymers showed a little more interesting wetting characteristics. When cast from DMF, a good solvent for both homopolymers, their contact angles were very close to that of PS and independent of composition, even with 85% PHEMA. This copolymer, however, was significantly more wettable when cast from methanol, a selective solvent for PHEMA. When heated to 150 °C, well above the T_g of PHEMA and PS, it gained non-wettable characteristics of PS. ^1H NMR study of the block copolymer solution in methanol showed micellar styrene core covered with HEMA. Authors argue that this structure- retained in the solid state as microphases- is responsible for the higher content of HEMA on the surface than in case of films cast from DMF. Heating above T_g drives the system to equilibrium, forcing the PS domains to migrate to the surface. These results on the effect of solvent seem to be reverse of those found earlier[28] or as might be expected from thermodynamics, presumably due to kinetics of migration of PS domains during the solvent evaporation.

2.1.2.2 Direct Methods. Clark, Peeling and O'Malley[39] studied surfaces of PS/PDMS AB block copolymers with the help of contact angles and XPS. Two copolymers containing 23% and 59% w/w PS were investigated. Contact angle measurements showed that both block copolymers had critical surface tensions of 22 dyn/cm. The casting

solvent was varied in the case of the 59% copolymer. Critical surface tensions values were found to be the same in each case. To complement the information by contact angle measurements, which is representative of the immediate surface of the film only, high resolution XPS was utilized which gives chemical information from the subsurface, typically 50 Å deep. Their quantitative treatment of the XPS data led to interesting conclusions regarding the nature of the PDMS surface layer. The thickness of this sublayer, assumed to be over a uniform bulk of the given copolymer composition, was found to vary from 13 Å for cyclohexane(preferential solvent to PDMS) cast films to 40 Å for styrene(preferential to PS) cast films. A study of the bulk morphology of the same system by Saam et al.[40] indicated earlier that the domain structure depended upon the solvent. It changed from spheres of PS surrounded by PDMS when cast from solvent selective for PDMS to spheres of PDMS surrounded by PS when cast from solvent selective for PS, through a variety of intermediate structures. Thus the study by Clark et al. clearly indicated that the surface morphology may differ considerably from the bulk morphology as long as the latter is definitely multiphase.

O'Malley and Thomas used angular dependent XPS to determine surface compositions and topographies of PEO/PS diblock[41] and triblock[42] copolymers. Studies on a number of copolymers having different composition disclosed that the PS concentration at the air-polymer interface was substantially higher than the bulk concentration of PS. The block architecture apparently did not affect the behavior. Note that the solubility parameters(or the polymer-polymer segment

interaction parameters) are much closer for PEO/PS relative to PSX/PS. Moreover, PEO may be semi-crystalline at room temperature. Careful angular dependence study gave an useful insight into the topography of these copolymers. Relation of the angle between the electron analyzer and the sample surface (proportional to the depth from which the analyzed electrons are emitted) and the surface composition pointed towards nonplanar topography. Cylinderical domains are slightly elevated above the PEO domains as shown in the Figure(2.3d) rather than the models shown in the Figures(2.3a-c). This study also revealed that in the surface region the two components are partially miscible and that the miscibility is a result of electronic interaction between the PEO and PS blocks in the copolymers. Complementary proof of this via, for example, Fourier transform-infrared (FT-IR) spectroscopy would be interesting. Similar investigation on PHMS/PDMS random block copolymers[43] indicated that PDMS never totally covers the surface. The segmented domain structure was evident in the surface to some degree. On the other hand, as it may be recalled, O'Malley and Stauffer's work described before on perfectly alternating PHMS/PDMS block copolymers[33] revealed an overlayer of PDMS on a microphase-separated bulk.

McGrath et al. studied[44] PBAC/Polysulfone(PSF) and PBAC/PDMS block copolymer surfaces with the help of XPS. In each case, the lower surface energy component dominated the surface i.e. PBAC in the PBAC/PS copolymer and PDMS in PDMS/PS copolymer. A number of PDMS/PC copolymers with various block length were examined by Riffle[45]. On review of the results it could be noted that the block

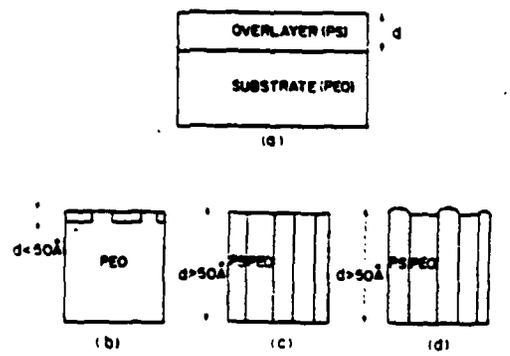

FIGURE(2.3). Models for the surface topography of polystyrene/poly(ethylene oxide) diblock copolymers. [from 41]

length of siloxane was the governing factor in determining the surface composition rather than the overall composition. Keeping the siloxane block length at 1800 g/mole(about 24 units) and varying the siloxane weight percentage as 11, 22, and 40, produced similar surfaces composed of about 60% w/w siloxane. Whereas, when the block length was increased to 5000 and 10000 g/mole each of approximately equal composition, surfaces of 82% and 92% siloxane respectively were obtained. When the copolymer of 1800 g/mole siloxane block was blended with PC homopolymer in different amounts, a notable behavior was observed. Siloxane was seen in considerable amounts even at 0.05% level in the bulk. A definite break was observed at about 1% siloxane by weight in the bulk at which the surface composition of siloxane jumped to a higher value as shown in the Figure(2.4). Presence of two plateau regions are evident in the figure- one where low amount of siloxane is detected at the surface (although higher than the bulk) and the other where there is a high surface siloxane approaching that displayed by the pure block copolymer. Analogous behavior was observed by Sha'aban et al.[15,46] in the system of polyurethane/PDMS blended with a poly(tetramethylene oxide)(PTMO)/polyurethane block copolymer, ESTANE®. XPS analysis on solvent(THF) cast films revealed a transition concentration of siloxane in the bulk at about 1% where the surface composition shoots up, eventually to level off as the surface characteristics of the neat block copolymer are approached. The Figure(2.5) depicts this behavior on a plot of %silicon(representative of the siloxane content) at the surface against the %siloxane in the bulk.

Recently Kugo and co-workers combined contact angle

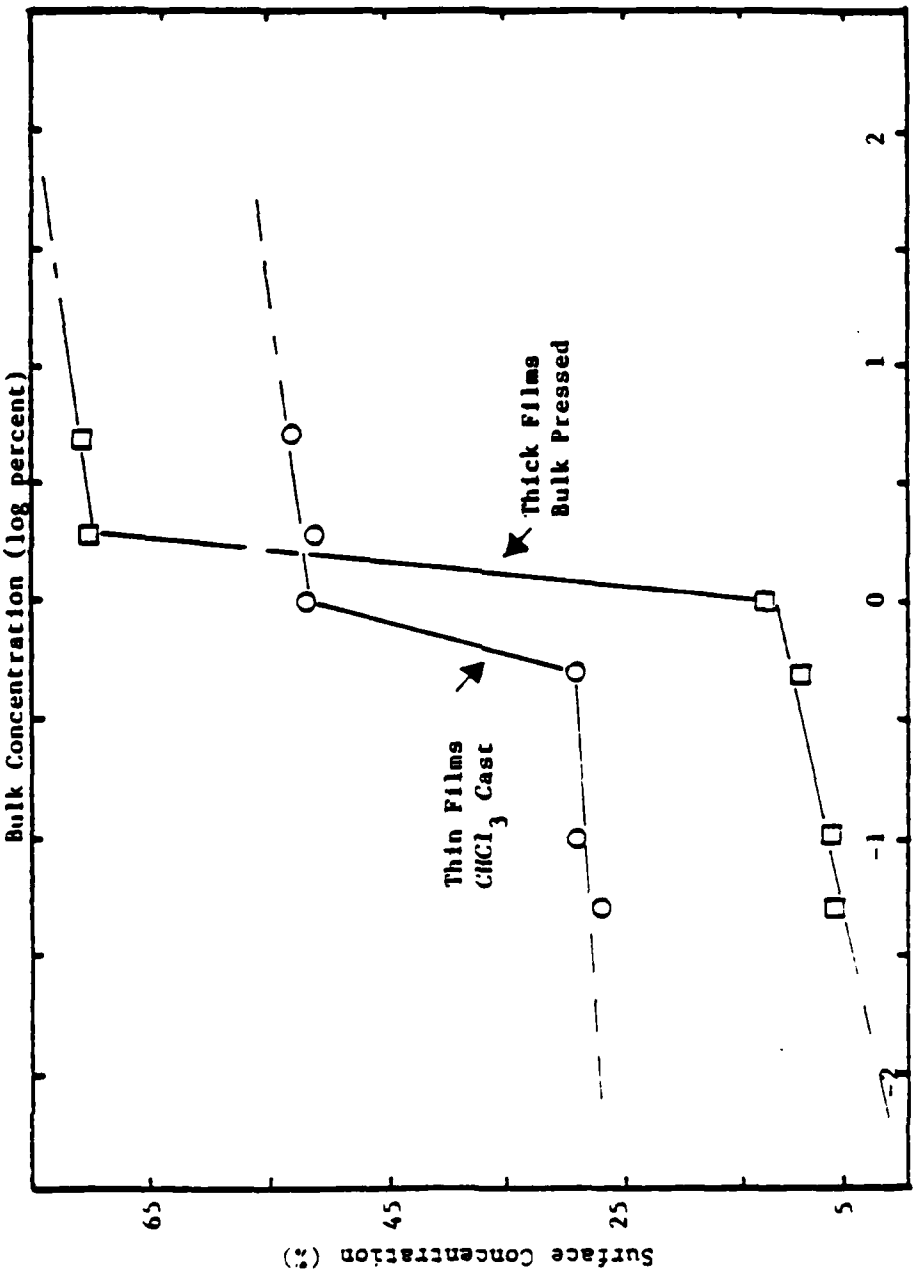

FIGURE(2.4). Surface segregation in polycarbonate/poly(dimethyl siloxane) block copolymer-homopolycarbonate blends. [from 45]

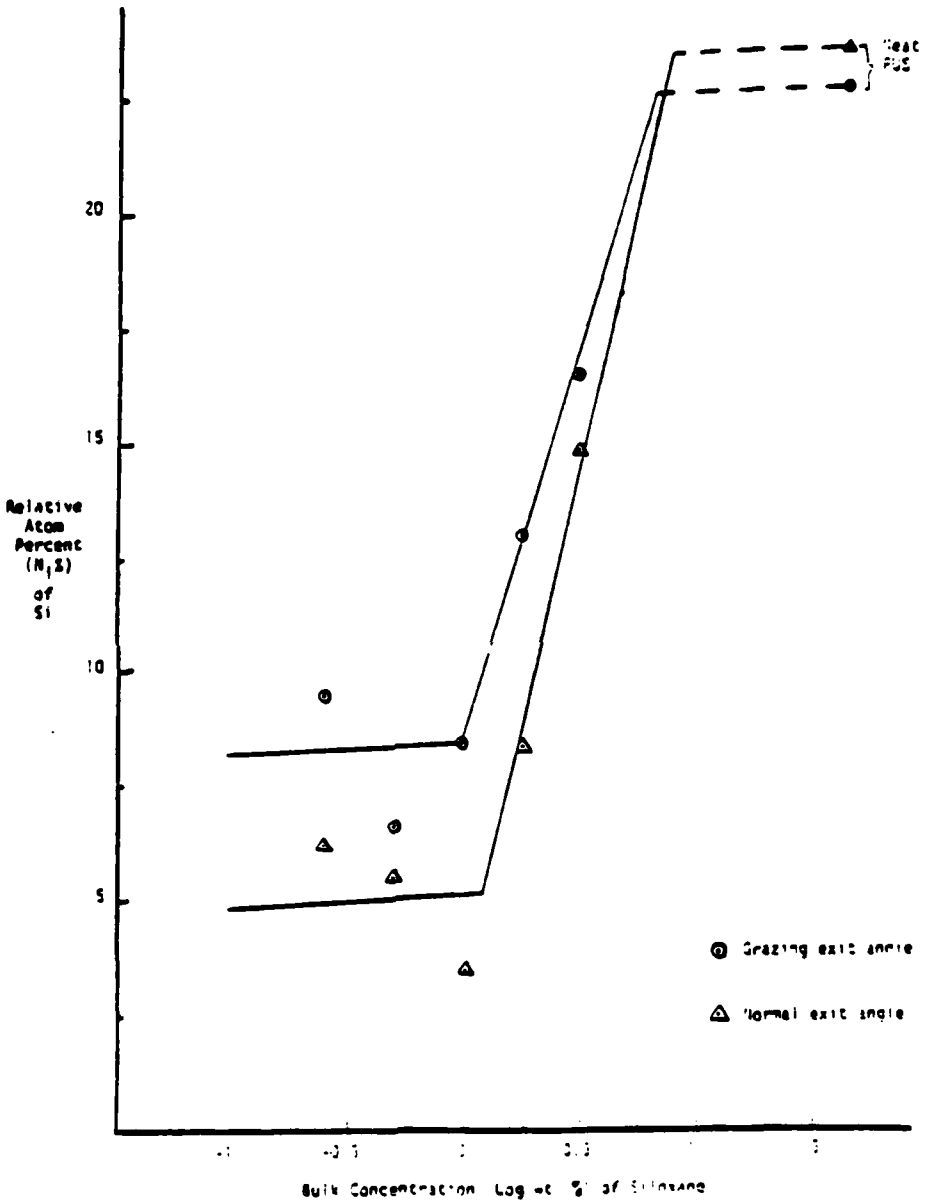

FIGURE(2.5). Surface segregation in polyurethane/poly(dimethyl siloxane) block copolymer blended with polyetherurethane. [from 46]

measurements, XPS, and replication electron microscopy to elucidate the surface composition and morphology of ABA triblock copolymers of poly(ε-N-benzyl carbonyl-L-lysine)(PBCL)/polybutadiene(PB)[47] and poly(α-methyl D,L-glutamate)(PMG)/PB[48]. PB, being of lower surface energy as compared to the other two counterparts, was expected to segregate at the surface. XPS on solvent cast films showed that this indeed was the case. It was found by replication electron micrographs that the block copolymer surface was uneven i.e. the PB domains were elevated above the PBCL matrix. Based on this micrographs, a surface model as shown in the Figure(2.6) was proposed. The presence of an interfacial region between α-helical PBCL component and PB component at the surface was well explained by contact angles. Similar results were obtained in the case of PMG/PB copolymers[48]. A microphase-separated bulk was observed by transmission electron microscopy. The surface retained this morphology as revealed by replication electron micrographs.

In the past few years, there has been a sizable research effort in the biomedical area to study polymeric surfaces which may be applied where biocompatibility (particularly, blood compatibilty) is necessary, in addition to good mechanical properties. Segmented polyurethanes were found to be the potential candidates for this application due to its elasticity(thermoplastic) and good biocompatibility. Two such commercially available polyurethanes-, Avcothane and Biomer, have been used in this application. However, their blood contact properties do not seem to be consistent and are found to be dependent on the fabrication process. This may be expected because the segmented

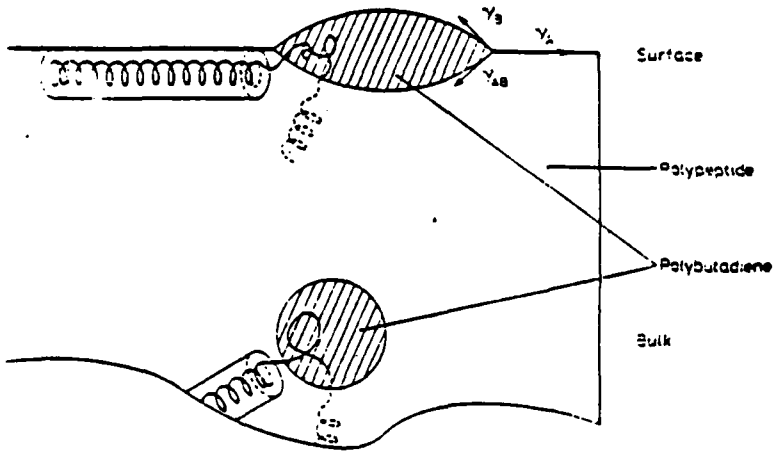

FIGURE(2.6). Cross section model for ABA triblock copolymers of poly(ε-N-benzyl carbonyl-L-lysine)/polybutadiene. [from 47]

polyurethanes being multicomponent, multiphase block copolymers, their bulk and surface properties would be sensitive to such parameters as substrate in contact, rate of evaporation, temperature etc. A number of studies have been done utilizing various surface analysis techniques such as contact angle measurements[49], attenuated internal reflection IR spectroscopy (ATR-IR)[49-51], auger electron spectroscopy (AES)[52], XPS[53-58], secondary ion mass spectroscopy (SIMS) and ion scattering spectroscopy (ISS)[57-58]. A brief review of their findings pertinent to our discussion will be presented here.

Nylias and Ward[51] observed that Avcothane, a complex polyurethane elastomer which has been loosely described as poly(ether urethane)/PDMS block copolymer, the biocompatible properties depended considerably on the rate of evaporation of solvent during the film preparation. ATR-IR spectroscopy showed that the surface was quite different from the bulk- having a larger amount of siloxane. The siloxane content at the surface was sensitive to the rate of evaporation. This is probably an example of kinetic factor playing a role in surface segregation. Effect of the substrate on the substrate side surface of a polyetherurethane was investigated by Stupp, Kauffman, and Carr[49]. ATR-IR spectroscopic characterization revealed surfaces cast on glass substrate showed a higher content of polyether segments whereas those cast on PET showed a higher content of aromatic segments. Similarly Paik Sung and co-workers showed that in solvent cast Avcothane and Biomer- a polyetherurethane, air side and substrate(glass) side surfaces had different chemical compositions, as revealed by fourier transform ATR-IR[50], AES[52], and XPS[54]. In the top few angstroms of

Avcothane, the air-side surface had considerably larger siloxane than the substrate side. In Biomer, the ether segments segregated(although weakly) to a greater extent at the air side than at the substrate side surface. Graham and Hercules[57,58] came to the same conclusions from their study with the help pf XPS, ISS, and SIMS combined. Ratner[56] reported segregation of the ether component in SOLITHANE®- a commercial polyetherurethane and of ester component in TYGOTHANE®- a commercial polyesterurethane.

2.2 THE BULK

Much attention is given in the last fifteen years or so to the study of micro-phase separation behavior of block copolymers since it is one of the most important factors imparting the physical and mechanical properties unique to these systems. More recently, a greater interest has been generated in morphological studies of binary or ternary systems containing block copolymers with corresponding homopolymers, mainly due to their applications in toughening of glassy polymers without adversely affecting the modulus and the softening temperature. The phenomenon of microscopic heterogeneities in block copolymers is reasonably well understood experimentally with further substantiation by thermodynamic and statistical calculations[59]. The situation in the blends is more complex. The morphology established by such systems range from highly miscible one phase systems to simple microheterogeneous structure persisting throughout the sample, to a variety of large isolated supermolecular features which may themselves

may have microscopic phases. A microheterogeneous structure implies the so-called 'solubilization' of the homopolymer into the existing frame of the block copolymer- much like the classical incorporation of an insoluble solute in micelles of surfactant molecules. Whereas the latter type of morphologies usually imply various degrees of incompatibility of the homopolymers and the block copolymer. A brief discussion of the above aspects is given as following.

2.2.1 PURE BLOCK COPOLYMERS.

Since this subject has been dealt with enormously in the literature[68], an attempt is made here to present only the basics. The physics controlling the morphology in block copolymers is quite simple, in principle. In any heterogeneous system composed of units of types A and B, which has a positive heat of mixing and a very small entropy of mixing, there is a tendency towards phase separation. The topology of the block copolymer molecules restricts this separation and induces the formation of microdomain structure. From a thermodynamic point of view, the process can be examined as a consequence of two opposing factors affecting the tendency of segregation. First is the surface free energy which decreases as the domains grow, providing the driving force. But at the same time, greater degree of phase separation means a higher randomness in the system- a state greatly opposed by nature. As a result a 'micro-phase' separated system is obtained. Several different types of morphologies have been confirmed by techniques of small angle x-ray diffraction and electron microscopy. These can be spherical, cylinderical, or lamellar as schematized in the Figure(2.7).

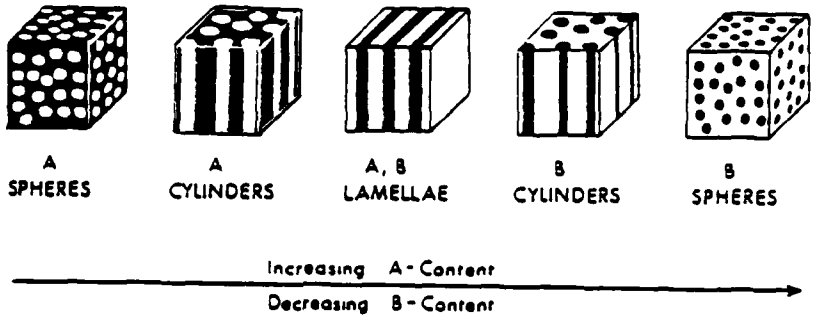

FIGURE(2.7). Scheme of block copolymer morphology. [from 3]

The type and extent of the domain structure in a particular system depends mainly on variables such as molecular weights, overall compositions and type of solvent in case of solvent-cast systems. Figures (2.8a) to (2.8c) give a clear evidence of this behavior in a system of PS/polyisoprene(PIP) block copolymers[61].

2.2.2 BLENDS OF BLOCK COPOLYMERS WITH HOMOPOLYMERS.

One of the earliest works in this area has been by Reiss et al.[62] on ternary blends of PS and PIP with PS/PIP block copolymers. By observing the transparency of the films, they concluded that the separation of the two homopolymers critically depended on the relative molecular weights of the homopolymers and the block copolymer segments. In a systematic study on blends of PS/PIP block copolymers with the corresponding homopolymers, Inoue et al.[5] found that homopolymer chains can be solubilized into block domains of the same type provided that the molecular weight of the former is same as or less than that of the latter. However, in the case when the molecular weight of the homopolymer is much larger than the corresponding block, macroscopic phase separation into the homopolymer phase and the block copolymer phase (which in turn is microphase separated) occured. A Comparison was made of two 80/20 blends by weight of a PS/PIP AB block copolymer with PS homopolymers- one of comparable and the other of much larger molecular weight than that of the corresponding PS block. In the former blend, the effect was of swelling the styrene spherical domains of the original block copolymer morphology, solubilizing the homopolymer. On the other hand, the latter blend

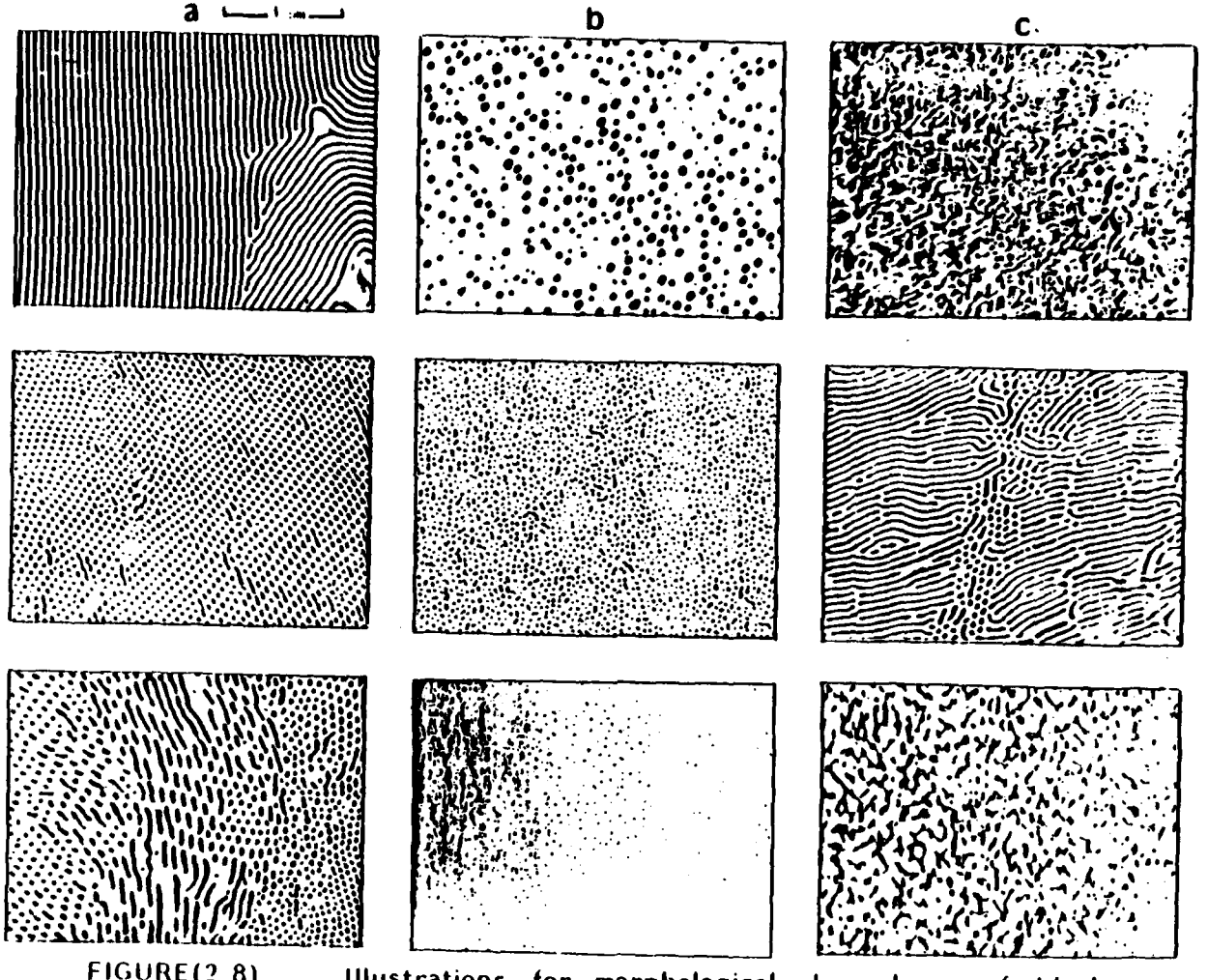

FIGURE(2.8). Illustrations for morphological dependence of block copolymers on various parameters, a. effect of fractional composition of the components, b. effect of molecular weights of the blocks, and c. effect of the type of solvent. [from 61]

revealed ellipsoidal styrene phases of about a micron in size dispersed randomly in a matrix of essentially same character as the neat block copolymer. Such supermolecular structures were also observed by Molau et al.[63] and Bradford[64] under certain circumstances although they offered no explanation for their existence. Dependence of the morphology on the molecular weight was also confirmed later Toy et al.[65], Reiss et al.[66] Kotaka et al.[67] and Kawai et al.[61], with evidences of both microscopic and mechanical nature.

Eastmond and Phillips[68,69] have presented a series of morphological studies on blends of the so-called nonlinear block copolymers or AB cross-linked copolymers(ABCPs) with their corresponding homopolymers. From the electron micrographs, they concluded that, contrary to the prior claims, homopolymers are essentially incompatible with the corresponding block copolymer- even if the their respective molecular weights are comparable. This conclusion is supported by Meier's theoretical results[70]. Meier's theory predicts that a very limited amount of a relatively high molecular weight homopolymer can be solubilized in the dry state. At the same time, the theory also shows that in the presence of a solvent, block copolymers can solubilize a considerable volume of homopolymer having a molecular weight not greatly different from the corresponding block. Meier points out that the discrepancies that may exist between the theory and experiments could be due to the non-equilibrium "freezing in" of domain features when domains first form in the presence of a solvent during sample preparation procedures.

Improved mechanical properties can be obtained by the

incompatibility between a block copolymer and a homopolymer. Aggarwal and Livigni[6] have shown that blending of 25 parts of a triblock copolymer having 40% styrene and 60% butadiene with 75 parts of PS produced a material tougher(in terms of impact strength) than a commercial high impact polystyrene(HIPS). Electron micrographs of both materials revealed the similarity and difference between the two. The similarity is that, as in HIPS, the blend also has as elastomeric phase (made of micro-phase separated PS/PB) dispersed in glassy PS. The difference lay in the fact that in the blend, the PS domains dispersed in the block copolymer phase are of submicroscopic size when compared to those in the dispersed phase of HIPS.

Very recently Jiang, Huang and Yu have investigated graft copolymer based blends[71]. Their electron microscopic study shows that in blends of PS and PS/PB graft copolymer with PS making the graft, there is a gradual variation of morphology with relative molecular weights of the PS chains in both components. When the molecular weight of homopolymer is much larger that of the grafts, they are completely incompatible. Solubilization increases as the two molecular weights come closer. It is almost complete when the homopolymer molecular weight is less than that of the grafts.

CHAPTER III

PRINCIPLES OF X-RAY PHOTOELECTRON SPECTROSCOPY

Although Einstein published his famous and controversial paper on photoelectric emission[72] much earlier, it was only in the mid 60's that the principle began to develop into an analytical tool in the form of photoelectron spectroscopy(PES). In 1967, Siegbahn and co-workers published their pioneering book[73] reporting results in which X-ray sources were used to study valence and core levels of molecules. This study revealed so much about chemical bonding that Siegbahn named the technique Electron Spectroscopy for Chemical Analysis or ESCA, more generally known as X-ray Photoelectron Spectroscopy(XPS) today. Since then XPS has evolved into one of the most successful analytical tools to study solid state band structure and atomic and molecular bonding in both the solid state and the gas phase, with developments being made to adapt it to liquid systems[74]. Out of all these uses, the most important one has been in the analysis of solid surfaces. Some of the reasons for which this technique has an edge over other surface analysis methods are its: non-destructive nature, capability of detecting of all elements except hydrogen and analyzing any solid that can withstand the vacuum and bombardment of x-rays, and sampling depth of only in tens of angstroms.

A great volume of literature in forms of books, reviews and research papers has been published in the last decade or so on XPS. The reader might be referred to one such publication which reports a comprehensive up-to-date list of literature published[75]. In the next sections a discussion of the basic concepts of XPS will be given particularly stressing the quantitative aspects that are used extensively in this work. A brief review of its use in study of polymers will be given later.

3.1 THE BASIC PROCESS.

The fundamental XPS experiment is shown schematically in the Figure(3.1a). X-ray photons, with energy $h\nu$, are bombarded onto the sample. The atoms in the sample absorb the photons with a simultaneous emission of *photo*electrons. Electrons from all the orbitals of the atom with binding energy E_b, less than the x-ray energy $h\nu$, are ejected with a certain kinetic energy E_k. Since electrons have different probabilities of emission, a spectrum with photoelectron peaks of variable peak intensities is obtained. From the conservation of energy one can write:

$$E_k = h\nu - E_b + \phi_s \qquad .....(3.1)$$

where ϕ_s is the 'spectrometric work function' which allows the binding energy of electrons to be referenced to the fermi level of the material. This makes the kinetic energy of any peak as measured in

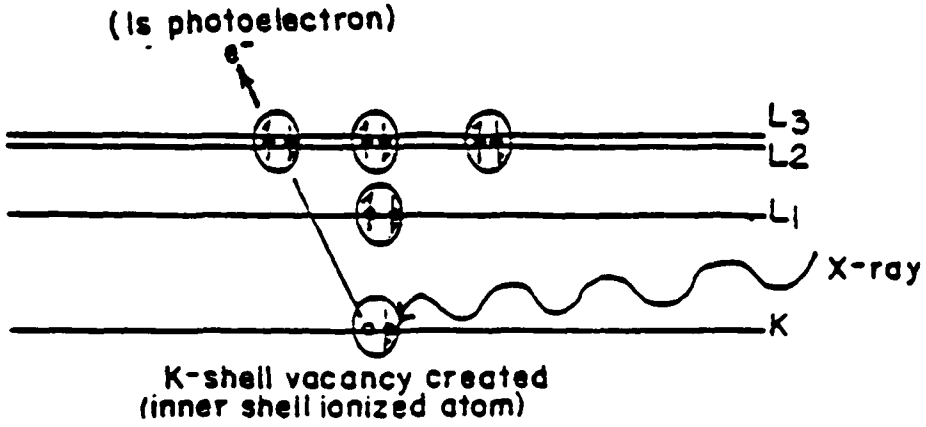

(a) The basic process.

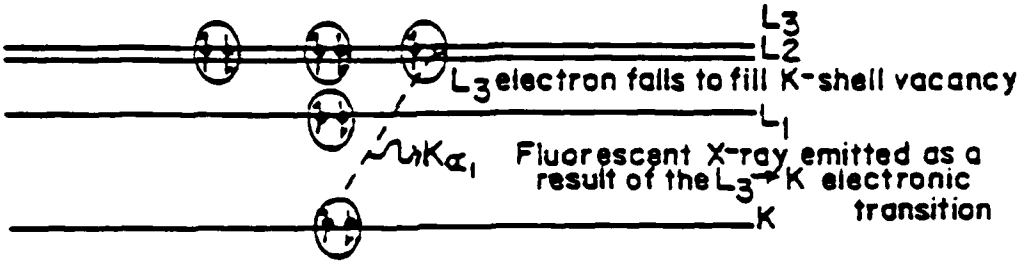

(b) Relaxation by x-ray flourescence.

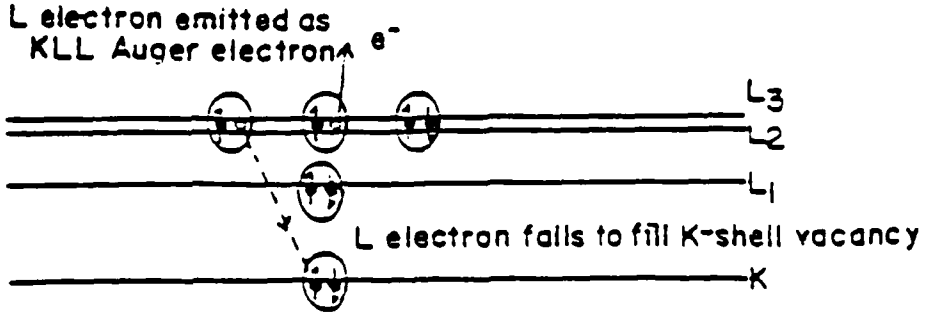

(c) Relaxation by the Auger process.

FIGURE(3.1) Processes occuring during the XPS experiment.

the spectrometer independent of the work function of the sample[76].

De-excitation of the hole state can occur either by fluorescence, as shown in the Figure(3.1b), or by the Auger process, as shown in the Figure(3.1c). The former produces secondary x-rays- and the latter auger electrons which are also detected along with the photoelectrons.

3.2 QUALITATIVE ANALYSIS.

Since binding energies of electrons in each element in the periodic table are distinct, except some instances where overlapping occurs, measurement of the positions of photoelectron peaks allows a quick identification of the elements present at the sample surface. A typical survey spectrum is shown in the Figure(3.2a). The chemical state of the elements may then be recognized by obtaining narrow scans of the regions of interest and measuring the exact peak position. For example, Figure(3.2b) shows two chemical states of Aluminium on a Al_{2p} spectrum. Published data on binding energies can be utilized for this purpose[73,79].

3.3 QUANTITATIVE ANALYSIS.

In this part the fundamentals of (semi)quantitative surface analysis by XPS i.e. how to convert intensities as measured in a spectrometer to atom percentages in the sampled volume, are described. Emphasis is provided on the origin and applicability of equations used later in the quantitation of data.

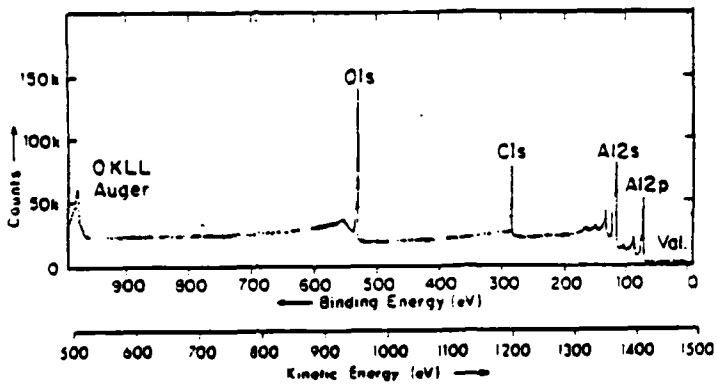

FIGURE(3.2a) Typical XPS spectra obtained from an oxidized aluminium specimen with a carbonaceous contaminant layer. [from 77]

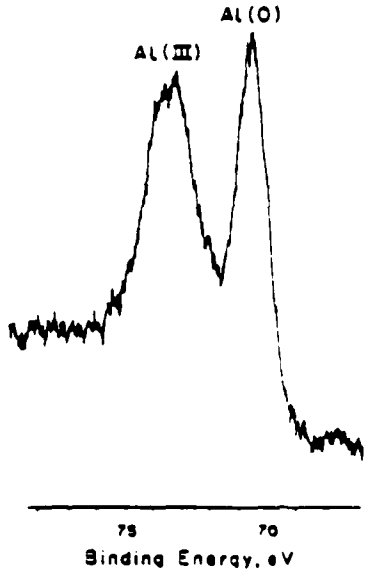

FIGURE(3.2b) Aluminium 2p spectrum from aluminium metal with a passivating overlayer showing chemical shift of Al(III) relative to Al(0). [from 78]

There are mainly three approaches for quantitative analysis:

(a) by standards;

(b) by elemental sensitivity factors; and

(c) by the first principle model.

The first method requires reliable local standards with surface composition similar to the unknown sample. It is obvious that this method is restricted to only certain circumstances such as routine analysis of samples with a limited range of compositions. The method of elemental sensitivity factors is developed and extensively used chiefly by Wagner[80] and Berthou and Jorgensen[81,82]. These authors have prepared a relative intensity scale in reference to the fluorine 1s intensity by analyzing a number of compounds. The calculations can then be performed by using the following equation:

$$n_1/n_2 = [I_1/S_1]/[I_2/S_2] \qquad .....(3.2)$$

where n is the atomic density; I is the intensity as measured in the XPS experiment; and S is the sensitivity factor referenced to F_{1s} line. The results with this method have been claimed to be better than 10% in general[80]. The 'first principle' method relates the measured intensities with the basic material and spectroscopic conditions via processes of x-ray bombardment, photoelectron creation, photoelectron transport to the surface and electron detection. The rest of the section is devoted to the understanding of this approach which is used in this research.

Figure(3.3) shows a typical sample/spectrometer geometry with nomenclature for various quantities labeled. A general expression for the number of photoelectrons dN emerging from a subshell nl as a function of θ, the electron take off angle, can be written as[83]:

$$dN_{nl}(\theta) = \begin{matrix} \text{x-ray flux at depth } z \\ \cdot \end{matrix} \begin{matrix} \text{number of atoms in volume} \\ \cdot \end{matrix} \begin{matrix} \text{probability for an nl level electron emission into } \Omega_o \\ \cdot \end{matrix} \begin{matrix} \text{fraction escaping in a no-loss peak} \\ \cdot \end{matrix} \begin{matrix} \text{factor due to spectrometric function for analysis and detection} \end{matrix} \quad \ldots\ldots(3.3)$$

or,

$$dN_{nl}(\theta) = \{I_o[1-R][\mathrm{Sin}\phi/\mathrm{sin}\phi']\mathrm{Exp}[-z/\lambda_x \mathrm{Sin}\phi]\} \cdot \{\rho[A_o/\mathrm{Sin}\theta]dz\} \cdot \{[\partial\sigma_{nl}/\partial\Omega]\Omega_o\} \cdot \{\mathrm{Exp}[-z/\lambda_e(E)\mathrm{Sin}\theta]\} \cdot \{T(E)\} \quad \ldots\ldots(3.4)$$

where R represents the x-ray reflection coefficient; ρ is the number density of the atom under consideration; $\partial\sigma_{nl}/\partial\Omega$ is the differential photoelectron cross-section for the nl subshell; λ_x and λ_e are the mean free paths of the x-rays and the electrons, respectively, under consideration; and T(E) represents a function describing the intensity change caused by retardation in the spectrometer.

For a homogeneous sample of atomically flat surface and infinite thickness the above equation after integration can be simplified to[83]:

$$N_{nl,\infty}(\theta) = N_{nl,\infty} = ST(E)\rho[\partial_{nl}/\partial\Omega]\lambda_e(E) \quad \ldots\ldots(3.5)$$

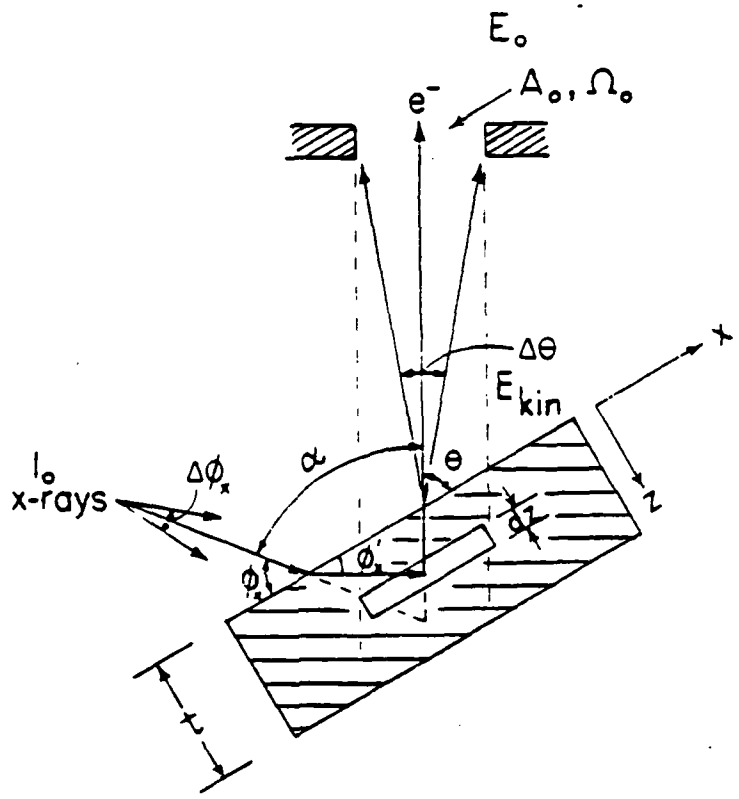

I_o = intensity of the oncoming x-rays

A_o = area of the spectrometer entrance aperture

Ω_o = geometrical solid angle of acceptance of the spectrometer

E_{kin} = energy of the electrons off the sample surface

E_o = energy of the electrons in the analyser after retardation

ϕ_x', ϕ_x = x-ray incident and refraction angles at the sample surface

θ = average electron exit angle

α = angle between the oncoming x-rays and the exiting electrons

$\Delta\phi_x$, $\Delta\theta$ = maximum uncertainity in ϕ_x and θ respectively

FIGURE(3.3). Idealized spectrometer geometry for calculating photoelectron peak intensities from solid specimens under XPS analysis. [from 77]

Here, S is a constant representing various factors that are dependent only on the spectrometer/sample configuration and independent of the electrons analysed. Similarly number of photoelectron emitted from n'l' level of an atomic species of density ρ' and energy E' can be written as:

$$N_{n'l',\infty}(\theta) = ST(E')\rho'[\partial_{n'l'}/\partial\Omega]\lambda_e(E') \qquad .....(3.6)$$

Using Equations (3.5) and (3.6), and rearranging we get:

$$\frac{\rho}{\rho'} \quad \frac{N_{nl,\infty}T(E')[\partial_{n'l'}/\partial\Omega]\lambda_e(E')}{N_{n'l',\infty}T(E)[\partial_{nl}/\partial\Omega]\lambda_e(E)} \qquad .....(3.7)$$

Three terms in the above equations demand a broader explanation. They are:

(a) Electron mean free path $\lambda_e(E)$, dependent on matrix properties;

(b) Differential Photoelectron Cross-section $\partial\sigma_{nl}/\partial\Omega$, dependent on atomic properties; and

(c) Transmission function T(E), dependent on spectrometer properties.

3.3.1 ELECTRON MEAN FREE PATH.

A great deal of work has been done on the measurement and prediction of electron mean free path as a function of its energy and the matrix through which it travels. Earliest work was by Penn[84] who proposed the following relation for energy dependence of mean free

paths:

$$\lambda(E) = E/\{a[\ln E + b]\} \qquad .....(3.8)$$

where a and b are material constants. This equation fits very well for free electron materials (believed to be better than 5%), but poorly for other materials. More recent compilation of experimental data and theoretical modeling suggest a power law relation[85-88]:

$$\lambda(E) = kE^{p} \qquad .....(3.9)$$

with k regarded as a material constant.

After extensive compilation of data, Seah and Dench[85] obtained 0.5 as the value of p for electrons greater than 150 eV. Szajman et al.[86] predicted 0.75 value for p from theoretical calculations for E > 300 eV. Wagner et al.[87] suggest that p is most likely to lie in the range 0.65-0.75 after comparing several sets of data. More recently Ashley and Tung[88] came to the conclusion on the basis of theory and experiment that an average p in the energy range 400 to 2000 eV is 0.73. They also showed that values by Equation(3.8) according to Penn[84] in this range fitted well to the power law model with an average p of 0.77. In the same range, the value of k, the material parameter, varies from 0.08 to 0.288. This parameter is less important since it cancels when a ratio of λ's is taken in the quantitative calculations.

3.3.2 DIFFERENTIAL PHOTOELECTRON CROSS-SECTION.

Emission of photoelectrons is generally not isotropic and is a

function of the angle ϕ between the directions of the photons and the electrons as shown in the Figure(3.3), given by[89]:

$$\partial\sigma/\partial\Omega = [\sigma_{total}/4\pi]\{1+0.5\beta[1.5Sin^2\phi-1]\} \quad .....(3.10)$$

where σ_{total} is the total cross-section and β is the asymmetry parameter. β ranges from +2 to -1 and is dependent on the photoelectron energy for p, d, and f orbitals, whereas it is constant at 2 for all s orbitals. Reilman et al.[90] have calculated values of β for all atomic levels excited by $Mg_{K\alpha1,2}$ and $Al_{K\alpha1,2}$ x-ray sources. The total cross-section σ_{total} have been calculated theoretically by Scofield[91] which are quite accurate up to about 10% for electron energies above 100 eV, as verified experimentally[92].

3.3.3 INSTRUMENT TRANSMISSION FUNCTION.

Most commercial XPS instruments have electrostatic deflection analyzers to separate the electrons of a definite energy from all other electrons. For such analyzers, the efficiency at which this separation is done is directly proportional to the electron energy in the analyzer, E_a[93]. Normally the electrons emitted from the sample are first retarded to a certain amount before analyzing since it improves the resolution[94]. Two modes of retardation are mainly used, viz: (i) Fixed Retarding Ratio (FRR), and (ii) Fixed Analyser Transmission (FAT). In FRR mode, as the name suggests, all electrons are retarted to the same fraction of their original energy. Hence, $E_a \propto E$. And since, as mentioned earlier, the efficiency of the analyzer is directly proportional to the electron energy E_a, we have $T(E) \propto E$. On the

other hand, in the FAT mode, the E_a is kept constant independent of the energy of the incoming electrons. Hence, in this mode T(E) is a constant independent of E. These relations are found to be valid both experimentally and theoretically[95].

3.4 ANGLE-DEPENDENT DEPTH PROFILING.

A greater surface sensitivity can be achieved by variation of the angle θ between the sample surface and the analyzer as shown in the Figure(3.3). This angle-dependent XPS studies have been reviewed by Fadley[96]. As shown in the Equations(3.3) and (3.4), the fraction of electrons escaping without loss of energy is an exponential function of the distance it travels given by:

$$\text{No loss fraction}, f \propto \text{Exp}[-z/\lambda_e(E)\text{Sin}\theta] \qquad .....(3.11)$$

This relation leads to a concept of 'sampling depth'. If the 'sampling depth' is arbitrarily defined as that depth in the sample at which the electrons have only 5% chances of escaping into the no loss peak, it can be shown that:

$$z/\text{Sin}\theta = 3\lambda_e(E) \qquad .....(3.12)$$

or,

$$z = 3\lambda_e(E)\text{Sin}\theta \qquad .....(3.13)$$

Thus by varying the electron take off angle, we can effectively

analyze at various depths in the solid. This is demonstrated in the Figure(3.4). Equation(3.7) can be used to calculate relative atomic fractions as a function of angle θ from experimental values of intensity measured at various angles. The results can not be easily converted to atomic fractions vs. depth in the sample due to the fact that: (i) atomic densities obtained thus are not point values but an exponential average over the sampling depth; and (ii) sampling depths for the two species would be different if their mean free paths are different. Nevertheless, the data can certainly be useful in obtaining a semi-quatitative idea of the concentration variation in the top few angstroms of the surface.

Accurate analysis can be done by postulating surface models in terms of concentration profiles, predicting the XPS intensity behavior by integration of the rigorous Equation(3.4) over these models and then comparing with experimental behavior to choose the model that fits the best[97,98]. This situation becomes more complicated when atomically rough surfaces are encountered, as may be expected in real samples, due to shadowing of the oncoming x-rays and the emerging electrons. Fadley and co-wokers have dealt with the subject in detail[83].

3.5 APPLICATION OF XPS TO POLYMERS.

Of all techniques available today, XPS has made the greatest impact on investigation of structure and reactivity of polymeric systems in the solid state. This is quite evident from the number of reviews[99]

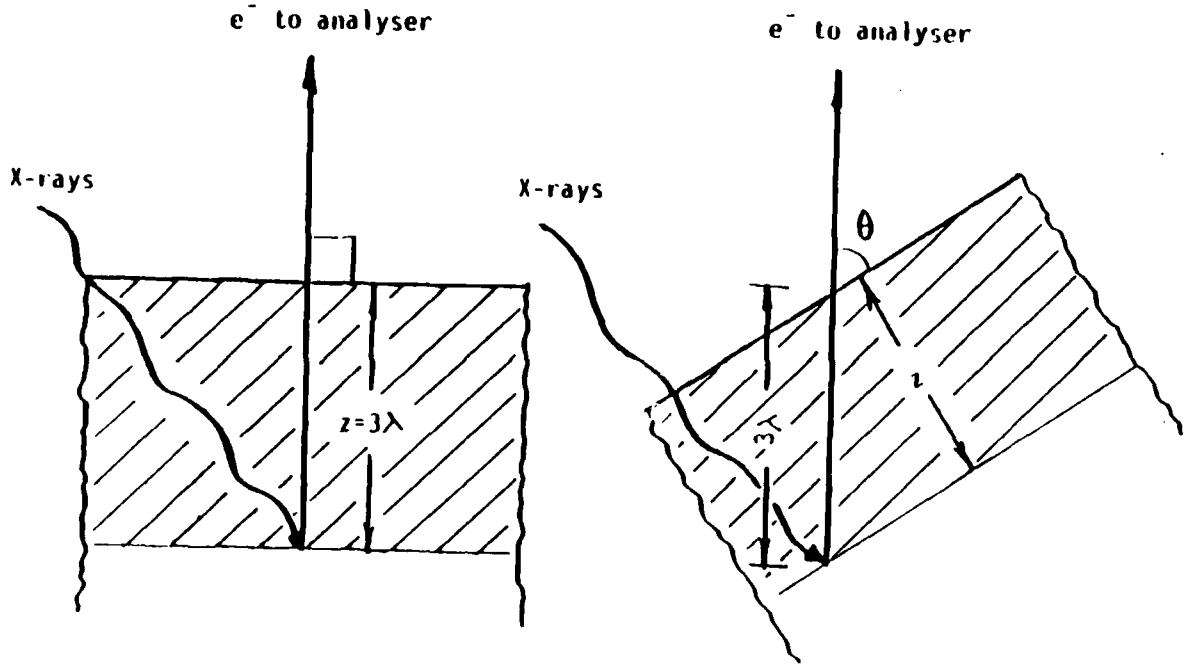

FIGURE(3.4) sampling depth 'z' as a function of the angle θ between the sample plane and the analyser.

appearing within only a decade after some of the first results of XPS studies on polymers were published by Clark and co-workers[100] and by Dwight and Riggs[101].

For surface analysis of polymers in particular, XPS is the most attractive method because of its non-destructive nature. Other popular surface sensitive techniques do not share this advantage. Auger Electron Spectroscopy(AES), which is widely applied to conductive materials, is difficult to use for study of polymers due to the latter's non-insulating nature and susceptibility to electron beam damage at current densities normally used. Similarly in case of ion spectroscopy, such as Ion Scattering Spectroscopy(ISS) and Secondary Ion Mass Spectroscopy(SIMS), ion beam damage (reduction, rearrangement etc.) can occur and much of the chemical information is lost while the spectra are being collected. Other techniques that may have applications for chemical information in polymers are infrared and Raman spectroscopic methods, although the depth of probing here is much greater than that with XPS.

In this section we will review the application of XPS to polymers, bringing out certain unique features of the combination which would explain the dominant use of the technique in this work.

3.5.1 INFORMATION CONTENT.

Table(3.1) summarizes the primary information available from XPS core level spectra of polymers on their chemistry and structure. Core level electrons are essentially localized on atoms, their energies being characteristic for the given element. But they are sensitive to the

electronic environment of the atom. This gives rise to a range of energies around the characteristic binding energy i.e. *chemical shifts* due to change in the type of bonding. Thus measurement of binding energies of photoelectrons in an XPS experiment provides not only the identification of the atom but also an idea of the chemical bond structure it has. It should be noted here that carbon bound to itself and/or to hydrogen has the same 1s binding energy no matter what state of hybridization. It requires more electronegative atoms or groups of atoms to obtain chemical shifts measurable with resolutions available in XPS instruments today.

The credit for the major volume of work on chemical shifts in polymers goes to Clark and Thomas[103-105]. A summary of their findings is depicted in the Figure(3.5). It can be noticed from the figure that the binding energy spreads for various cores are rather small, largest being that of C_{1s} of about 10 eV. Also the secondary effects induced by neighboring groups are usually too small in polymers for detection, demanding caution in interpretation of raw data. For example, a C_{1s} peak at 286.5 eV (compared to hydrocarbon C_{1s} at 285.0) may mean any of the following structures:

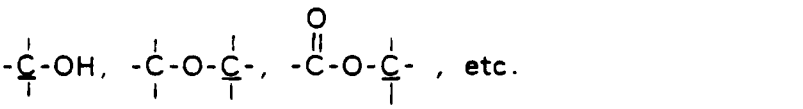

This lack of long range effect on chemical shifts is advantageous, in fact, in theoretical determination of binding energies since it allows one to model the complex macromolecules by considering only short segments of the chain. Instead of the more difficult exact(ab initio) calculations, analysis has been based on the so-called charge potential

TABLE(3.1) Information obtained from XPS spectra of polymers. [from 102]

Spectral Feature	Information
Main peak position	Atom identification
Chemical shift	Oxidation state
Peak-area ratios	Stoichiometry
Shake-up satellites	$\pi \rightarrow \pi^*$ Transitions

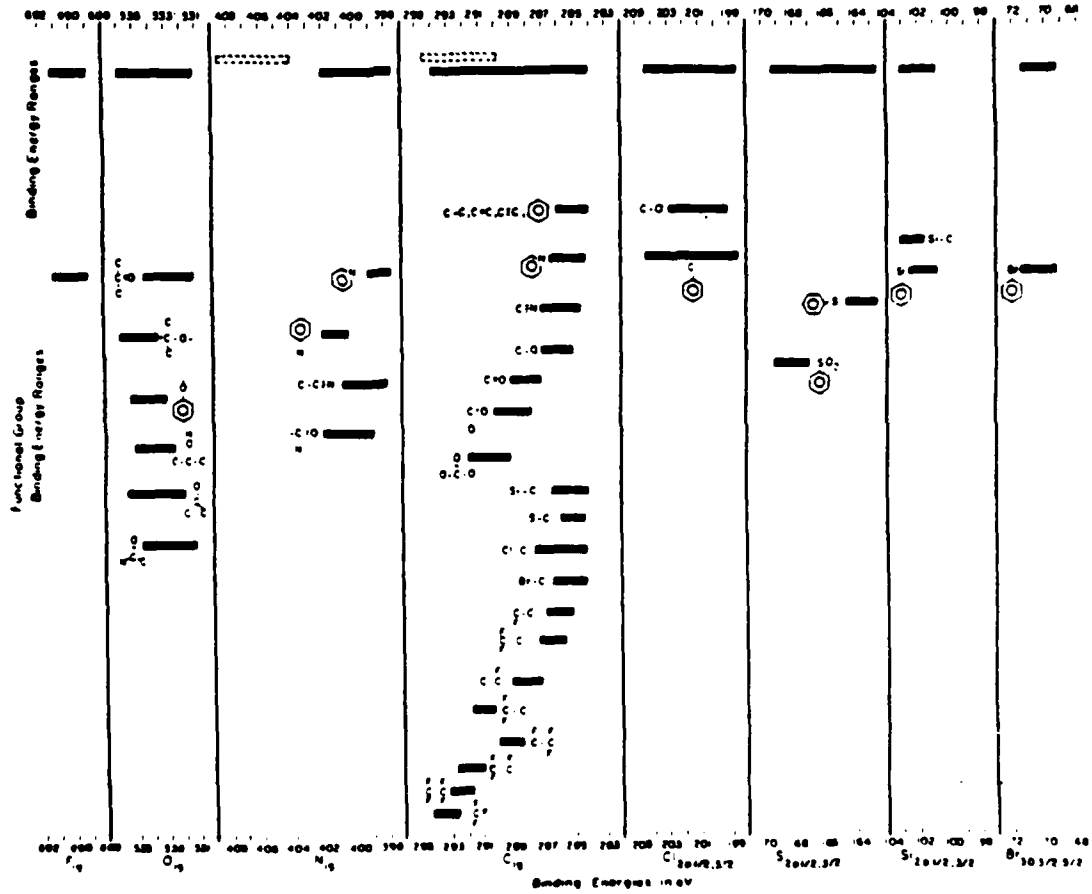

FIGURE(3.5) Summary of chemical shifts found in polymers. [from 103]

model[106] approximated from Koopmans' theorem[107]. Clark, Cromarty and Dilks[108] have used a semi-empirical LCAO MO SCF formalism to calculate the charge distributions in model organic systems containing oxygen and computed absolute binding energies which are in excellent agreement with experiment. Calculations on nitrogen-containing systems have given similar results[109].

The most pronounced chemical shift is observed in fluoropolymers due to the very high electronegativity of fluorine, e.g. C_{1s} from $-CF_2-CF_2-$ is at approximately 7 eV higher energy than C from a hydrocarbon[100]. Typically a multifunctional surface will give rise to a broadened spectrum called peak 'envelope' containing overlapping peaks. This envelope can be separated into its component peaks by deconvolution or curve resolution techniques. For instance, the C_{1s} peak from poly(ethylene terephthalate)(PET)[102] is shown in the Figure(3.6) to have composed of three main peaks, together with a *shake-up satellite* peak. The latter occurs due to the shake-up phenomenon accompanying the main photoionization whereby reorganization of the valence electron occurs in response to the effective increase in nuclear charge. Figure(3.7) depicts this process. In systems having unsaturation in either the backbone or pendant groups, such as the aromatic ring in PE, the shake-up satellites arising from $\pi \rightarrow \pi^*$ transitions are of considerable intensity. Thus the presence of a shake-up satellite can provide an additional level of information. In fact, it has become clear that for purely hydrocarbon polymers, it often provides the only level of information concerning the type of bonding[103].

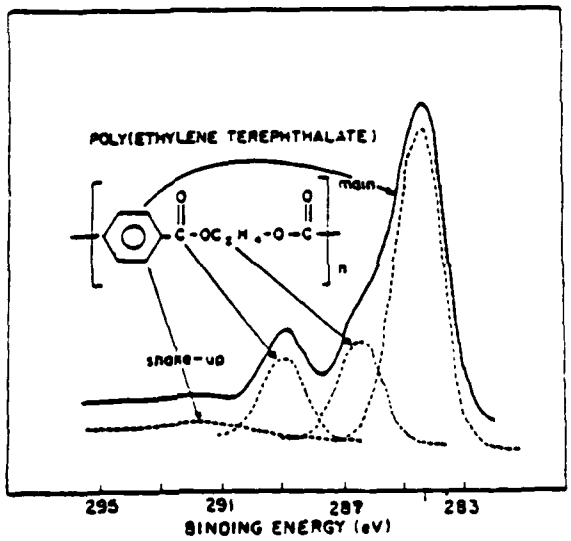

FIGURE(3.6) Carbon 1s spectrum from PET film. Experimental peak shape is shown by the solid line, dashed lines show the component peaks. [from 102]

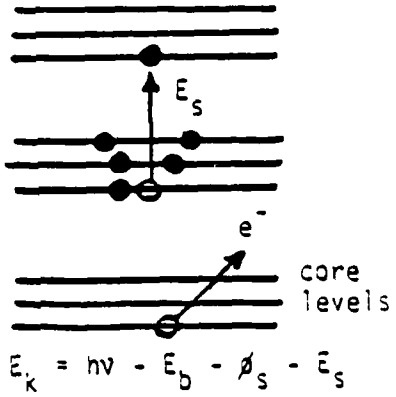

FIGURE(3.7) Shake-up phenomenon resulting into reduction in the kinetic energy of the photoelectron.

An alternate route to distinguish between surface functional groups whose peaks overlap has been used recently[110]. It involves 'derivatization' whereby an unique element, preferably with high photoelectron cross-section, is introduced via a reagent which derivatizes a specific functional group.

3.5.2 INFORMATION DEPTH.

Much of the earlier work on measurement of mean free paths in polymers has been of debate[111]. Results of Cadman, Gossedge, and Scott[112] suggested much larger MFPs in polymers as compared to typical metals, insulators, and semiconductors, i.e. 100 Å for C_{1s} at 970 eV. Evans[113] also maintained that MFPs in polymers were one order of magnitude higher than those in metals. On the other hand, work of Steinhardt, Hudis, and Perlman[114] by substrate-overlayer technique gave an estimate of 15 Å for 970 eV electrons, thus showing a similarity to other materials. With computer calculations from data pertaining to surface fluorination of polyethylene, Clark and co-workers[115] also proposed similar figures stressing that the maximum sampling depth(3λ) for organic materials does not exceed 100 Å. Siegbahn's own work[73] had also indirectly implied 100 Å as the sampling depth in organic compounds, though not in the context of MFP. Confirmation of this is also evident in a more recent investigation by Clark et al.[116] and by Roberts and co-wokers[117], both through the substrate-overlayer technique with poly(paraxylene) and poly(methyl methacrylate) respectively.

CHAPTER IV

EXPERIMENTAL

As it might be clear from the discussion so far, the combined surface and bulk phase separation behavior in block copolymers and their blends with homopolymers must depend on a number of factors. Some of these factors are: (a) chemical and physical nature of the blocks- in terms of surface free energy, solubility parameter, crystallizability etc.; (b) architecture and structural integrity of the blocks mainly in terms of either perfectly alternating(di, tri, or multiblock) or randomly coupled, or star blocks; (c) length of the blocks- individual or in relation to the other block; and (d) film preparation conditions- solvent cast(type of solvent) or compression-molded(time, temperature, pressure etc.). In case of blends the additional factors are amount of block copolymer added, the molecular weight of homopolymer, and the mixing techniques and fabrication methods, e.g. extrusion, injection molding, etc.

In this research,effect of some of these factors are addressed by studying a number of block copolymers-homopolymers systems.

4.1 MATERIALS.

The materials investigated can be divided into four different block copolymer-homopolymer systems. All block copolymers had polysiloxane as the lower surface energy component. Table(4.1) gives a list of these polymer systems by their generic names. Details regarding their structures and relevant characterization data have been given on Tables(4.2) through (4.5). Table(4.1) also shows the solvent used in each system for preparation of films.A pure poly(dimethyl siloxane) standard, designated as PDMS-STD, was used as a reference to compare photoelectron peaks from the polymers. All polymer samples were gratefully acquired from Prof. J. E. Mcgrath's polymer synthesis laboratory in the Department of Chemistry.

4.2 METHODS.

The general experimental strategy used here was to first use XPS to obtain the surface composition as compared to the overall or bulk composition. First the neat block copolymers were investigated. Their blends with the corresponding homopolymers were studied next with compositions varying from very small(<0.1%) to very high(>50%) content of the block copolymer. TEM was utilized to probe the bulk morphology at several selected compositions.

4.2.1 SAMPLE PREPARATION.

4.2.1.1 XPS. Most of the samples were prepared by casting them from their solutions in a solvent as listed in Table(4.1).

Table(4.1). Summary of the copolymer-homopolymer systems studied.

system	Block Copolymer	Homopolymer	Solvent
1	Polysulfone/Polysiloxane	Polysulfone	Chloroform
2	Polyester/Polysiloxane	Polyester	Chloroform
3	Polyurea/Polysiloxane	Polyurethane	Tetrahydrofuran
4	Polyimide/Polysiloxane	----	Dimethylacetamide +Tetrahydrofuran

Table(4.2). Polymer System 1.

BLOCK COPOLYMER:

POLY(BISPHENOL-A-SULFONE)/POLY(DIMETHYL SILOXANE)[a]

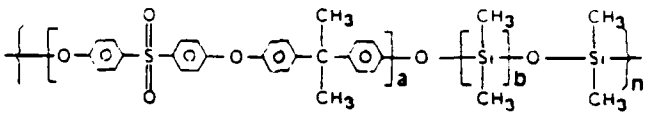

Sulfone Siloxane

HOMOPOLYMER:

POLY(BISPHENOL-A-SULFONE)

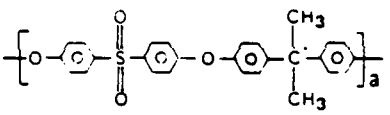

CHARACTERIZATION DATA:

Polymer Designation	Polysiloxane Block length Mn, g/mole	Polysulfone Block length Mn, g/mole	Weight Percentage Siloxane	CHCl [η], dl/g 25°C
PSFPSX-1	4400	4900	47.3	0.67
PSFPSX-2	4400	8600	34.0	0.67
PSFPSX-3	12800	4900	72.2	0.55
PSFPSX-4	12800	9700	56.9	1.27
PSF-1[b]	-----	----	0.0	----

[a]See also ref. 118, 119, 120

[b]commercial product UDEL® from Union Carbide Corporation

Table(4.3). Polymer System 2.

BLOCK COPOLYMER:

POLYARYLESTER/POLY(DIMETHYL SILOXANE)[a]

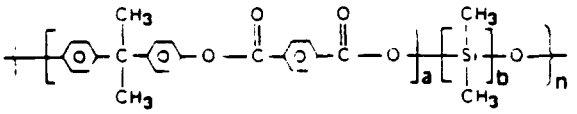

Ester Siloxane

HOMOPOLYMER:

POLYARYLESTER

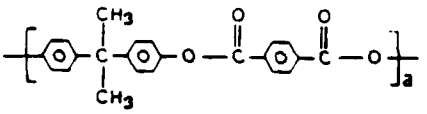

CHARACTERIZATION DATA:

Polymer Designation	Polysiloxane Block length M_n, g/mole	Polyester Block length M_n, g/mole	Weight Percentage Siloxane	CH Cl $[\eta]$, dl/g 25°C
PEPSX-1[b]	6700	5000	57.3	2.34
PEPSX-2[c]	4500	----	4.9	0.41
PEPSX-3[c]	2700	----	4.8	0.72
PE-1[d]	----	----	0.0	----

[a]See also ref. 118, 121

[b]perfectly alternating multi-blocks

[c]random block copolymers

[d]commercial product ARDEL® from Union Carbide Corporation

Table(4.3). Polymer System 3.

BLOCK COPOLYMER:

POLYUREA/POLY(DIMETHYL SILOXANE)[a]

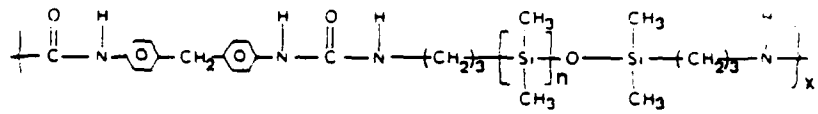

Urea Siloxane

HOMOPOLYMER:

POLYETHERURETHANE

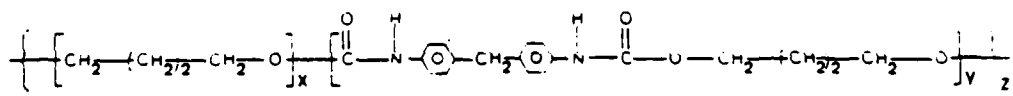

Ether Urethane

CHARACTERIZATION DATA:

Polymer Designation	Polysiloxane Block length M_n, g/mole	Polyurea Block length M_n, g/mole	Weight Percentage Siloxane	THF $[\eta]$, dl/g 25°C
PUPSX-1[b]	1140	250	82.0	0.24
PUPSX-2[b]	2420	250	90.6	0.83
PURTH-1[c]	----	---	0.0	----

[a]See also ref. 15, 46, 122

[b]alternating segmented copolymers

[c]commercial product ESTANE C-5® by B. F. Goodrich

Table(4.5). Polymer System 4.

BLOCK COPOLYMER:

POLYIMIDE/POLY(DIMETHYL SILOXANE)[a]

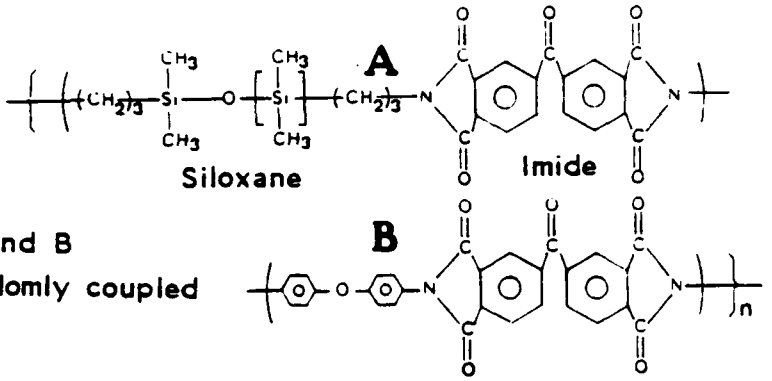

CHARACTERIZATION DATA:

Polymer Designation	Polysiloxane Block length M_n, g/mole	Weight Percentage Siloxane
PIPSX-1[b]	720	5.0
PIPSX-2	720	10.0
PIPSX-3	2130	10.0

[a]See also ref. 120, 123, 124

[b]*in situ* randomly coupled oxydianiline, benzophenone tetracarboxylic dianhydride thermally cured system

Typically about a gram of polymer containing the appropriate proportions of the block copolymer and the homopolymer were weighed into a glass vial and dissolved in about 20 ml of the solvent to yield clear transparent homogeneous solutions. Films of approximately 0.5 mm thickness were then cast on scrupulously cleaned stainless steel strips of dimensions 1"x1/4" suitable for direct attachment to the spectrometer probe. Atmospheric solvent evaporation of at least 2 hours was followed by vacuum drying. As far as possible, the samples were analysed right after that to ensure minimum possible atmospheric contamination, if any.

Some compression-molded samples of blends of PSFPSX-4 with PSF-1 were obtained from Dr. Dean Webster of the Department of Chemistry and the Materials Engineering and Science program. The samples were prepared by first dissolving the appropriate amounts of polymers in chloroform, then coagulating the mixture in excess methanol. The dried blend was then extruded at 300 °C. The extrudate obtained was subsequently compression-molded at 290-300 °C in a hydraulic press between two photographic plates without a mold release agent.

4.2.1.2 TEM. The same solutions prepared for XPS analysis were used to cast thin samples for TEM analysis. A drop of solution was spread onto a water surface using a disposable pipette. The thin film thus formed composed of different color regions, each color signifying different film thickness. The gold region- supposed to represent approximately 1000 Å thickness- was then lifted off onto TEM grids of 3 mm diameter. Special staining techniques to differentia-

various phases are unnecessary here because of the differences in adsorption and scattering of electrons of the siloxane blocks and the other blocks. Due to higher mean atomic number of siloxane, it always comes out darker than the other components such as the poly(arylene ether sulfone) or the aromatic polyester.

4.2.2 INSTRUMENTATION.

4.2.2.1 XPS. The x-ray photoelectron spectrometer used for surface analysis was a XSAM 800 model manufactured by KRATOS, Ltd., England. The instrument is a state-of-the-art in commercial spectrometers, equipped with a dual anode x-ray source and hemispherical electron energy analyser- two of its distinct features. A DEC RT-11 computer system with a software package interfaced to the spectrometer enables automatic acquisition of data and simultaneous manipulation of the same. Figure(4.1) shows the set up with relevant parts labeled.

The stainless steel strips on which the polymer films were cast were attached to the sample holder with the help of either screws or double stick adhesive tape. All spectra were collected using $Mg_{k\alpha 1,2}$ x-ray source, normally run at 15 kV and 20 ma. The pressure in the sample chamber maintained at approximately 10^{-9} mm of Hg during spectra collection. Narrow scans were obtained at the high resolution option and analyzer slit width of 2 mm to ensure detection of fine features. The analyzer was operated in the Fixed Retarding Ratio(FRR) mode.

Angle-dependent depth profiling(whose principles have been presented at length in the previous chapter) was done on all samples.

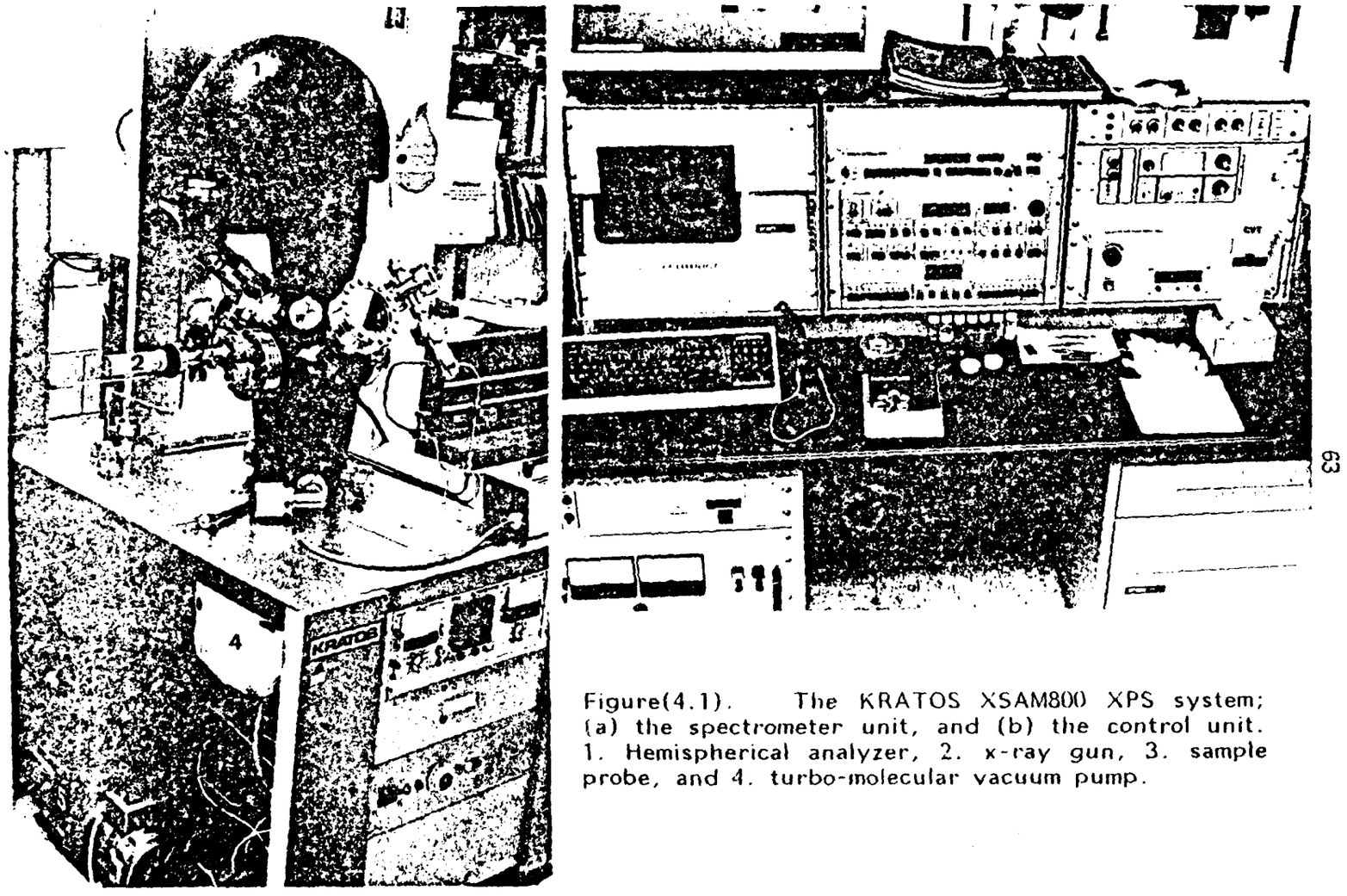

Figure(4.1). The KRATOS XSAM800 XPS system; (a) the spectrometer unit, and (b) the control unit. 1. Hemispherical analyzer, 2. x-ray gun, 3. sample probe, and 4. turbo-molecular vacuum pump.

The variation in electron take-off angle θ between the analyser and the sample surface could be simply brought about by rotating the circular probe rod to a required degree. Angles ranging from 90° to 10° were used in most cases.

4.2.2.2 TEM. A JEOL Model-100C electron microscope was at 80 kV was used for the purpose.

4.3 QUANTITATION OF THE XPS DATA.

In this section the general procedure employed for converting the XPS signal intensities into useful numbers, such as weight percentage of different components involved will be described briefly. Since all systems investigated here have siloxane as the lower surface free energy component, the main concern here is to obtain the amount of siloxane present at the surface as seen by XPS.

Equation(3.7) was used to first calculate the atomic fraction ratio of carbon to silicon, C/Si. The levels chosen for the calculation were C_{1s} and Si_{2s}. Although Si_{2s} signal is of lower intensity than Si_{2p} signal, the former was used because of two reasons. Comparison of two s level electrons eliminates the use of asymmetry parameter and the angle φ between the x-rays and the analyser, allowing one to use the total cross sections instead of the differential cross-sections in the Equation(3.7). In addition to this, since the mean free paths of the two electron levels are very close, the angle θ can be directly related to the depth of analysis. Transmission function T(E) was simply E- the energy of the electron since the mode of operation wa. FRR.

Table(4.6). XPS parameters for the calculation of atomic fractions of Carbon and Silicon from their peak intensities.

Parameter	CARBON 1s level	SILICON 1s level
Electron kinetic energy, eV	970	1105
Photoelectron cross-section,[9,1] kilobarns	22.2	19.0
Mean free path,[8,6] angstroms	18.2	20.0

Table(4.7). Sampling depth, z, for an average electron mean free path of 19.1 Å as a function of the electron exit angle, θ.

θ, degrees	z, angstroms
90	57.3
60	49.6
45	40.5
30	28.7
20	19.6
10	10.0

Table(4.6) shows the various values required by the Equation(3.7) for the C_{1s} and Si_{2s} levels.

Conversion of the calculated C/Si ratio to weight %siloxane was then done with the help of stoichiometric relations between the two components involved as outlined in the Appendix(A). For the blends of polyurea/polysiloxane with polyurethane and polyimide copolymers, this calculations could not be carried out due to complications(such as the random coupling) in their structure. In any case, the C/Si value gives a qualitative idea regarding the percentage siloxane when compared to 2.0- the value for pure poly(dimethyl siloxane).

The sampling depth z, as a function of θ can be calculated by using the Equation(3.13). Using the average of mean free paths of C_{1s} and Si_{2s} electrons, an approximate relation between z and θ is presented in the Table(4.7).

CHAPTER V

RESULTS AND DISCUSSION

This chapter is divided into two sections, one devoted to the neat block copolymers and the other to the blends of the same with homopolymers. Although the major portion of this work depends on the quantitative XPS, an attempt is made in some instances to also present a qualitative picture of the surfaces of the polymers by way of spectral features of various atomic levels involved.

5.1 NEAT BLOCK COPOLYMERS.

Figure(5.1) shows the C_{1s} and the O_{1s} XPS spectra collected at normal angle from the polysulfone/polysiloxane block copolymers as compared to those from pure polysulfone PSF-1 and pure poly(dimethyl siloxane) PDMS-STD. Boxes in the figure depict the components of the C_{1s} peak and the O_{1s} peak of PSF-1 and origins of the same labeled on the structure. It can be clearly seen that the spectra from the block copolymers resemble closely those from PDMS-STD which are composed of single symmetric peaks at 285.0 eV for C_{1s} and 532.4 eV for O_{1s}. The absence of (or very small) shake up satellite at 292.0 eV on C_{1s} peaks speaks of the dominance of siloxane at the surface.

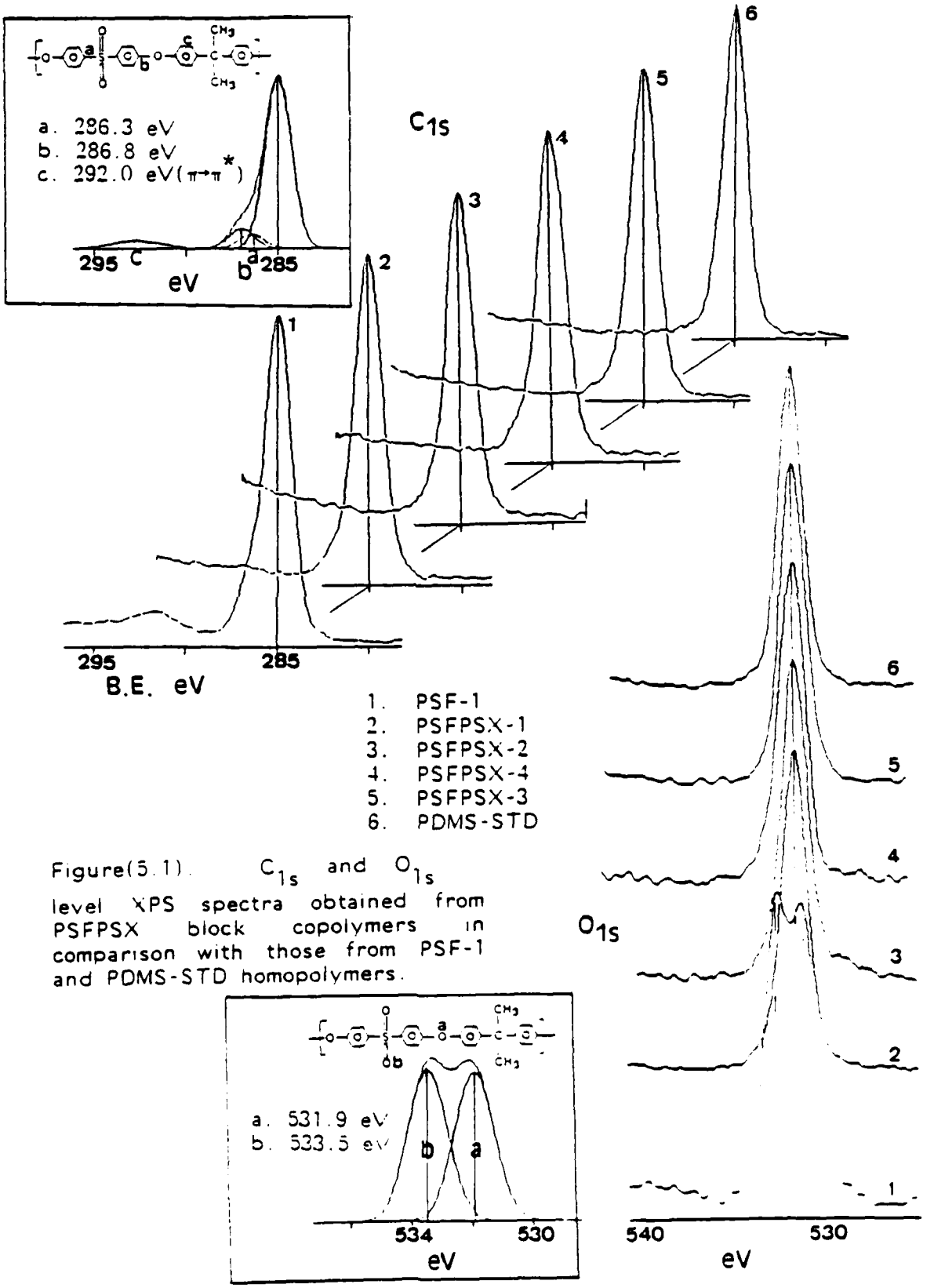

Figure(5.1). C_{1s} and O_{1s} level XPS spectra obtained from PSFPSX block copolymers in comparison with those from PSF-1 and PDMS-STD homopolymers.

at the surface. In case of O_{1s} peaks, the ones from the block copolymers occur at 532.4 eV- same as that from PDMS-STD. The percentage of oxygen in homopolysulfone itself being very small, the shifts at 531.9 eV and 533.5 eV occuring due to S=O=S and C-O bonds respectively are not detected to considerable levels in the O_{1s} peaks from the block copolymers. Figure(5.2) illustrates the angle-dependent C_{1s} and O_{1s} spectra from PSFPSX-1. Once again the O_{1s} peaks can be seen to be very similar to that from PDMS-STD, regardless of the electron exit angle. Slight variation can be observed in the C_{1s} peak as the angle is changed. At $\theta=90°$, a small shake-up satellite and asymmetry on the left side of the main peak signifies some mixing of polysulfone. At $\theta=10°$, both these effects vanish completely showing a slight concentration variation as one goes from the subsurface to the surface. This qualitative judgement of a high surface segregation of poly(dimethyl siloxane) is further strengthened by quantitation of the XPS data by the procedure outlined in the previous chapter.

Figure(5.3) depicts the weight% siloxane as seen by XPS vs. $\sin\theta$(which represents the sampling depth as given in the Equation(3.13)) behavior of the four polysulfone/polysiloxane copolymers. Two important deductions can be made from this figure. Considering the individual polymers, the weight% siloxane at the surface does not vary too much as the electron exit angle is changed. This implies a relatively homogeneous sublayer at the surface. Comparison of the four curves provides information on the effect of block lengths and/or overall composition of the copolymers. For example, PSFPSX-1, which has the same sulfone block length as in PSFPSX-3(4900 g/mole)

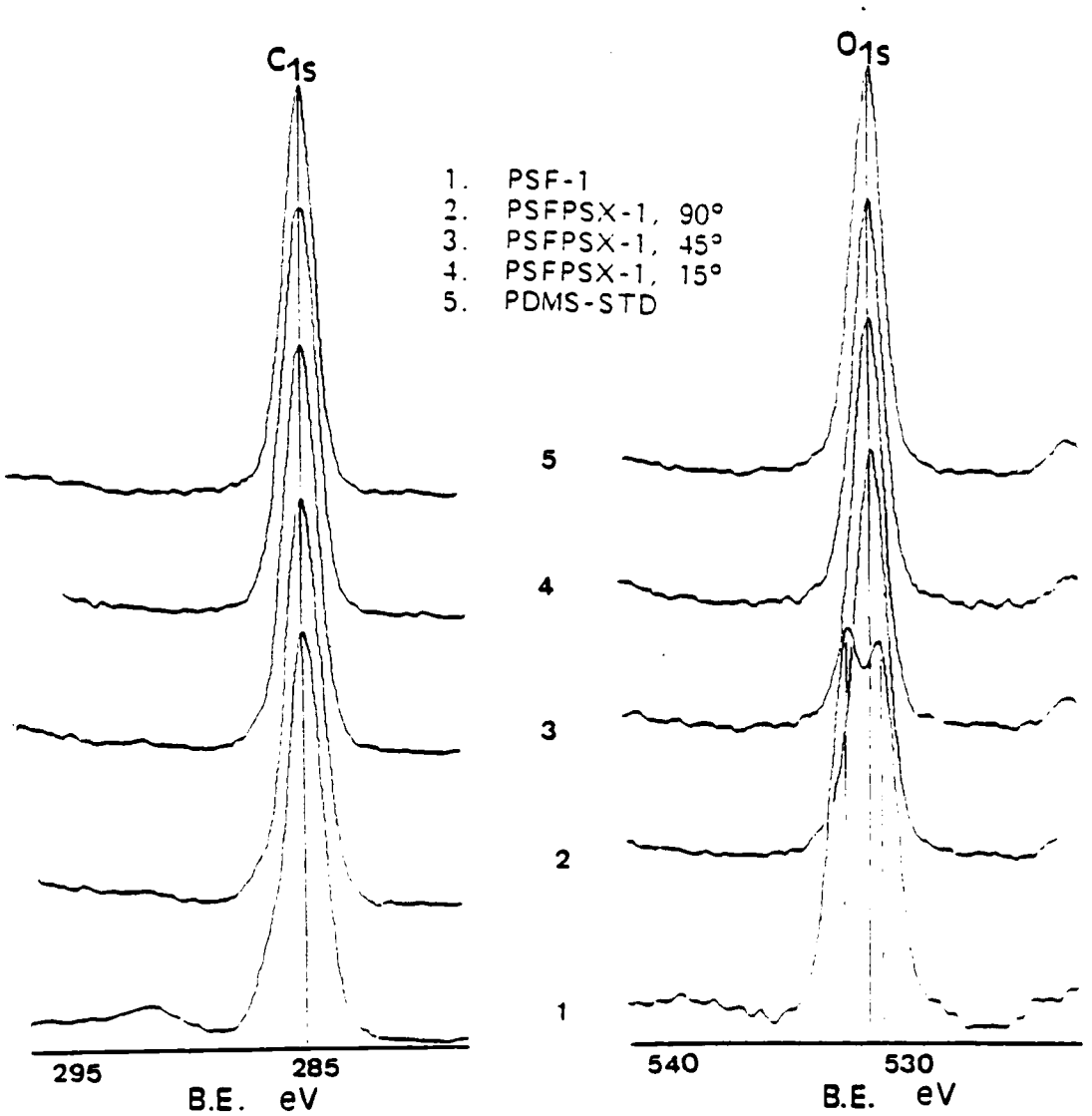

Figure(5.2). Spectral angular-dependent behavior of PSFPSX-1.

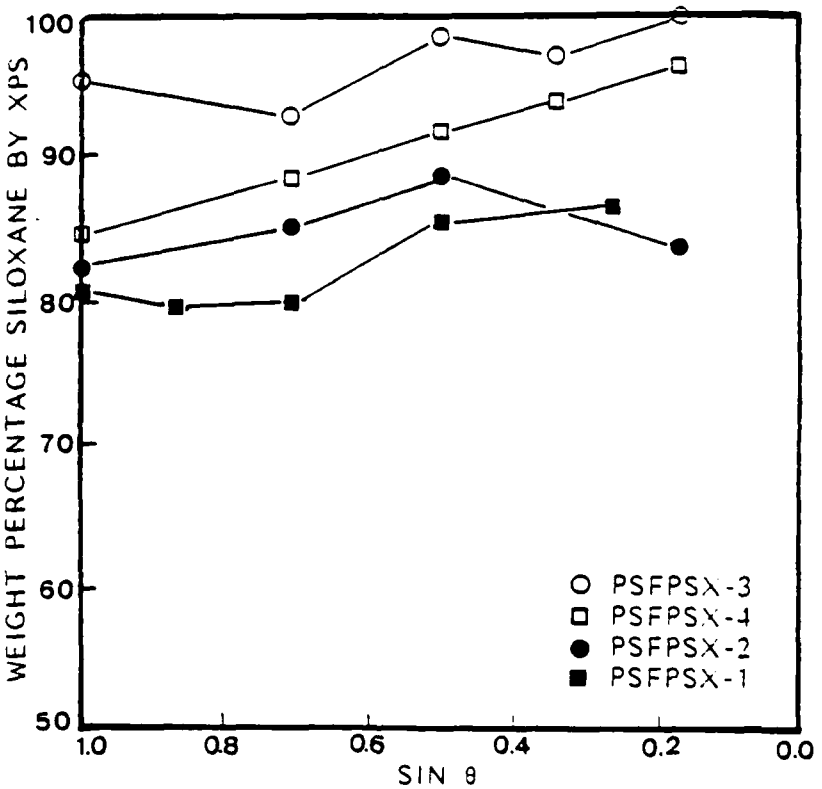

Figure(5.3). Quantitative angular-dependent behavior of PSFPSX block copolymers.

but a smaller siloxane block length(4400 g/mole vs. 12800 g/mole) or overall siloxane content(47% vs. 72%), shows a lesser extent of surface segregation. In fact, in case of PSFPSX-3, the surface seems to be made of close to 100% siloxane throughout the depth of analysis. On the other hand, PSFPSX-4 has the same siloxane block length as PSFPSX-3 and a longer sulfone block. This is reflected in the lower position of the curve for the former. The overall compositions of PSFPSX-4 and PSFPSX-1 are relatively close(47% vs. 56%), the former having longer siloxane blocks. Comparison of the curves for these two polymers confirms the importance of the block length of the lower surface energy component in order to achieve a purer phase at the surface. The surface behavior of PSFPSX-2 seems to be out of place. Considering that its overall siloxane content is only 34%, it still shows higher siloxane at the surface than that in PSFPSX-1. The reason of this *mis*behavior may be attributed to presence of unreacted siloxane oligomers which is not an uncommon occurance in siloxane containing polymers.

Figure(5.4) through (5.7) show the TEM photomicrographs of PSFPSX-1, 2, 3 and 4 respectively. Figures(5.4) and (5.5) clearly indicate that while PSFPSX-1 has a well phase-separated bulk, PSFPSX-2 has a sort of patchy structure reflecting impurity of the copolymer. Microphase separations are evident also in PSFPSX-3 and PSFPSX-4. All polymers have spherical microdomain structure. In PSFPSX-1, siloxane seems to be the spherical phase, with sulfone making the matrix. The situation is reversed in PSFPSX-3 and PSFPSX-4. Also it can be noted that the size of the domains are

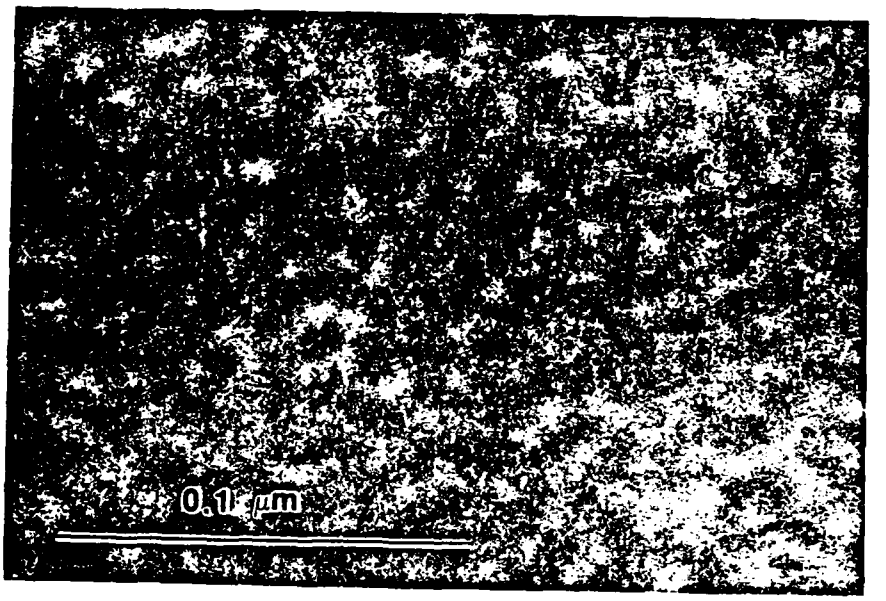

Figure(5.4). TEM photomicrograph of PSFPSX-1.

Figure(5.5). TEM photomicrograph of PSFPSX-2.

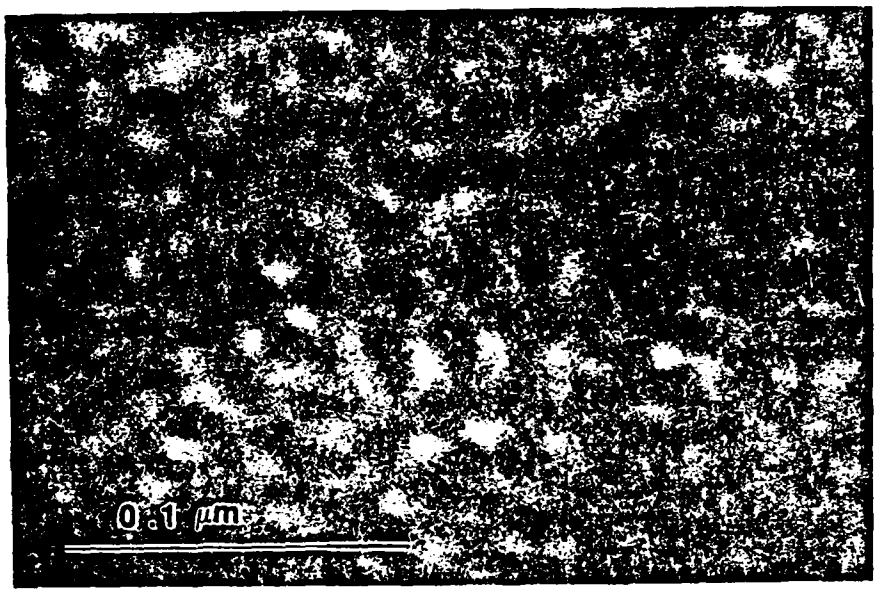

Figure(5.6). TEM photomicrograph of PSFPSX-3.

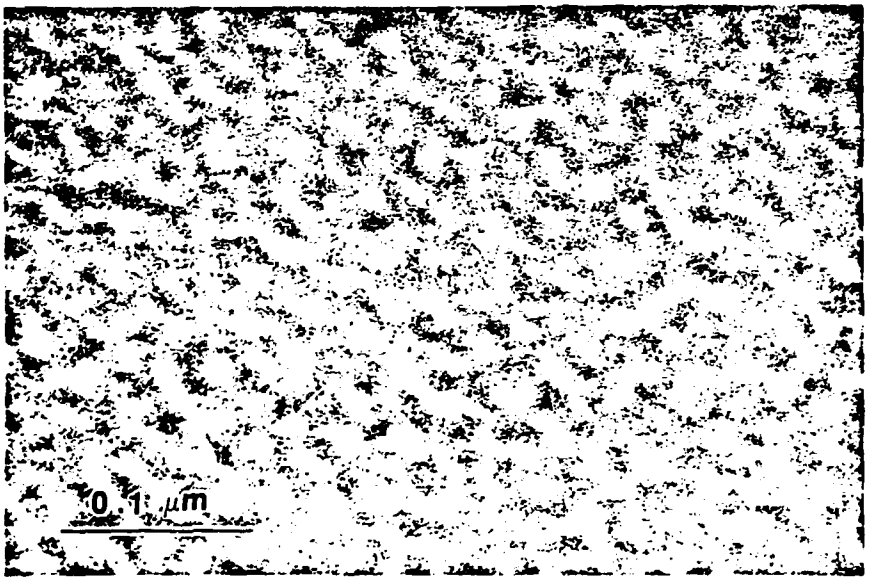

Figure(5.7). TEM photomicrograph of PSFPSX-4.

smaller in PSFPSX-1 compared to those in the other two. This can be explained well by the fact that the former has smaller block lengths. Without going into any further details regarding the bulk of the polymer, it suffices to point out that the XPS and TEM, both combined, project different phase separation behavior at the surface and at the bulk respectively. The surface seems to be composed of an overlayer of predominantly siloxane of at least about 60 Å, which is the sampling depth at normal exit angle. The effect of molecular weight can be seen as the degree of mixing in this siloxane rich phase. The longer the siloxane blocks, the weaker will be the long-range interactions from the sulfone blocks- attached on both sides in case of a perfectly alternating block copolymers. This results in a less hindrance to the siloxane chains to align themselves at the surface in a fashion most suitable to minimize the surface free energy. The XPS data suggests that the alignment of the siloxane segments at the surface in these polymers may be that of a closely packed chains perpendicular to the interface.

The results of XPS analysis on the polyester/polysiloxane polymers have been summarized on the Figures(5.8) to (5.10). Figure(5.8) qualitatively compares the nature of the surfaces of PEPSX-1(perfectly alternating) and PEPSX-2,3(random) block copolymers to the surfaces of the homopolyester PE-1 and PDMS-STD via their C_{1s} level peaks. The box shows the C_{1s} peak of PE-1 decomposed into its component peaks- at 291.8 eV due to the $\pi \rightarrow \pi^*$ shake-up, 289.3 eV from $-\underset{\underset{O}{\|}}{C}-O$ species, 286.5 eV due to $-\underset{|}{C}-O$ species and 285.0 eV from the remaining hydrocarbons. Again here the smaller peaks due to the shake-up and $\underset{\underset{O}{\|}}{C}-O$, and more symmetric main peak at 285.0 eV in each of the

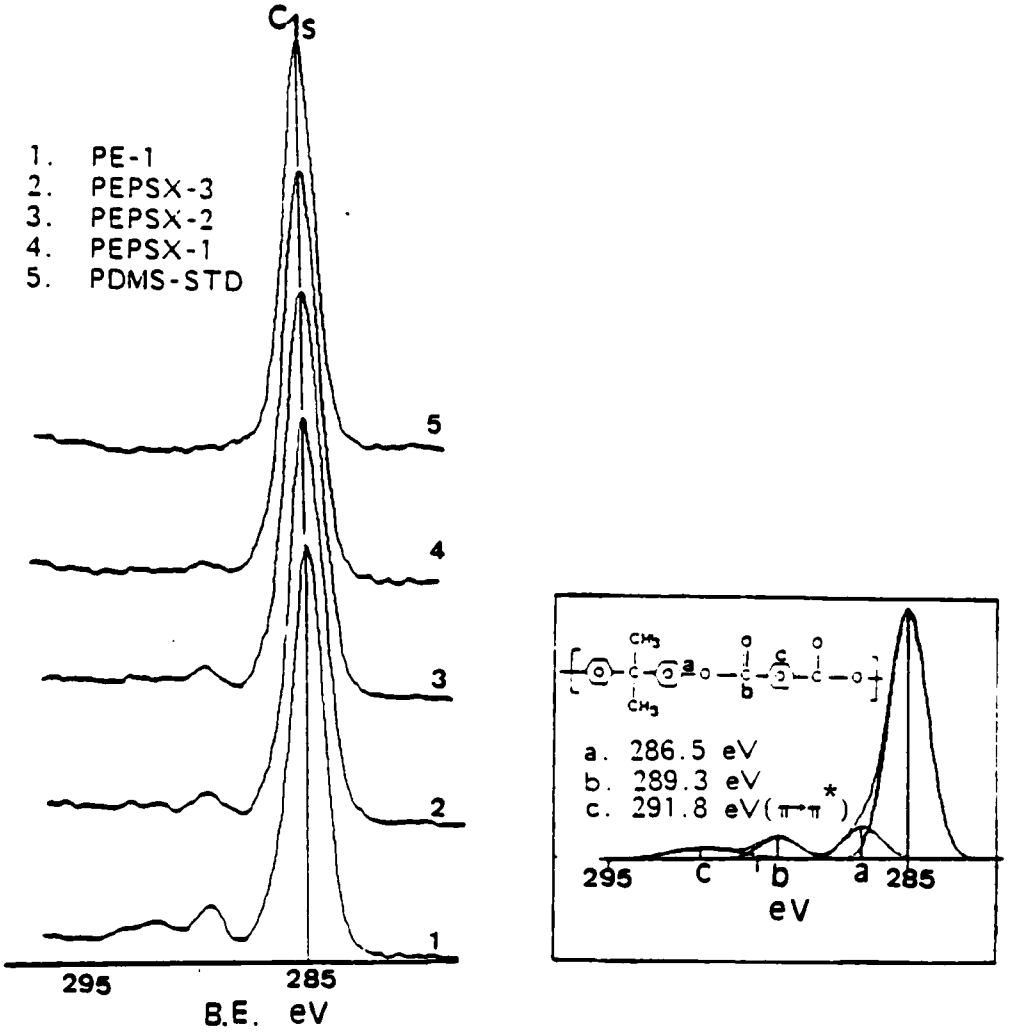

Figure(5.8) C_{1s} level XPS spectra from various PEPSX block copolymers in comparison to those from PE-1 and PDMS-STD homopolymers.

copolymers suggest the surface segregation of siloxane. Figure(5.9) depicts the angular dependence of the O_{1s} peak from PEPSX-2. As shown in the accompanying box, the O_{1s} peak of PE-1 is made up of two equal size component peaks- one at 532.2eV due to C-O-C and the other at 533.9 due to $\overset{O}{\overset{\|}{C}}$. At θ=90°, the double peak shape is lost readily with dominance of the Si-O-Si peak at 532.4 eV. A shoulder to the left still indicates the presence of some ester. The shoulder vanishes as θ is decreased. Quantitative results are presented on the Figure(5.10) in the form of weight% siloxane at the surface vs. Sinθ. Unfortunately, a direct comparison of the perfectly alternating and the random block copolymers is not possible because of the vast difference in their siloxane contents(57% in the former and 5% in the latter two). Behavior of PEPSX-1 is very similar to that observed in case of PSFPSX series, indicating again an overlayer type of surface morphology although with some degree of mixing. The behavior of PEPSX-2 and 3 random block copolymers is interesting. It appears that the fact that the two polymers had different block lengths of siloxane oligomers to start with does not affect the surface segregation as long as the overall composition is the same. The large variation in the surface composition(from 60% to 90%) as the angle of analysis changes from 90° to 10° signifies that the surface is not made of an overlayer of siloxane. The bulk of PEPSX-1 is found to be microphase-separated with spherical domains of ester(light areas) and siloxane matrix(dark areas) shown in the photomicrograph reproduced in the Figure(5.11). Once again, the surface morphology differs from the bulk morphology.

The two polymers investigated in the system of

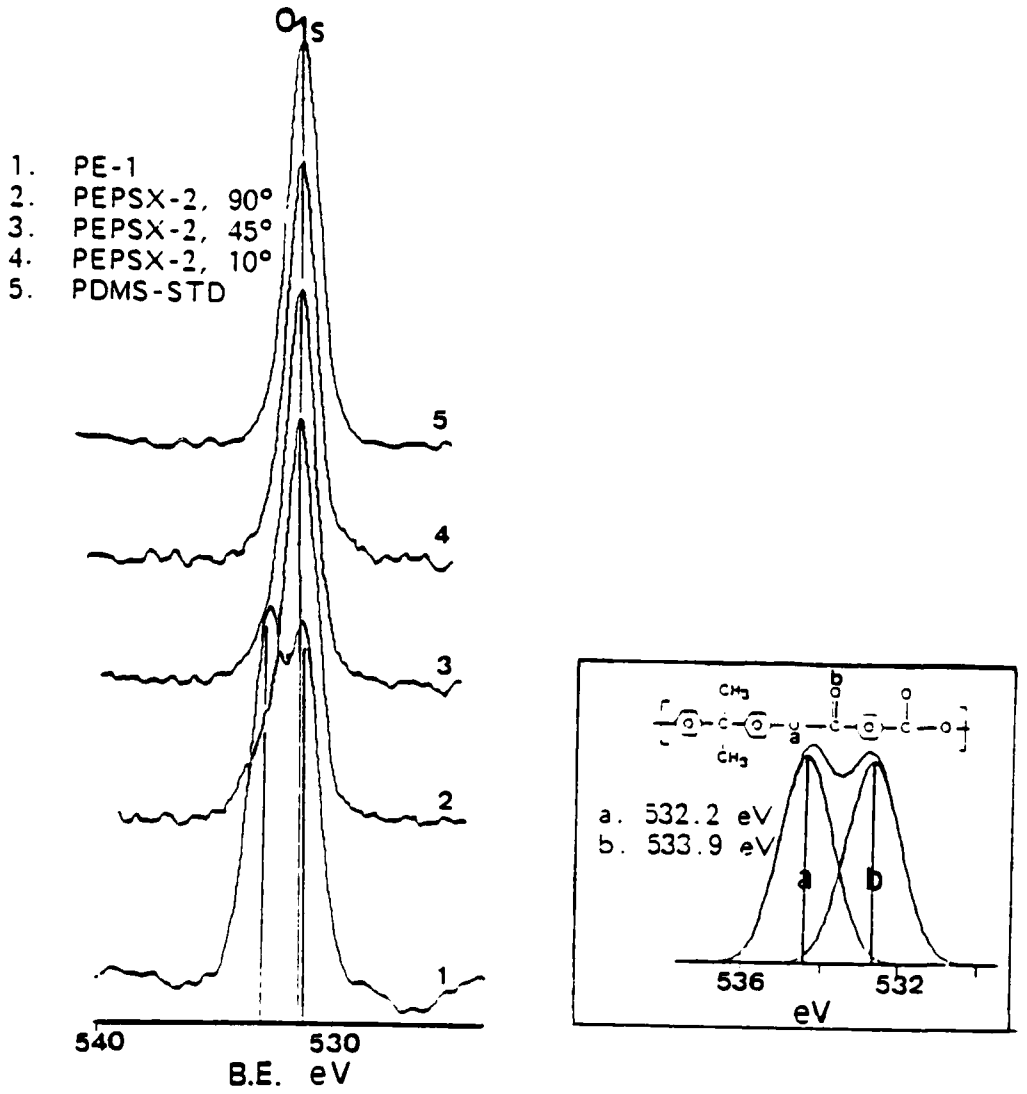

Figure(5.9) Spectral angular-dependent behavior of PEPSX-1.

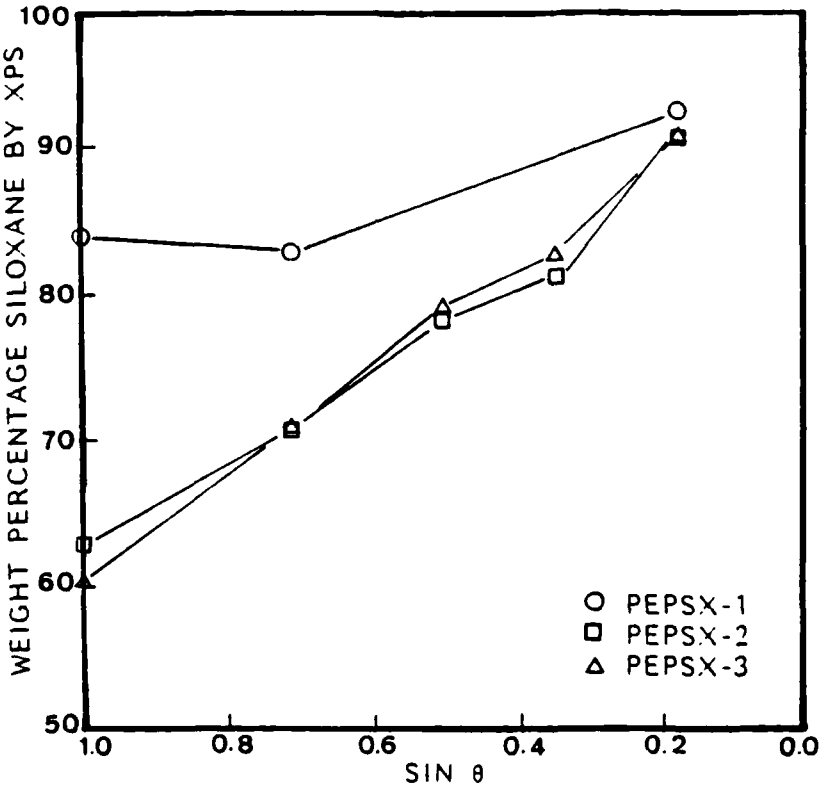

Figure(5.10). Quantitative angular-dependent behavior of PEPSX block copolymers.

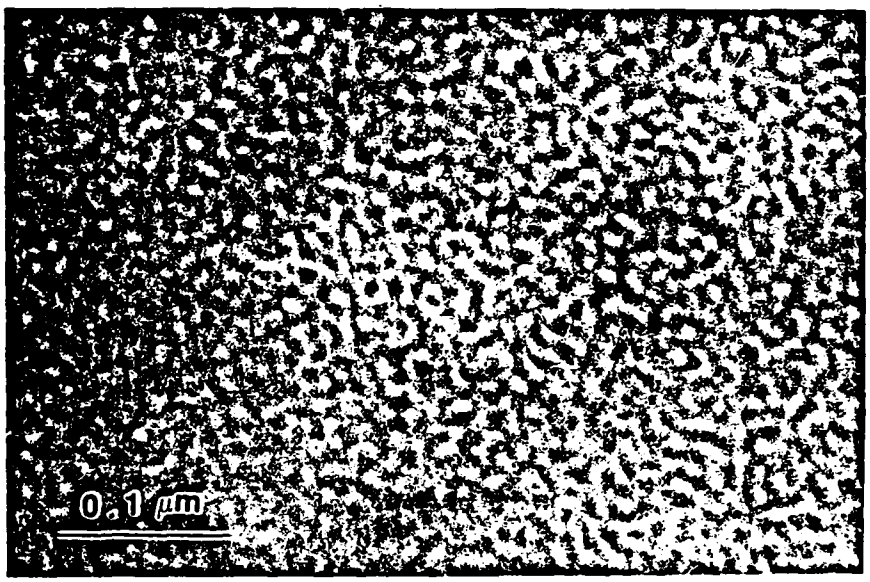

Figure(5.11). TEM photomicrograph of PEPSX-1.

polyurea/polysiloxane polymers, PUPSX-1 and PUPSX-2, have different siloxane block lengths, 1140 and 2420 g/mole respectively. The urea block remaining the same, this results into a difference in their overall composition- i.e. PUPSX-1 has 82.0% w/w and PUPSX-2 has 90% w/w siloxane. This composition difference reflects in their surface properties. Figure(5.12) shows the C_{1s} spectra from the two polymers as compared to that from PDMS-STD. It also shows that polyurea C_{1s} peak should have two characteristic chemical shifts away from the normal hydrocarbon peak at 285.0 eV. One would occur at 285.6 eV due to the C-N bond and the other at 289.0 eV due to N-$\underset{\underset{O}{\|}}{C}$-N. PUPSX-2 shows none of these chemical shifts at any electron exit angles. In PUPSX-1, a small peak at 289.0 is visible and also a slight asymmetry of the main peak indicates the presence of C-N species, although in very small amounts. Both these effects tend to vanish as the angle θ is decreased. Quantitative results are plotted on the Figure(5.13). Understandably, PUPSX-2 has a higher surface siloxane. Both have fairly uniform surface layers indicated by the very small change in the siloxane as seen by XPS with angular variation.

Here it might be pointed out that the surface segregation, if measured by the difference between the bulk and the surface compositions, in both the above polymers does not seem to be very pronounced. Comparison can be made with PSFPSX-3 block copolymer which has about 72% w/w siloxane in the bulk but shows a near pure siloxane at the interface. The difference lies in the length of the siloxane block which is very small in the polyurea/polysiloxane copolymers.

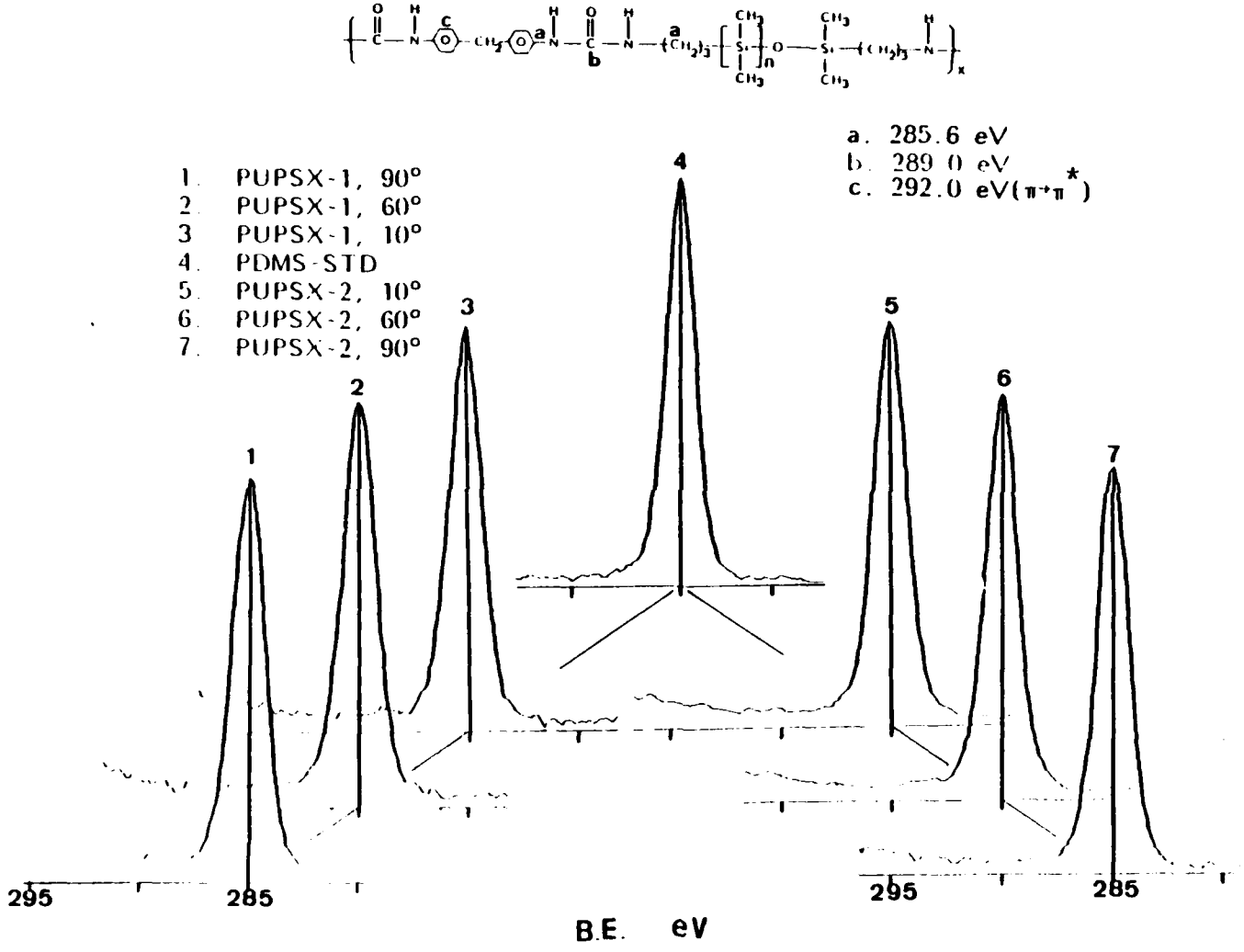

Figure(5.12) C_{1s} level XPS spectra from PUPSX-1 and PUPSX-2 block copolymers in comparison to that from PDMS-STD homopolymer.

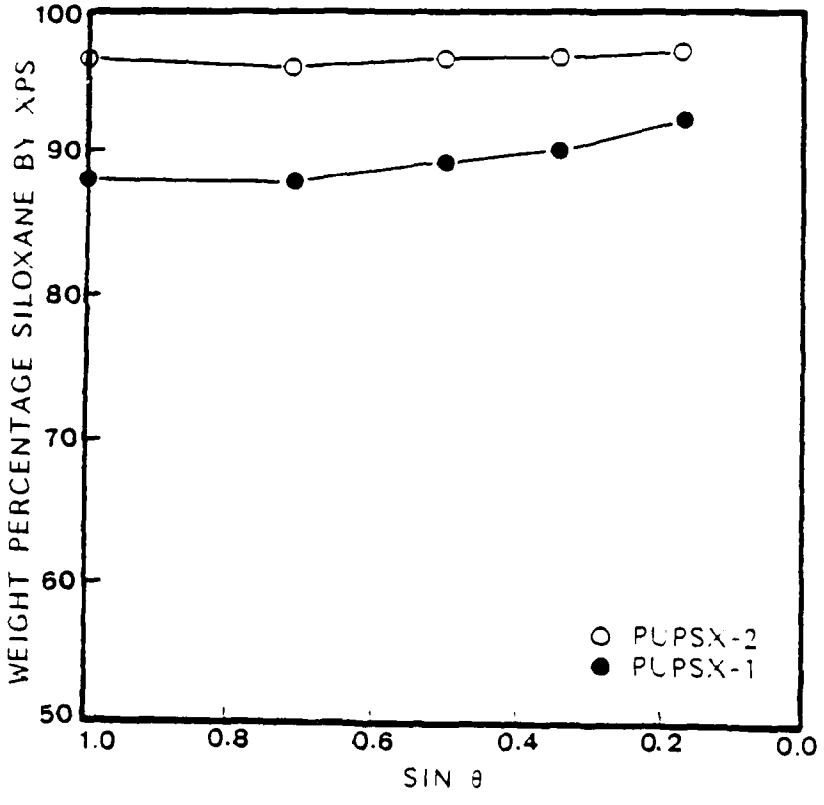

Figure(5.13). Quantitative angular-dependent behavior of PUPSX block copolymers.

AD-A140 020 SURFACE AND BULK PHASE SEPARATIONS IN BLOCK COPOLYMERS AND THEIR BLENDS(U) VIRGINIA POLYTECHNIC INST AND STATE UNIV BLACKSBURG N M PATEL ET AL. MAR 84 VPI-E-84-7 2/2

UNCLASSIFIED N00014-82-K-0185 F/G 11/9 NL

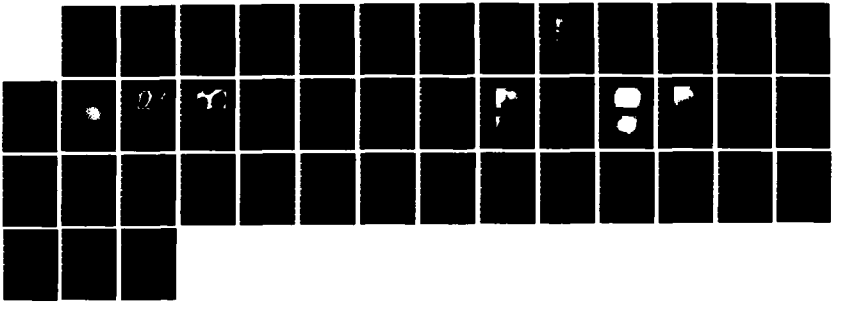

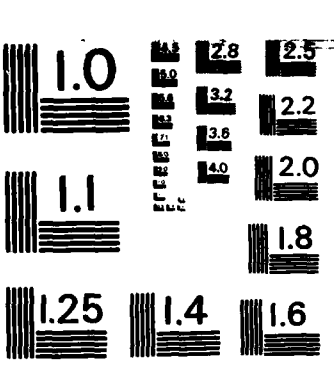

MICROCOPY RESOLUTION TEST CHART
NATIONAL BUREAU OF STANDARDS-1963-A

In case of polyimide/polysiloxane block copolymers the XPS signal intensities of C_{1s} and Si_{2s} peaks were converted to C/Si atomic ratios. For pure poly(dimethyl siloxane) this ratio would be 2.0. Hence closeness of the actual value to 2.0 would indicate the extent of siloxane at the surface. Figure(5.14) shows this ratio as a function of the electron take off angle, θ. Comparing the curves for PIPSX-1 and PIPSX-2, which have same siloxane block lengths, it can be noticed that the concentration gradient is lower for PIPSX-2- having a higher bulk siloxane. On the other hand, PIPSX-2 and PIPSX-3 have the same bulk siloxane at 10% w/w, but the latter has longer siloxane blocks. This is reflected in a more flat curve for PIPSX-3. As the same time, it might be noted that the absolute values C/Si ratio at each angle are in increasing order as one goes from PIPSX-1 to PIPSX-3.

On comparing the results from each system, the importance of sufficient block length of siloxane emerges. This is consistent with the findings of Riffle[45] on polycarbonate/polysiloxane copolymers and other previous works[23,27]. Also all polymers seem to have a surface morphology of an overlayer of siloxane as compared to a spherical microdomain structure in the bulk demonstrated by the micrographs on some samples. Gaines[13] has put forward a rationale for such observations. He suggested that the thermodynamic criterion of liquid spreading[125] should apply in block copolymer systems to explain their surface morphologies. For a liquid b to spread over the surface of liquid a, one must have a positive spreading coefficient. The spreading coefficient

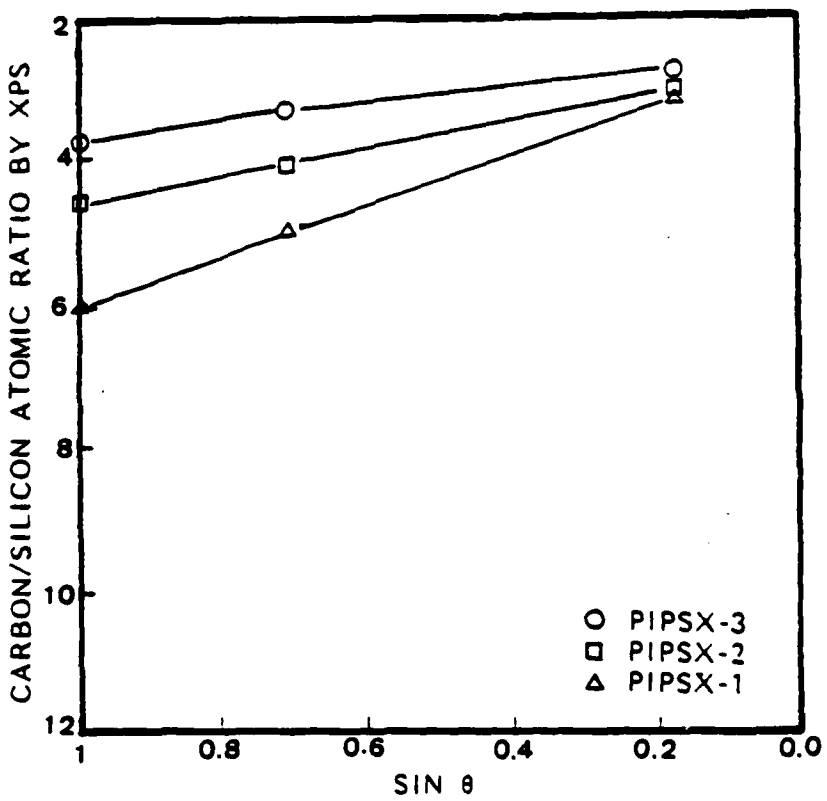

Figure(5.14). Quantitative angular-dependent behavior of PIPSX block copolymers.

is defined as:

$$S_{b/a} = \gamma_a - (\gamma_b + \gamma_{ab}) \qquad .....(5.1)$$

where γ_a and γ_b are the surface tensions of liquids a and b and γ_{ab} is the interfacial tension between the liquids. For $S_{b/a}$(or $S_{a/b}$) to be positive, $|\gamma_a - \gamma_b|$ must be greater than or equal to γ_{ab}. If this condition is fulfilled at the block copolymer surface during its film formation, such as during solvent casting, an overlayer type of surface morphology may be obtained. Otherwise an isolated domain type morphology from the bulk would be retained at the surface.

The surface tension of poly(dimethyl siloxane) is at least 10 dyn/cm lower than most other polymers, and the interfacial tensions between polymers rarely exceed this value[126,127]. Thus, Gaines pointed out that siloxane would almost always form an overlayer in a block copolymer where it is one of the components. Using compiled values from the literature[126], γ for polystyrene at 150 °C is 30.8 dyn/cm, that for poly(dimethyl siloxane) is 13.6 dyn/cm, and γ_{ab} for the polymers is 5.1 dyn/cm. This leads to a $S_{PDMS/PS}$ of +12.1 dyn/cm. Hence poly(dimethyl siloxane) can be expected to have an overlayer which is what has been observed by Clark et al.[39]. The criteria also seems to apply to other cases such as poly(ethylene oxide)/poly(propylene oxide)- for overlayer type of morphology[27], and poly(ethylene oxide)/poly(styrene)- for a isolated domain type of morphology[41]. These arguments appear to fit well in the siloxane-containing systems studied here, although the surface tension data for

the other components used are not available in the literature.

After this simplistic approach, the complexities may be introduced from a number of variables in the system. Type of solvent, temperature, molecular weights etc. govern the surface tension of polymers. In the higher range(greater than 3000), the molecular weight dependence of surface tension is found to be negligible[116]. Hence for a given system of block copolymer, it might be said that the type of surface that can be obtained is fixed. The effect of molecular weight then, as far as the overlayer-type surface is concerned, can be seen to come about in two ways based on the above observations. The first is the thickness of the overlayer which will be smaller for copolymers having shorter blocks. Secondly, as has been mentioned before, there will be a difference in the extent of phase mixing depending on the block length the overlayer component. The latter effect would be dependent on the architecture of the copolymer also. It might be expected that the diblock copolymer would have less phase mixing than a triblock(with the lower energy block in the middle) or a multiblock due to the fact that the chains are constrained at both ends in the latter two.

Before making any further quantitative judgements, more research needs to be done on block copolymers of variety of combinations. Also more confident values of surface and interfacial tension are required than those available in the current literature.

5.2 BLENDS OF BLOCK COPOLYMERS WITH HOMOPOLYMERS.

Three blend systems- PSFPSX copolymers with PSF-1, PEPSX-1 with PE-1, and PUPSX-1 with PURTH-1 were studied in detail. Results are presented here by taking each block copolymer-homopolymer pair individually and making comparisons on the way. The quantitative results are given in the form of weight% siloxane as detected by XPS representing the top few angstroms at the surface plotted against the weight %siloxane in the bulk. The latter is calculated simply from the knowledge of the siloxane content in the block copolymer and the block copolymer content in the blend.

Figure(5.15) shows the results of XPS analysis on blends of PSFPSX-1 with PSF-1. Spectra were collected at three electron exit angles viz: 90°, 45°, and 15°. The distance between the three curves obtained from each angle signifies the extent to which concentration changes occur in the top 60 A or so. In going from below 0.1% to above 10% siloxane in the bulk, the three curves come closer to each other implying that the surface region is becoming more homogeneous in terms of composition. Taking each curve individually, it can be noted that there is no sharp break at any *critical* concentration as observed by Riffle[45] and Sha'aban[46]. Nonetheless, there are three distinct phases, or regions, which may represent different physical phenomena occuring in the system. The first region is the lower plateau at concentrations below about 0.05% bulk siloxane where the surface composition seems to be independent of the bulk value, although there is still a considerable extent of surface segregation (compare 55%

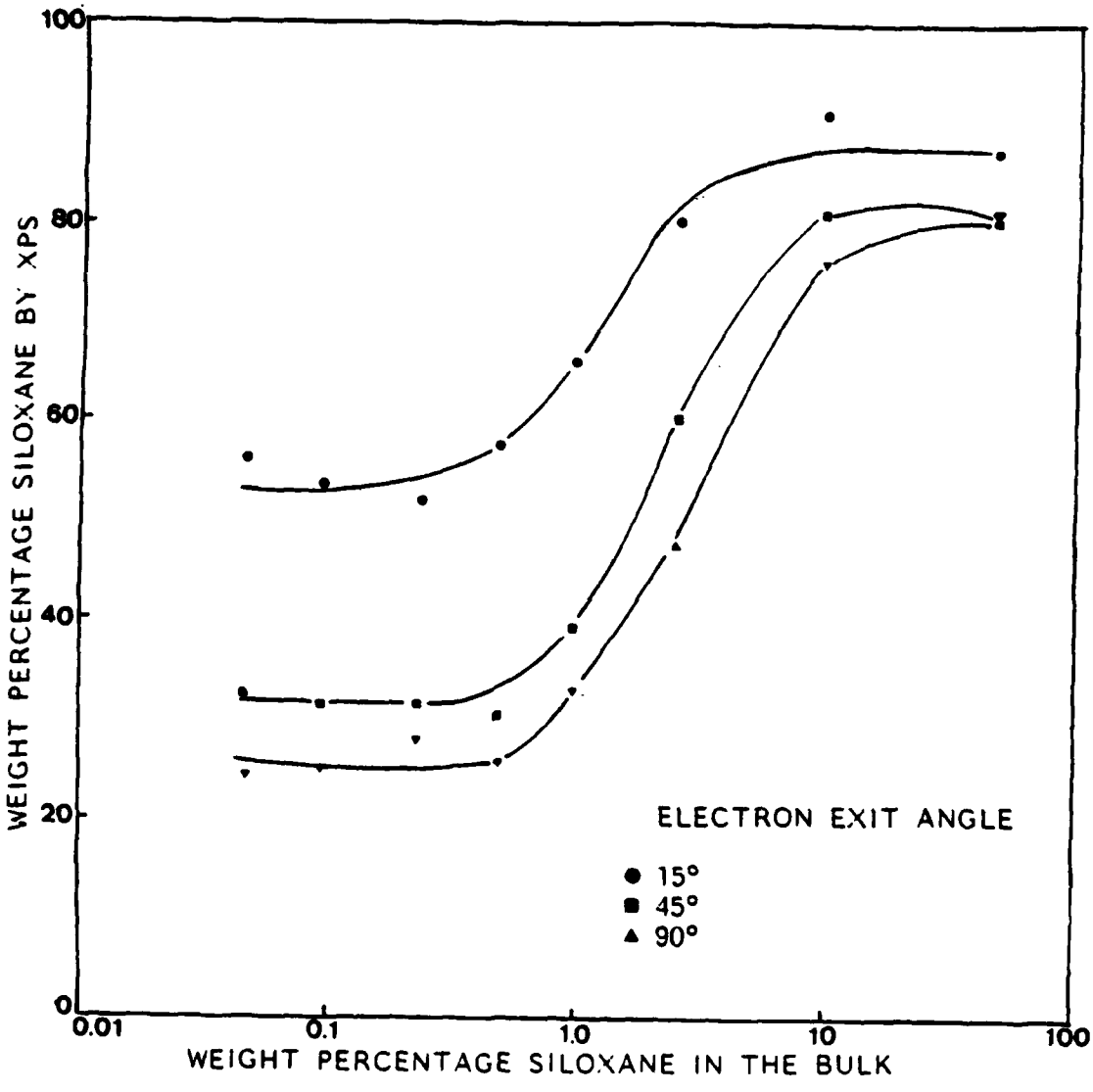

Figure(5.15). Surface behavior of PSFPSX-1/PSF-1 blends.

siloxane in the top 15 Å to 0.05% siloxane in the bulk). The other region also creates a plateau at the bulk concentrations higher than about 10% siloxane. Here the surface seems to be very similar to that of the pure block copolymer PSFPSX-1. The two plateau regions are connected through an intermediate region whereby the surface siloxane content continuously increases.

At this point it is tempting to compare the above polymeric behavior to the behavior of a soap solution, with which many parallels have been drawn in the past. Just as a break in a surface property in a soap solution(corresponding to the c.m.c) is connected to the morphological changes occuring in the bulk, it might be expected that the changes in the bulk may have a bearing on the surfaces of the block copolymer-homopolymer systems, too. Of course, the comparison is only qualitative in nature, and one-to-one relations of various quantities can not be hoped for due to many more complexities involved in the polymer systems such as effects of molecular weights, architecture of the block copolymer, polymer-solvent interactions, etc. TEM was done on two representative samples- 0.5% and 5% bulk siloxane respectively- to delve into a possible role of bulk morphology that could explain the observed surface behavior. At 0.5% siloxane, belonging to the lower plateau, the bulk was found to be homogeneous signifying that the two components of the blends are well-mixed. Figures(5.16) shows the photomicrographs of the bulk of the 5% siloxane sample. This composition belongs to the intermediate region. It can be clearly seen that there are two large scale phases existing in the system. The block copolymer is no longer capable of mixing with the

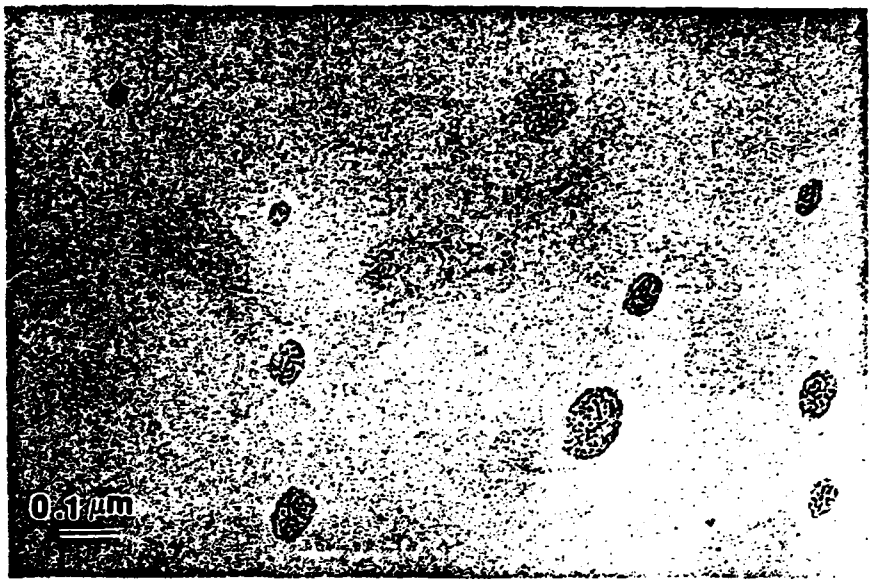

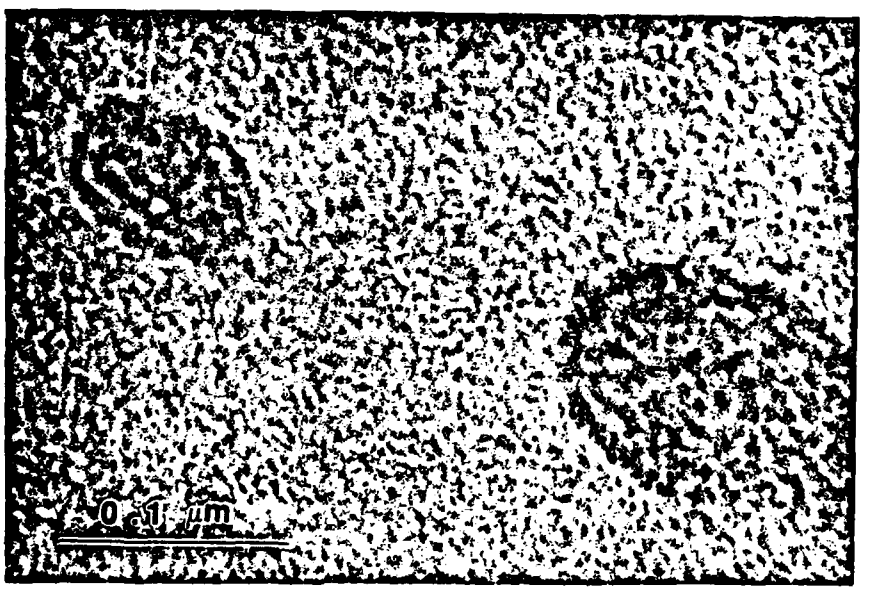

Figure(5.16). TEM photomicrographs of a 4.5% bulk siloxane blend of PSFPSX-1 with PSF-1; (a) low magnification, and (b) high magnification.

homopolymer since the positive heat of mixing, now large enough, drives the system away from the natural tendency of achieving a low entropy state by complete mixing. PSFPSX-1 exist in a form of spherical or ellipsoidal domains of sizes varying from very small to about 0.1 microns. These domains are also responsible for the increased fracture toughness of these blends[119].

The above *macro*structures contain the inherent microdomains of the original copolymer. Similarity between the microphases in terms of size and shape in the Figures(5.16b) and (5.4) can be easily noted. The onset of formation of *macro*heterogeneous bulk can be looked upon as responsible for the end of the lower plateau and the beginning of the intermediate region. At this point, the macrodomains formed of the block copolymer may themselves preferentially migrate towards the surface causing the increase in signals representing siloxane in the XPS spectra. The confirmation of this suggestion can come from surface imaging by high resolution S(T)EM analysis. Work in this regard is in progress.

The results of XPS analysis on PSFPSX-3 blended with PSF-1 are shown on the Figure(5.17). Comparing the Figures(5.15) and (5.17), it is clearly seen that the extent of surface segregation of siloxane at any given bulk concentration is much larger in the latter than in the former- a manifestation of the longer siloxane blocks in the latter. The general trend in this system has remained similar to the previous one. Absence of a conspicuous lower plateau may also be a result of the longer siloxane blocks. Figures(5.18) through (5.23) show micrographs of the bulk of several of these blends. The morphology changes from

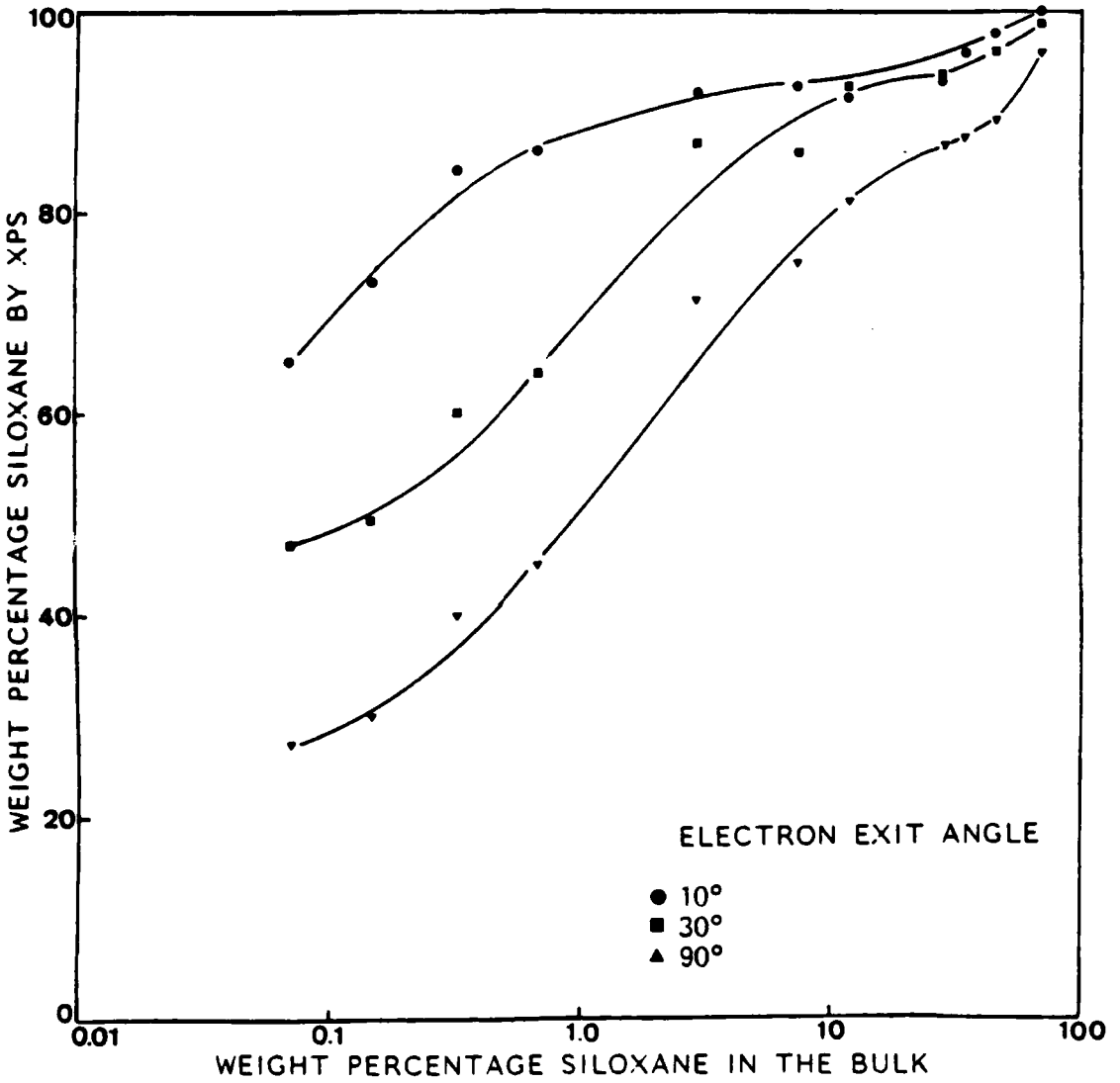

Figure(5.17). Surface behavior of PSFPSX-3/PSF-1 blends.

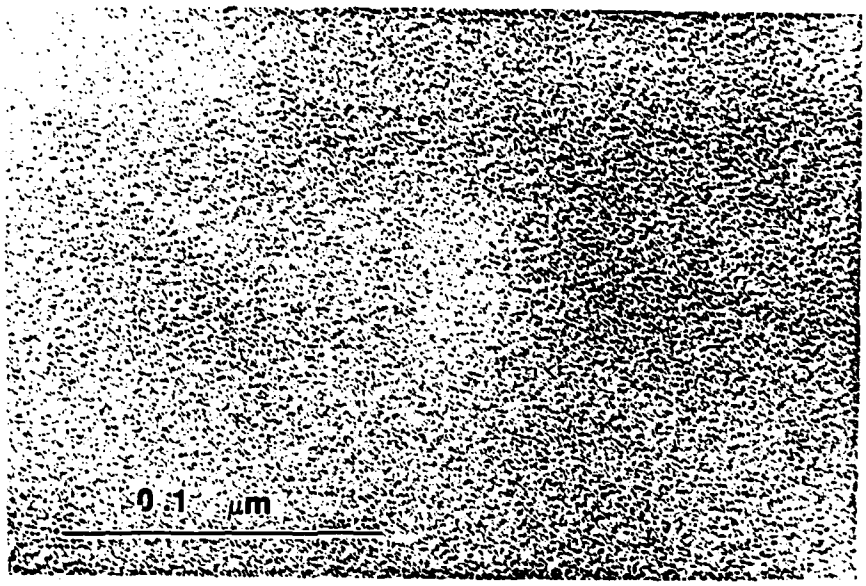

Figure(5.18). TEM photomicrograph of a 0.7% bulk siloxane blend of PSFPSX-3 with PSF-1.

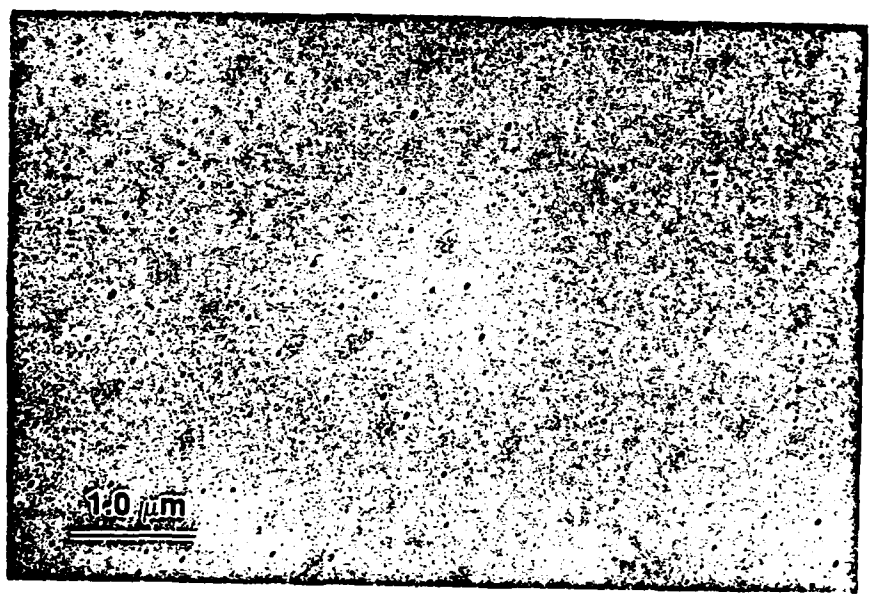

Figure(5.19). TEM photomicrograph of a 3.0% bulk siloxane blend of PSFPSX-3 with PSF-1.

that of a homogeneous one at 0.7%(Figure(5.18)) to that having macroheterogeneities at 3% siloxane(Figure(5.19)) in the bulk. Figures(5.20a) and (5.20b) show the phases in a 7.5% blend demonstrating the simultaneous existence of a homogeneous phase and a microheterogeneous phase. Figure(5.21) shows a detailed picture of a approximately micron-size ellipsoid of block copolymer having spherical polysulfone microdomains(light) in a matrix of siloxane(dark). At higher copolymer concentrations, there is a 'macro'phase-inversion, i.e. PSFPSX-3 makes the continuous phase with large dispersed phases of PSF-1 in it. Figure(5.22b) is a higher magnification photomicrograph of the interfacial region between the dark and the light regions showing the microdomain structure in the former. A similar morphology is also observed in a 45.5% siloxane blend as depicted in the Figures(5.23a) and (5.23b). It seems logical that the surface of these two blends would be similar to that in the neat block copolymer PSFPSX-3.

Figure(5.24) displays the XPS data from the above blends as a function of electron take-off angle, θ. At lower siloxane concentrations, the variation of the surface siloxane with the angle, and hence with the depth, is that of a continuous increase. Above 3% bulk siloxane, the surface siloxane becomes relatively insensitive to the angle, especially below 30° representing a depth of about 30 Å. The fact that macroheterogeneous bulk morphology is also observed above 3% siloxane establishes that there must be some relation between the bulk and surface behaviors.

The results from blends of PSFPSX-4 and PSFPSX-2 with PSF-1 are depicted on the Figures(5.25) and (5.26) respectively. Again same

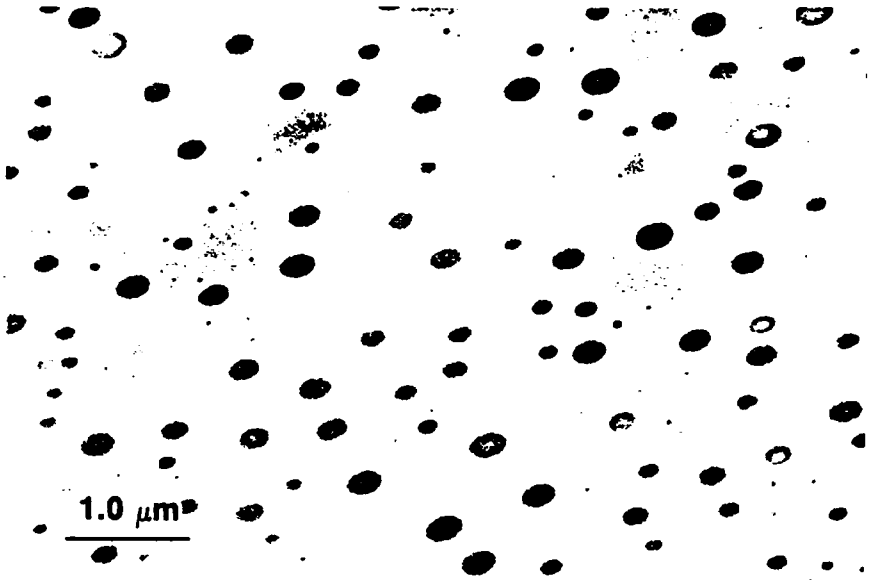

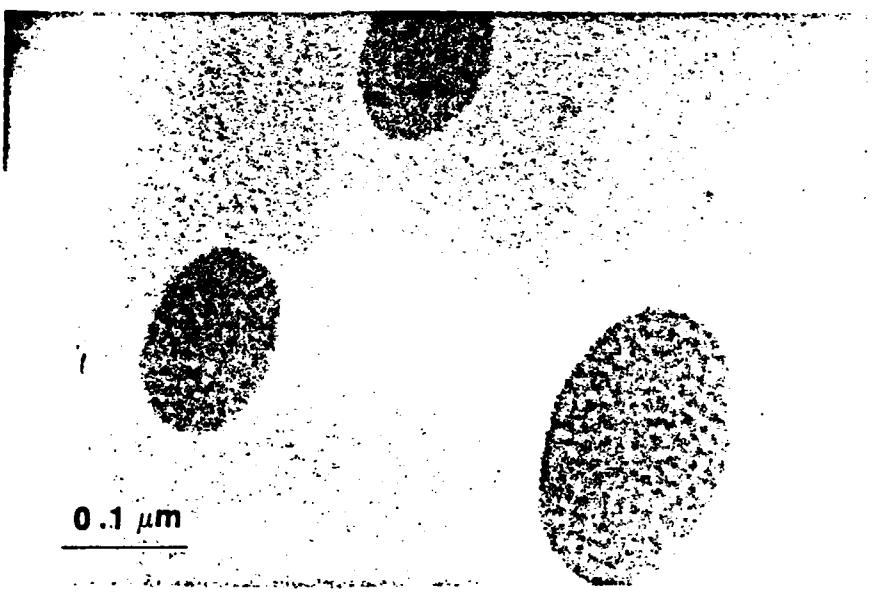

Figure(5.20). TEM photomicrographs of a 7.5% bulk siloxane blend of PSFPSX-3 with PSF-1; (a) low magnification, and (b) high magnification.

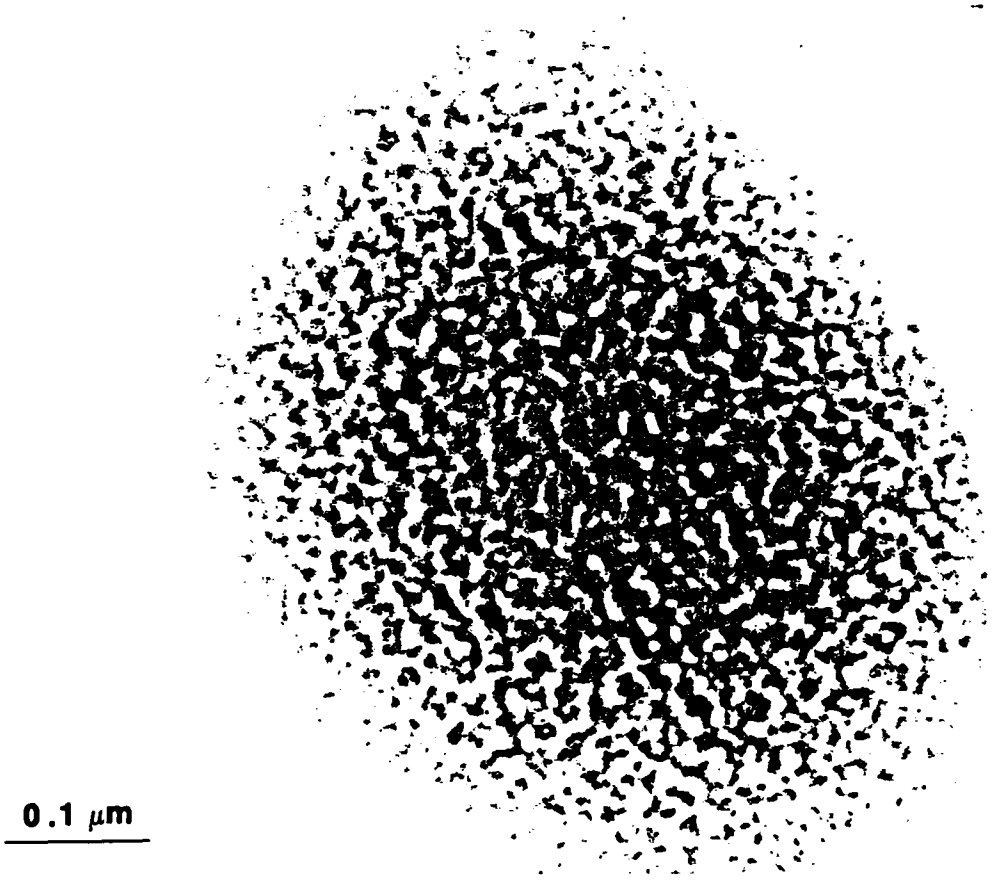

Figure(5.21) TEM photomicrograph of a 9.7% bulk siloxane blend of PSFPSX-3 with PSF-1. A Philips EM-400 electron microscope at University of Virginia was used for this micrograph.

Figure(5.22). TEM photomicrographs of a 35.4% bulk siloxane blend of PSFPSX-3 with PSF-1; (a) low magnification, and (b) high magnification showing the interfacial region.

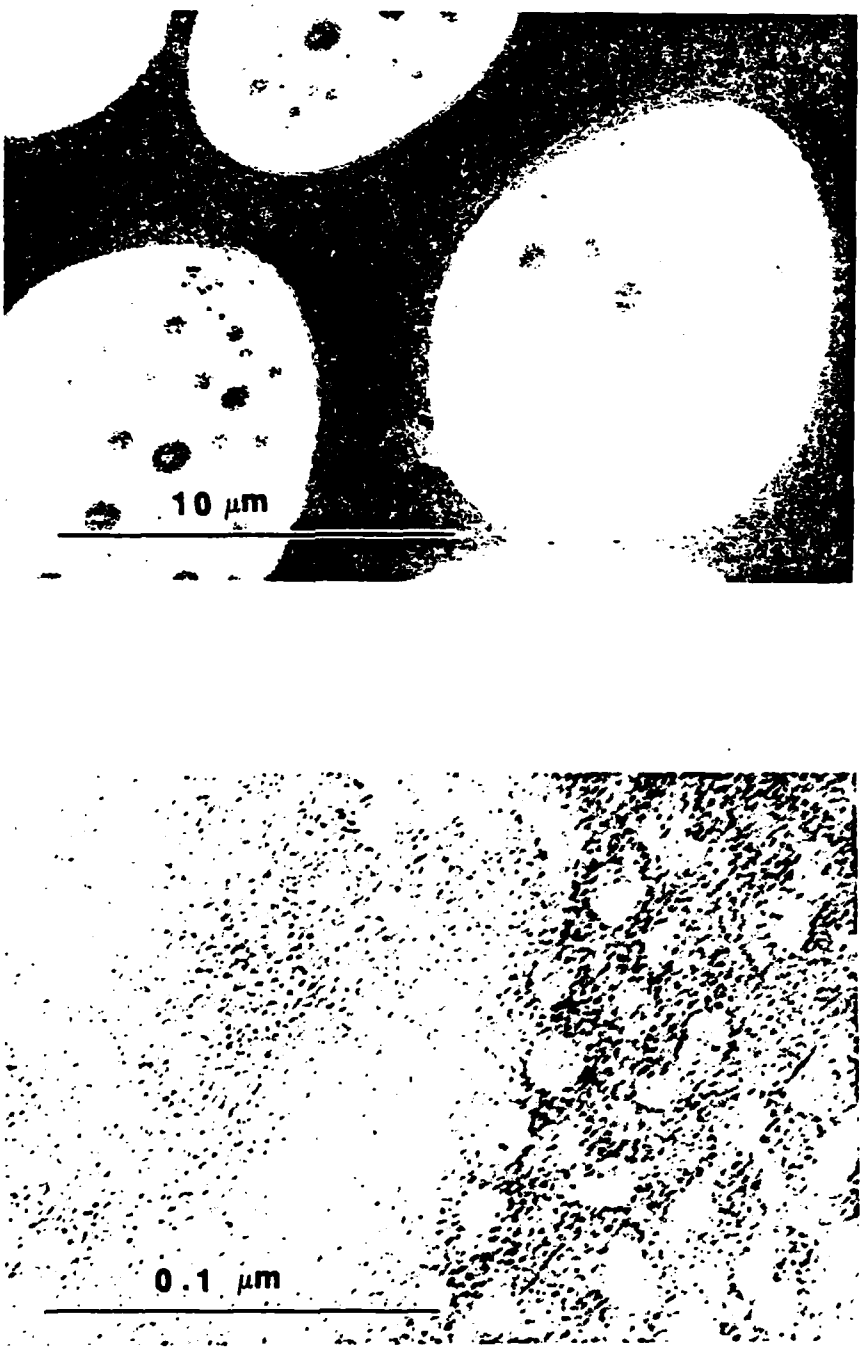

Figure(5.23). TEM photomicrographs of a 45.5% bulk siloxane blend of PSFPSX-3 with PSF-1; (a) low magnification, and (b) high magnification showing the interfacial region.

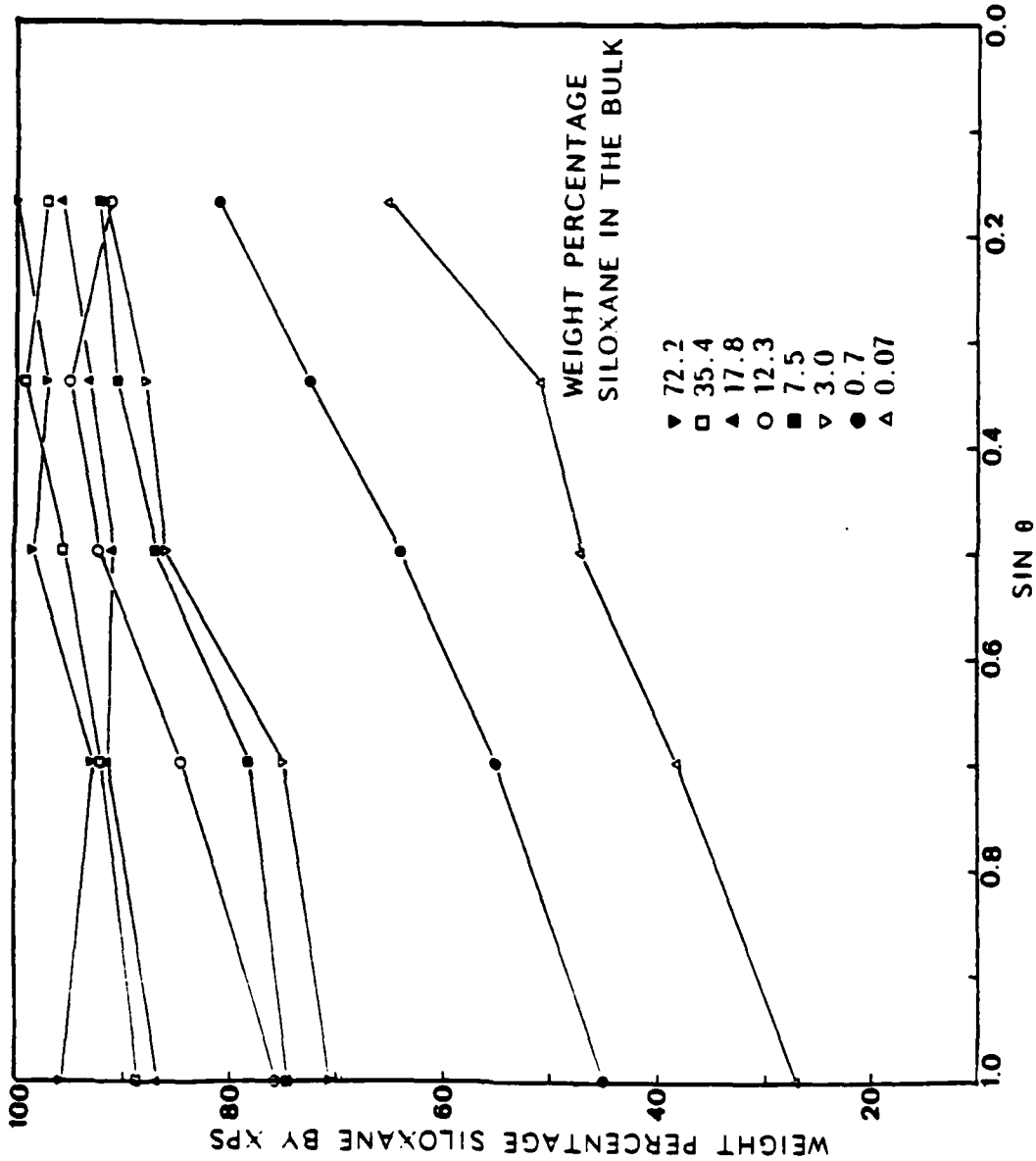

Figure(5.24). Quantitative angular-dependent behavior of various blends of PSF/PSX-3/PSF-1.

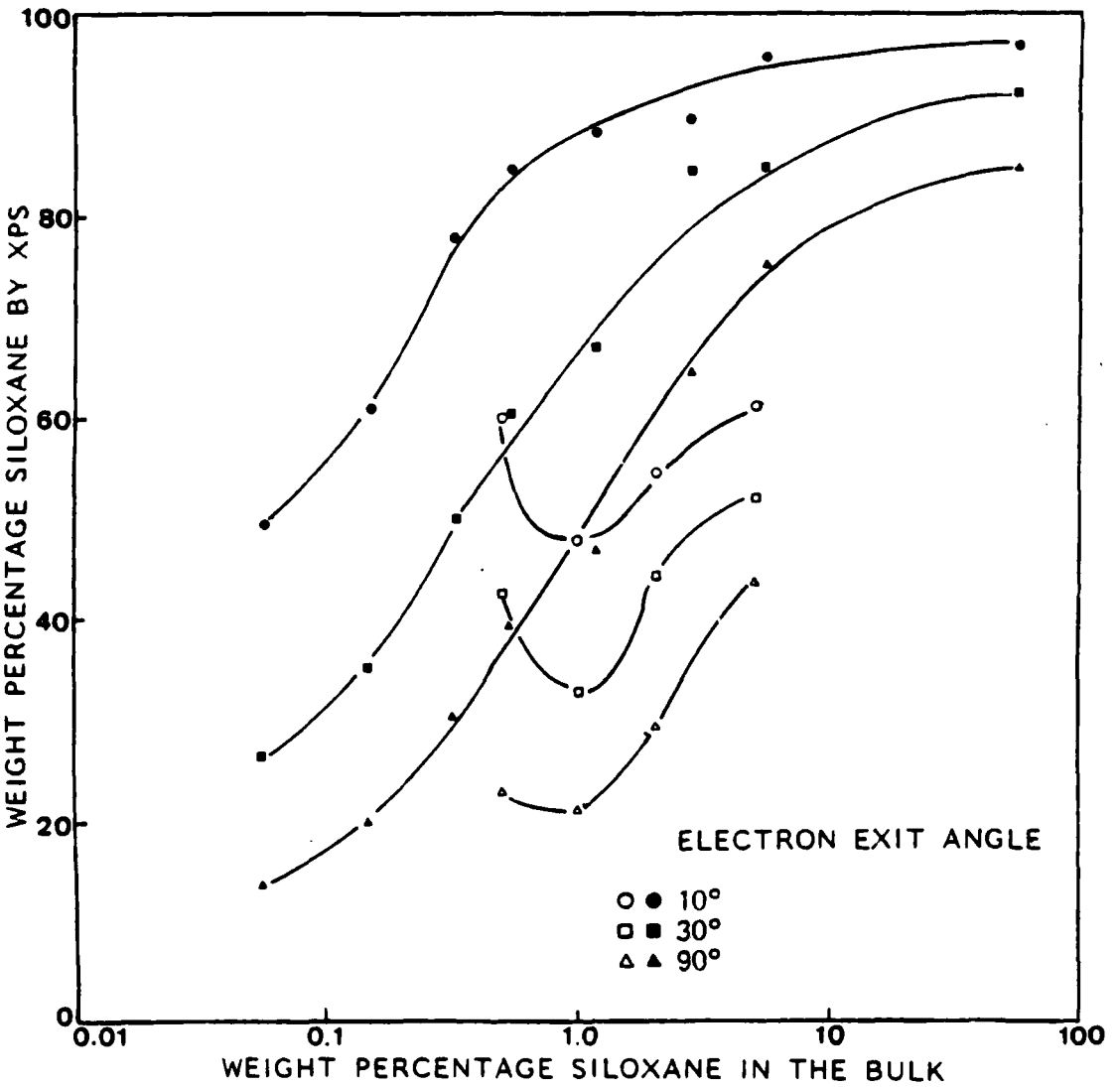

Figure(5.25). Surface behavior of PSFPSX-4/PSF-1 blends. The light symbols represent the compression molded films.

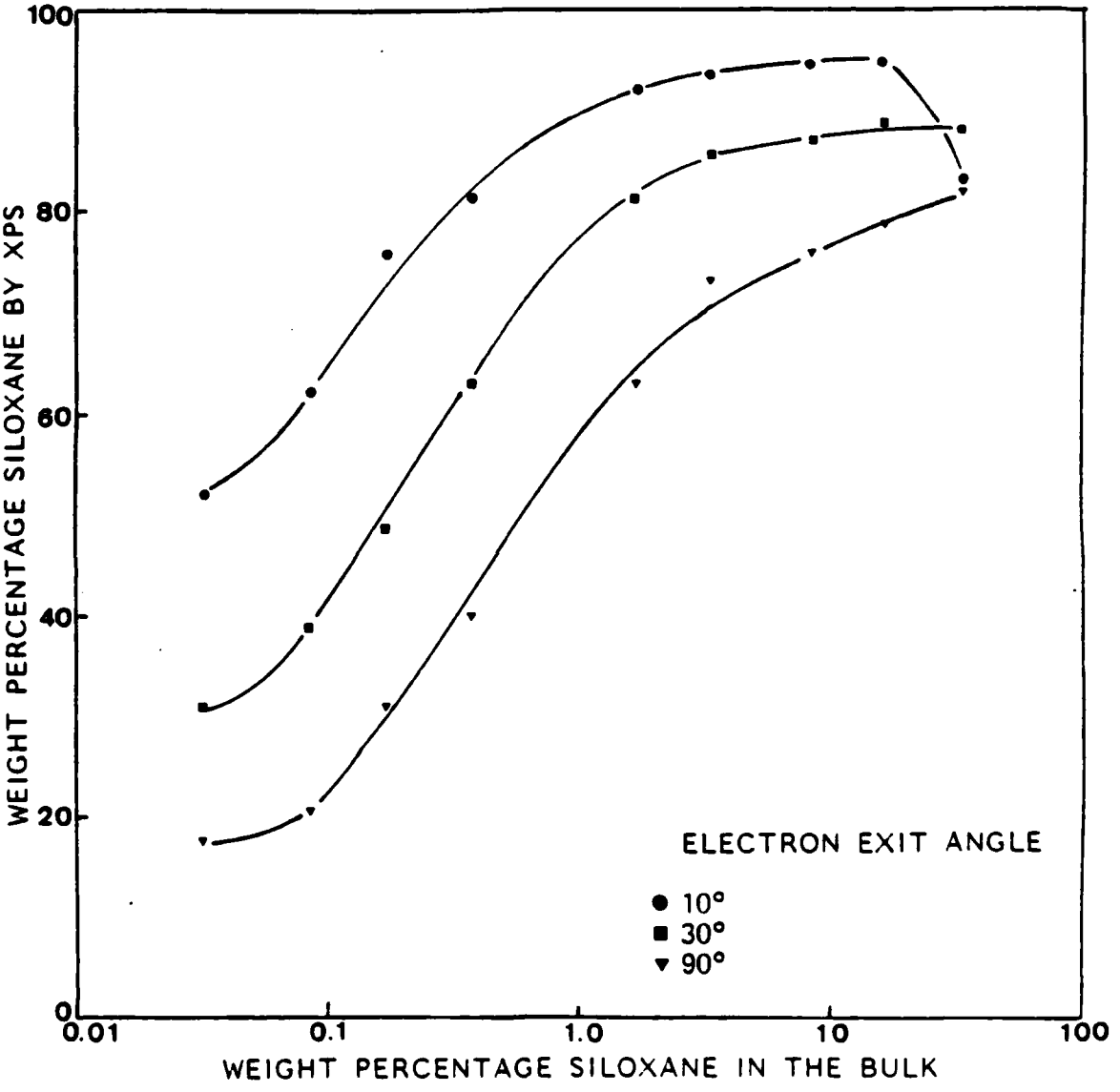

Figure(5.26). Surface behavior of PSFPSX-2/PSF-1 blends.

general behavior is obtained. Comparison of Figures(5.25) and (5.17) reveals that at any fixed bulk composition, the surface siloxane is higher in the latter. It is not surprising noting the difference in lengths of the sulfone blocks, with those of siloxane blocks remaining the same, in the two copolymers concerned.

Figures(5.27) and (5.28) show photomicrographs of two blends of PSFPSX-4 with PSF-1. The former displays the bulk of a 1.2% siloxane blend with macroheterogeneities similar to ones seen in the other systems. Figure(5.28) shows a single microheterogeneous structure of a 45% siloxane blend. The Block copolymer content in this blend is 80% by weight. It seems that at this high content of block copolymer, thermodynamics favors solubilization of PSF-1 into the sulfone domains of the block copolymer instead of forming separate phases.

Figure(5.25) also shows results of surface analysis on compression molded films of PSFPSX-4/PSF-1 blends. The siloxane content in each was found to be lower than the corresponding value in solvent cast samples. This can be due to two reasons. There might have been some transfer of the top surface layer while removal, to the surfaces between which the molding was carried out. On the other hand, it is possible that the time provided during molding was not enough to allow the surface to achieve an equilibrium state. Such kinetic effects have been observed by Gaines and Bender[32].

Blends of the polyester/polysiloxane copolymer PEPSX-1 with the homopolyester PE-1 also display similar behavior as evident from the Figure(5.29). Figures(5.30) through (5.34) display the TEM photomicrographs for these blends. Similar characteristics are found

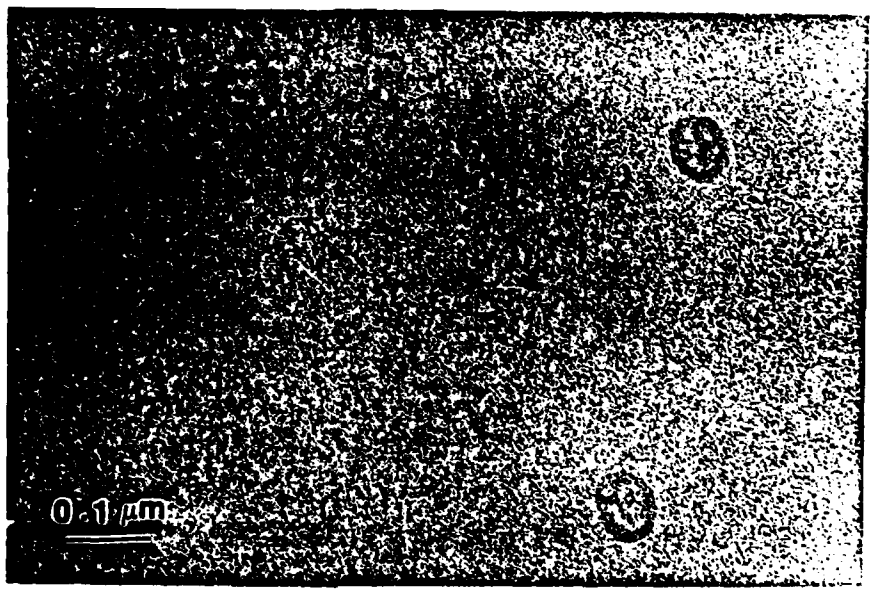

Figure(5.27). TEM photomicrograph of a 1.2% bulk siloxane blend of PSFPSX-4 with PSF-1.

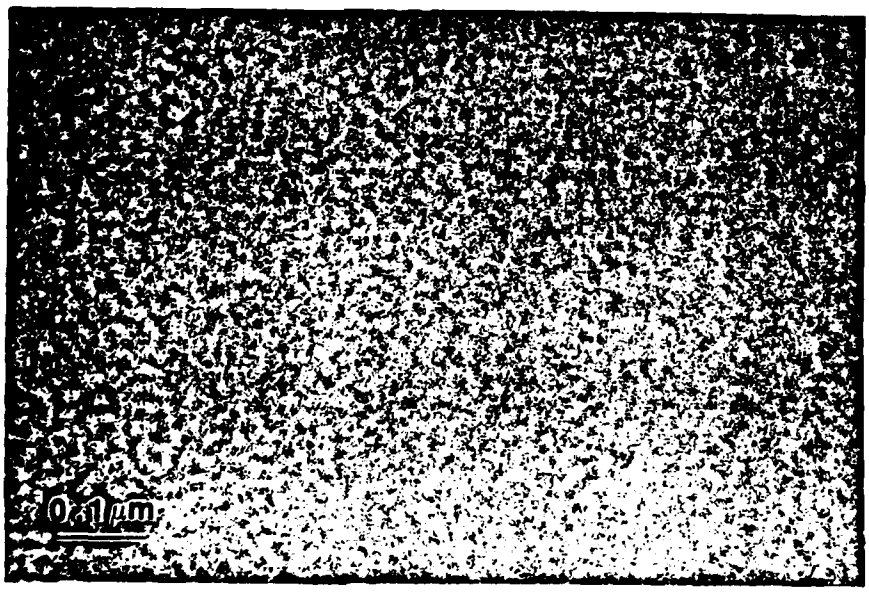

Figure(5.28). TEM photomicrograph of a 45% bulk siloxane blend of PSFPSX-4 with PSF-1.

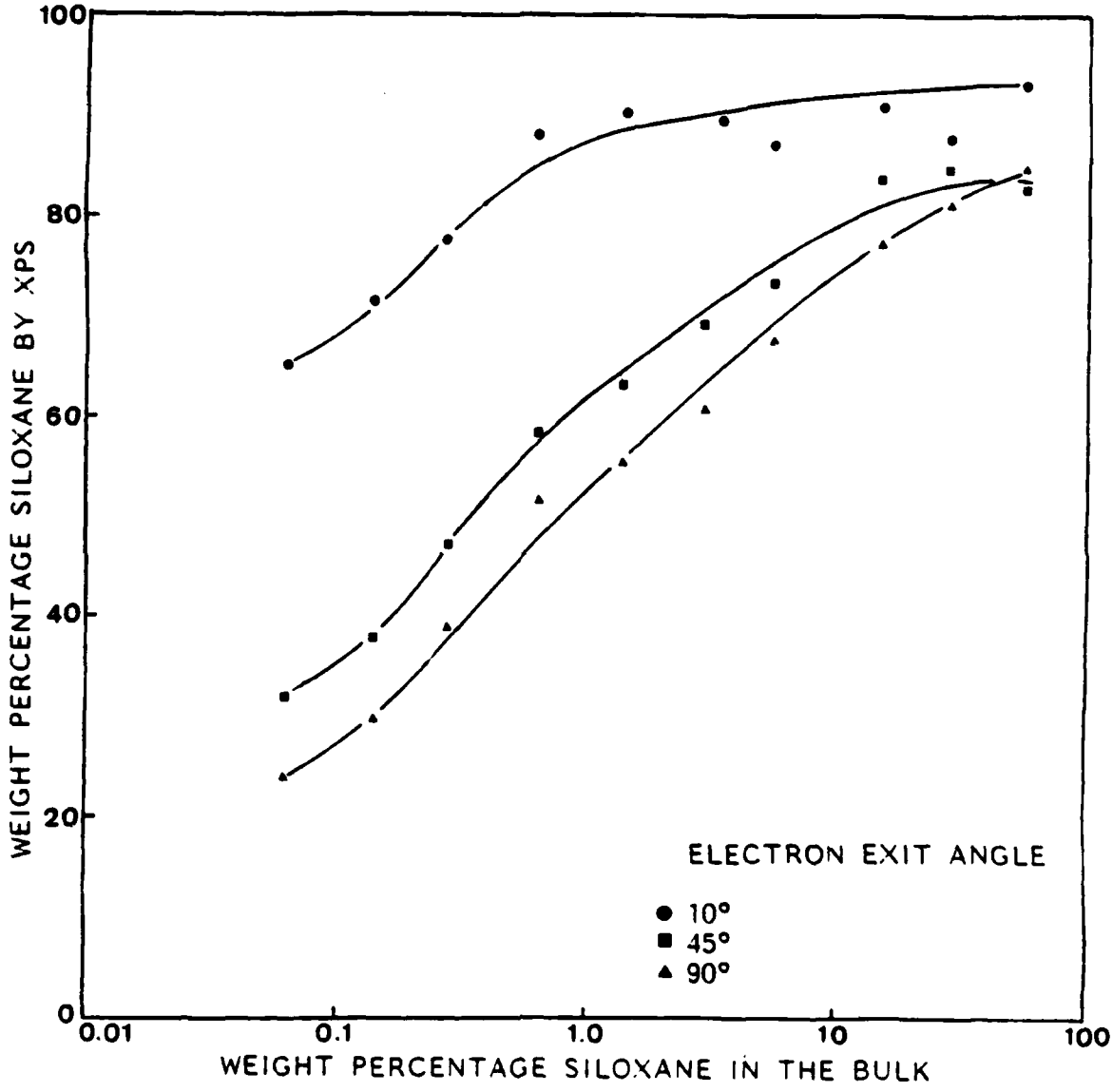

Figure(5.29). Surface behavior of PEPSX-1/PE-1 blends.

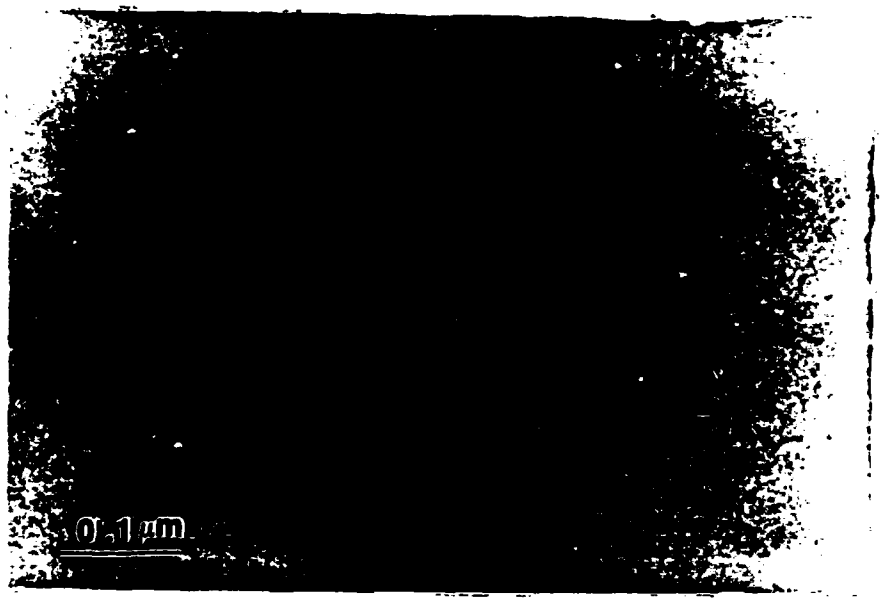

Figure(5.30). TEM photomicrograph of a 2.4% bulk siloxane blend of PEPSX-1 with PE-1.

Figure(5.31). TEM photomicrograph of a 5.2% bulk siloxane blend of PEPSX-1 with PE-1.

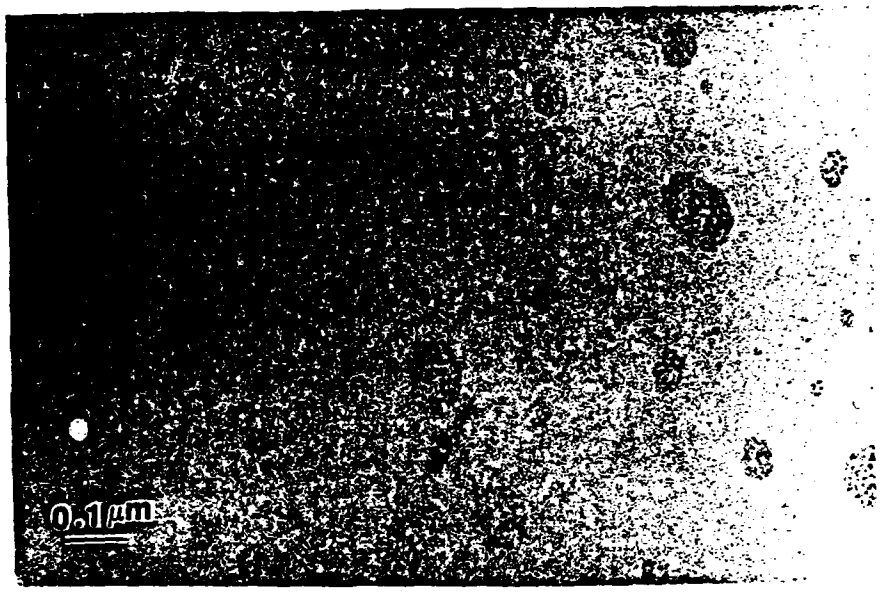

Figure(5.32). TEM photomicrograph of a 9.8% bulk siloxane blend of PEPSX-1 with PE-1.

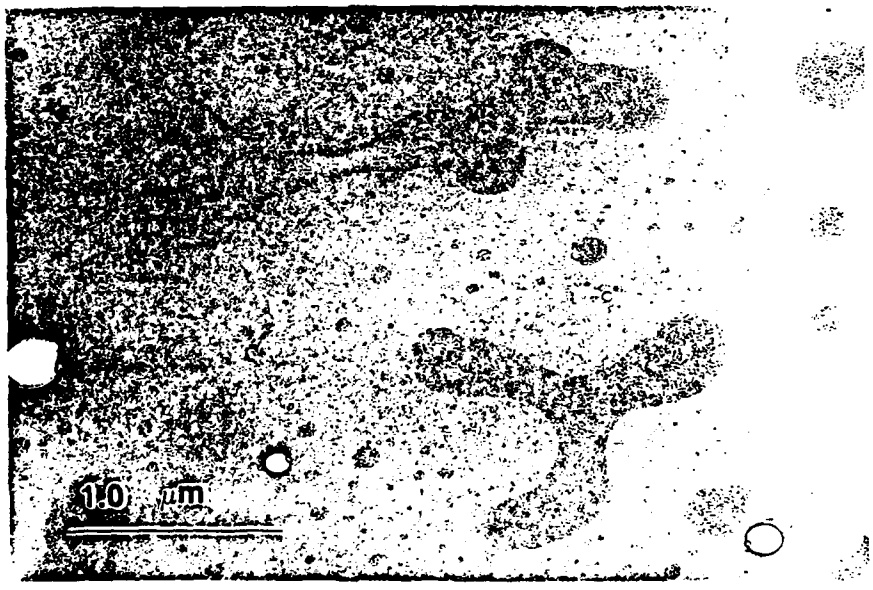

Figure(5.33). TEM photomicrograph of a 25.8% bulk siloxane blend of PEPSX-1 with PE-1.

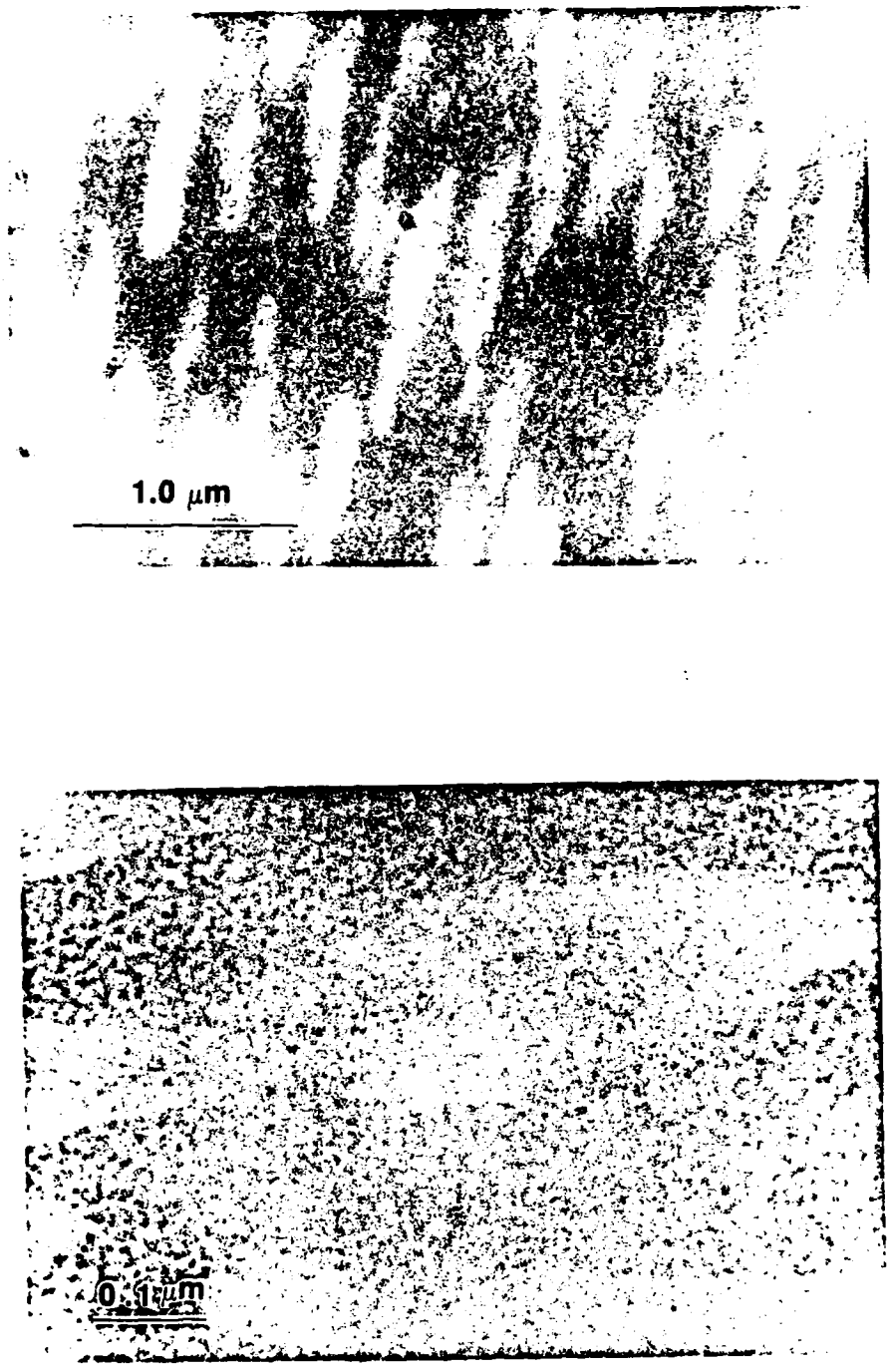

Figure(5.34). TEM photomicrographs of a 50% bulk siloxane blend of PEPSX-1 with PE-1; (a) low magnification, and (b) high magnification.

here too, i.e. two phase system with homopolyester and the copolymer PEPSX-1 making the phases. At 2.4% bulk siloxane, the block copolymer phases of sizes below 0.1μ are dispersed in the homopolymer matrix. These phases get bigger and numerous as one goes through 5.2%, 9.8%, and 25.8% bulk siloxane as shown on the Figures(5.31) to (5.33) respectively. The phases ultimately merge together to make a continuous phase. Each dark phase representing the block copolymer very clearly shows the siloxane continuous-ester spherical microdomain structure resembling those of the pure block copolymer in the Figure(5.11).

The results from blends of PUPSX-1 and PURTH-1 polymers have been depicted on the Figure(5.35). Here the surface composition is expressed in terms of carbon to silicon atomic ratio.

On examining the surface compositions of each systems at very low angles of analysis, such as 10° or 15°, an additional level of information is obtained. Even at very low concentrations, there is a great amount of siloxane detected by XPS which readily acquires a constant value on increasing the siloxane to about 2-3%. An analogy can be drawn with contact angle measurements on such blends by several workers[11,28,31] who also observed similar behaviors. The depth of analysis at 10° being only to the order of 10 Å, the XPS results might be expected to conform to those of contact angles. The fact that the macrophase separation also begins in each case at concentrations in the range of 2-3% siloxane points towards a possible correlation between the surface and the bulk phenomena. The bulk phenomenon might be responsible for the observed surface behavior or the two might be

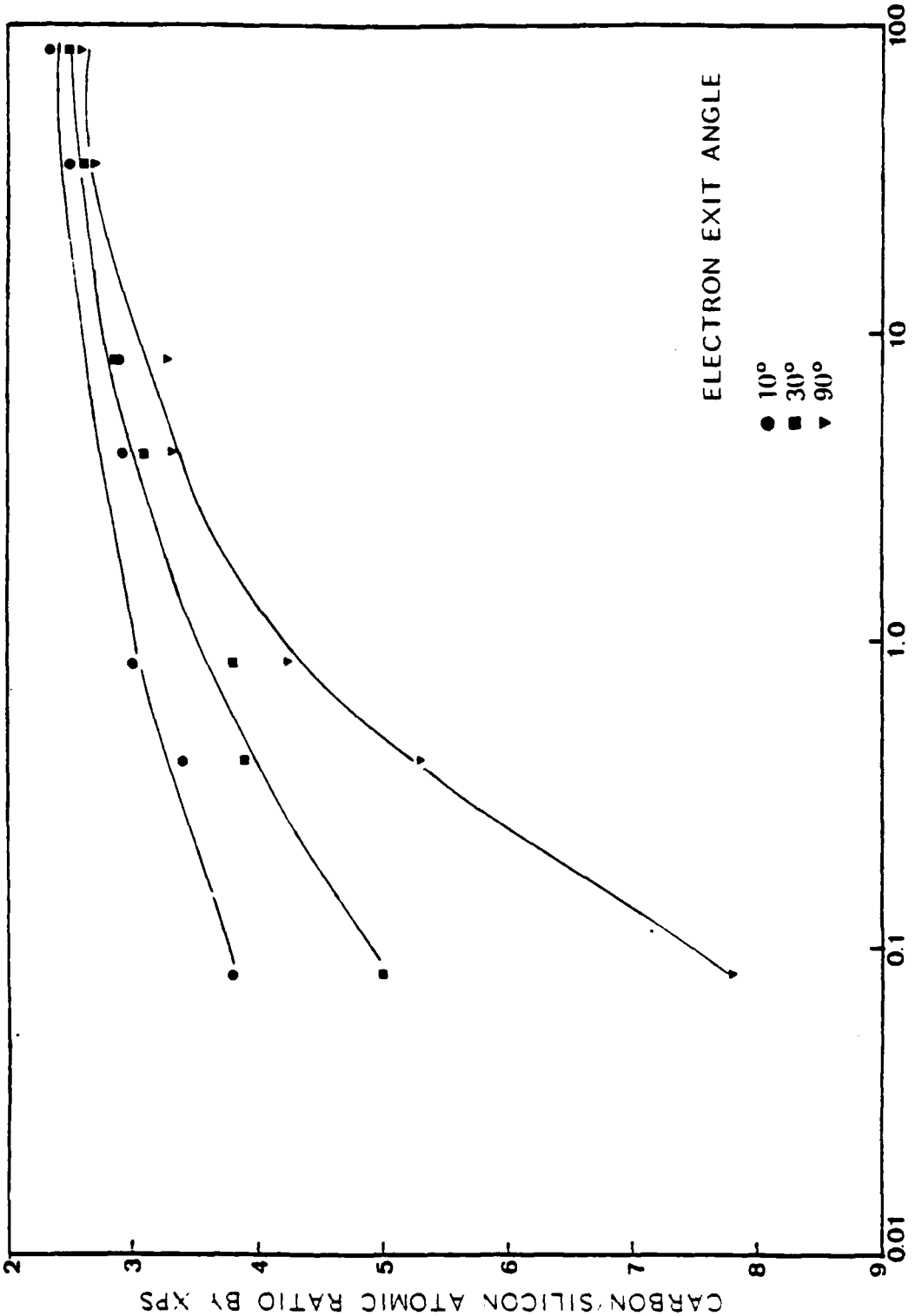

Figure(5.35). Surface behavior of PUPSX-1/PURTH-1 blends.

occuring parallel with a common physical origin. But again, unless the exact surface morphology is known, erroneous interpretations can be easily made from the XPS data. For example, if the phase separated block copolymer domains of about 0.1μ observed here are aligned at the surface in an elevated position even in small numbers, the shadowing of the photoelectrons arising from the rest of the analysis area will be responsible for the high siloxane content detection by XPS. At the same time, similar data can also be obtained if the siloxane blocks are just forming a monolayer like uniform film at the surface. Both possibilities seem equally valid at this point. An absolute confirmation of one over the other can only be made with the help of surface topographical information by techniques such as Replication Electron Microscopy or Scanning Transmission Electron Microscopy.

CHAPTER VI

CONCLUSIONS

There are several points of conclusions that can be drawn from the present study.

For the neat block copolymers investigated here, containing siloxane as the lower surface energy component:

(a) The surface is made of a compositionally homogeneous overlayer which is siloxane-rich.

(b) In constrast to the above, the bulk is microphase-separated with spherical domains, showing that the surface and bulk morphologies can differ.

(c) The purity of the overlayer in terms of siloxane content depends on the block length of siloxane and the overall siloxane content in the copolymer. Increase in both results in higher surface siloxane.

For blends of copolymers with homopolymers corresponding to the higher surface energy component:

(a) Very high surface segregation of siloxane is displayed even at concentrations as low as 0.1%.

(b) On increasing the bulk siloxane content, initially there is a slow rate of increase in the surface siloxane which then increases rapidly to reach values typical of the pure block copolymer. At a fixed

siloxane content in the bulk, longer siloxane block results into enhancement of surface segregation.

(c) Parallel to the above, the bulk shows a homogeneous mixed phase at low concentrations.

(d) Gross phase separation of the block copolymer from the homopolymer occurs at higher concentrations.

(e) These block copolymer phases themselves contain microdomain structure similar to the pure block copolymer.

(f) The surface behavior and the morphological changes in the bulk seem to be related to each other. More work in the direction of surface morphology need to be done before any confirmation of this can be established.

REFERENCES

1. J. W. Gibbs, "*The Scientific Papers of J. Willard Gibbs*", *Vol I*, Dover, New York(1961), p219.

2. G. Holden, and R. Milkovich, *U. S. Patent*, No.3,265,765(1966).

3. G. E. Molau in "*Colloidal and Morphological Behavior of Block and Graft Copolymers*", G. E. Molau, ed., Plenum, New York(1971), p79.

4. D. R. Paul in "*Polymer Blends*", *Vol. 2*, D. R. Paul, and S. Newman, eds., Academic Press, New York(1978), p35.

5. T. Inoue, T. Soen, T. Hashimoto, and H. Kawai, *Macromolecules*, 3(1), 87(1970).

6. S. L. Aggarwal, and R. A. Livigni, *Polym. Engg. Sci.*, 17(1), 498(1977).

7. A. Noshay, M. Matzner, B. P. Barth, and R. K. Walton, *Div. Organ. Coatings Plast. Chem. Prepr., Am. Chem. Soc.*, 217(1974).

8. D. F. Kagan, V. V. Prokopenko, Y. M. Malinskii, and N. F. Bakeyev, *Polym. Sci. U. S. S. R.*, 32, 124(1972).

9. P. O. Sherman, S. Smith, and B. Jahannessen, *Textile Res. J.*, 39, 449(1969).

10. J. H. Sanders, *Rubber Rev.*, 33, 1293(1960).

11. M. J. Owen, and J. Thompson, *British Polym. J.*, 4, 297(1972).

12. D. T. Clark in "*Advances in Polymer Friction and Wear*",*Vol 5A*, L. H. Lee, ed., Plenum, New York(1975), p241.

13. G. L. Gaines, Jr., *Macromolecules*, 14, 208(1981).

14. D. W. Dwight, J. E. McGrath, A. R. Beck, and J. S. Riffle, *Polym. Prepr., Div. Polym. Chem., Am. Chem. Soc.*, 20(1), 702(1979).

15. A. K. Sha'aban, S. McCartney, N. Patel, I. Yilgor, J. S. Riffle, D. W. Dwight, and J. E. McGrath, *ibid.*, 24(2), 130(1983).

16. A. J. G. Allan, *J. Colloid Sci.*, 14, 206(1959).

17. R. C. Bowers, W. C. Clinton, and W. A. Zisman, *Ind. Eng. Chem.*, 46, 2416(1954).

18. R. C. Bowers, W. C. Clinton, and W. A Zisman, *J. Appl. Phys.*, 24, 1066(1953).

19. N. L. Jarvis, R. B. Fox, and W. A. Zisman, *Adv. Chem. Ser. No. 43*, 317(1964).

20. D. R. Jackson, and L. G. Lundsted, *U. S. Patent*, No. 2,677,700(1954).

21. L. G. Lundsted, and I. R. Schmolka, in "*Block and Graft Copolymerizations*", R. J. Ceresa, ed., Wiley, London(1976), p113.

22. B. Kanner, W. G. Reid, abd I. H. Peterson, *Ind. Eng. Chem. Prod. Res. Devlop.* 6, 88(1967).

23. T. C. Kendrick, B. M. Kingston, N. C. Lloyd, *J. Coll. Interface. Sci.* 24, 135(1967).

24. H. W. Fox, P. W. Taylor, and W. A. Zisman, *Ind. Eng. Chem.* 39, 1401(1947).

25. P. J. Flory, in "*Principles of Polymer Chemistry*", Cornell University Press, Ithaca, New York(1953), p411.

26. M. J. Owen, and T. C. Kendrick, *Proc. Intern. Congr. Surface Activity, 5th, Barcelona, 1968*, 571(1970).

27. A. K. Rastogi, and L. E. St. Pierre, *J. Coll. Interface. Sci.*, 31(2), 168(1969).

28. M. J. Owen, and T. C. Kendrick, *Macromolecules*, 3, 458(1970).

29. A. Takahashi, and Y. Yamashita, in "*Copolymers, Polyblends, and Composites*", N. A. J. Platzer, ed., *Adv. Chem. Ser. No.142*, ACS, Washington D.C.(1975), p267.

30. Y. Yamashita, *J. Macromol. Sci.-Chem.*, A13(3), 401(1979).

31. D. G. Legrand, and G. L. Gaines, Jr., *Polym. Prepr., Div. Polym. Chem., Am. Chem. Soc.*, 11, 442(1970).

32. G. L. Gaines, Jr., and G. W. Bender, *Macromolecules*, 5,

82(1972).

33. J. J. O'Malley, W. J. Stauffer, *Polym. Eng. Sci.*, 17(1), 510(1977).

34. M. Litt, and J. Herz, *Polym. Prepr., Div. Polym. Chem., Am. Chem. Soc.*, 10, 905(1969).

35. M. Litt, and T. Matsuda, in "*Copolymers, Polyblends, and Composites*", N. A. J. Platzer, ed., *Adv. Chem. Ser. No.142*, ACS, Washinton D. C.(1975), p320.

36. M. Litt, F. Rahl, and L. G. Rolden, *J. Polym. Sci. Part A-2*, 7, 463(1969).

37. Y. Yamashita, Y. Tsukahara, K. Ito, K. Okada, Y. Tajima, *Polym. Bull.*, 12, 849(1980).

38. K. Ito, Y. Masuda, T. Shintani, T. KItaro, and Y. Yamashita, *Polym. J.*, 15(6), 443(1983).

39. D. T. Clark, J. Peeling, and J. J. O'Malley, *J. Polym. Sci. Polym. Chem. Ed.*, 14, 543(1976).

40. J. C. Saam, and F. W. G. Fearon, *Ind. Eng. Chem. Prod. Res. Develop.*, 10, 10(1971).

41. H. R. Thomas, and J. J. O'Malley, *Macromolecules*, 12(3), 323(1979).

42. J. J. O'Malley, H. R. Thomas, and G. M. Lee, *Macromolecules*, 12(5), 996(1979).

43. H. R. Thomas, and J. J. O'Malley, in "*Photon, Electron, and Ion Probes of Polymeric Structure and Properties*", D. W. Dwight, T. J. Fabish, and H. R. Thomas, eds., *ACS Symp. Ser. No.162*, ACS, Washington D. C.(1981), p319.

44. J. E. McGrath, D. W. Dwight, J. S. Riffle, T. F. Davidson, D. C. Webster, and R. Visvanathan, *Polym. Prepr., Div. Polymr. Chem., Am. Chem. Soc.*, 20(2), 528(1979).

45. (a) J. S. Riffle, *PhD Dissertation*, VPI&SU(1980); (b) J. S. Riffle et al., *Macromolecules*, in press(1984).

46. A. Sha'aban, *M. S. Thesis*, VPI&SU(1983).

47. K. Kugo, Y. Hata, T. Hayashi, and A. Nakajima, *Polym. J.*, 14(5), 401(1982).

48. K. Kugo, M. Murashima, T. Hayashi, and A. Nakajima, *Polym.*

J., 15(4), 267(1983).

49. S. I. Stupp, J. W. Kauffman, and S. H. Carr, *J. Biomed. Mater. Res.*, 11, 237(1977).

50. C. S. P. Sung, C. B. Hu, E. W. Merrill, and E. W. Salzman, *ibid.*, 12, 791(1978).

51. E. Nyilas, and R. S. Ward, Jr., *J. Biomed. Mater. Res. Symp.*, 8, 69(1977).

52. C. S. P. Sung, and C. B. Hu, *J. Biomed. Mater. Res.*, 13, 45(1979).

53. D. J. Lyman, K. Knutson, B. McNeill, and K. Shibatani, *Tran. Am. Soc. Artif. Int. Organs.*, 21, 49(1975).

54. C. S. P. Sung, and C. B. Hu, *J. Biomed. Mat. Res.*, 13, 161(1979).

55. J. D. Andrade, G. K. Iwamoto, and B. McNeill, in "*Advances in Characterization of Metal and Polymer Surfaces*", L. H. Lee, ed., Academic Press, New York(1976).

56. B. D. Ratner, in *Reference 43*, p371.

57. S. W. Graham, and D. M. Hercules, *J. Biomed. Mat. Res.*, 15, 465(1981).

58. S. W. Graham, and D. M. Hercules, *ibid.*, 15, 349(1981).

59. (a) D. J. Meier, *J. Polym. Sci. Part C*, 26, 85(1969). (b) E. Helfand, *Acc. Chem. Res.*, 8, 295(1975). (c) E. Helfand, and Z. R. Wasserman, *Macromolecules*, 13, 994(1980). (d) L. Leibler, *Macromolecules*, 13, 1602(1980).

60. For general references, see (a) *J. Polym. Sci. Part C*, 26(1969), (b) "*Block Copolymers*", S. Aggarwal, ed., Plenum, New York(1970), (c) "*Block and Graft Copolymers*", J. J. Burke, and V. Weiss, ed., Syracuse Univ. Press, Syracuse, NY(1973),(d) "*Recent Advances in Blends, Grafts, and Blocks*", L. H. Sperling, ed., Plenum, New York(1974), (e) *Polym. Eng. Sci.*, 17(8) (1977), (f) A. Noshay, and J. E. McGrath, "*Block Copolymers: Overview and Critical Survey*", Academic Press, New York(1977).

61. H. Kawai, K. Hashimoto, K. Miyoshi, H. Uno, and M. Fujimura, *Macromol. Sci.-Phys. B*, 11(3), 281(1975).

62. G. Reiss, J. Kohler, C. Tournut and A. Banderet, *Macromol. Chem.*, 101, 58(1967)

63. G. E. Molau and W. M. Witbrodt, *Macromolecules*, 1, 260(1968)

64. E. B. Bradford in "*Colloidal and Morphological Behavior of Block and Graft Copolymers*", G. E. Molau, Ed., Plenum, N.Y.(1971), p21.

65. L. Toy, M. Niinomi and M. J. Shen, *Macromol. Sci. - Phys. B*, 11(3), 281(1975).

66. G. Reiss, M. Schlienger and S. Masti, *J.Macromol. Sci. - Phys. B*, 17(2), 355(1980).

67. J. Kotaka, T. Miki and K. Arai *J. Macromol. Sci. - Phys. B*, 17(2), 303(1980).

68. G. C. Eastmond and D. G. Phillips, in "*Polymer Alloys*", D. Klempner and K. C. Frisch eds.,Plenum, New York(1977), p.141

69. D. J. Meier, *Polym. Prepr., Div. Polym. Chem., Am. Chem. Soc.*, 18(1), 340(1977).

70. G. C. Eastmond and D. G. Phillips, *Polymer*, 20, 1501(1979).

71. M. Jiang, X. Huang and T. Yu *Polymer*, 24, 1259(1983).

72. A. Einstein, *Ann. Phys. Leipzig*, 17, 132(1905).

73. K. Siegbahn et al, "*ESCA- Atomic, Molecular and Solid State Structure Studied by means of Electron Spectroscopy*", Almquist and Wiksell, Uppsala, Sweden(1967).

74. K. Siegbahn, *Pure Appl. Chem.*, 48, 77(1976).

75. P. K. Ghosh, "*Introduction to Photoelectron Spectroscopy*", John Wiley and Son, New York(1983).

76. P. S. Swingle and W. M. Riggs, "*C.R.C. Critical Reviews in Analytical Chemistry*", 269(1975).

77. C. S. Fadley, in "*Electron Spectroscopy: Theory, Techniques, and Applications*", *Vol 2*, C. S. Brundle, and A. D. Baker, eds., Academic Press, London(1978), p1.

78. W. M. Riggs, and M. J. Parker, in "*Methods and Phenomena 1: Methods of Surface Analysis*", A. W. Czanderna, ed., Elsevier, Amsterdam(1975), p157.

79. C. D. Wagner et al, "*Handbook of XPS*", Perkin Elmer Corp.(1979).

80. C. D. Wagner, *Analytical Chem.*, 44, 1050(1972).

81. C. K. Jorgensen and H. Berthon, *Chem. Soc. Far. Disc.*, 54, 269(1973).

82. C. K. Jorgensen and H. Berthon, *Anal. Chem.*, 47, 482(1975).

83. C. S. Fadley et al., *J. Elec. Spec. Rel. Phen.*, 4, 93(1974).

84. D. R. Penn, *J. Elec. Spec. Rel. Phen.*, 9, 29(1976).

85. M. P. Seah and W. A. Dench, *Surf. Interface. Anal.*, 1, 2(1979).

86. J. Szajman et al., *J. Elec. Spec. Rel. Phen.*, 23, 97(1981).

87. C. D. Wagner, L. E. Davis and W. M. Riggs, *Surf. Interface Anal.*, 2, 53(1980).

88. J. C. Ashley and C. J. Tung, *Surf. Interface Anal.*, 4(2), 52(1982).

89. J. W. Cooper and S. T. Manson, *Phys. Rev.*, 177, 157(1969).

90. R. F. Reilman, A. Msezane and S. T. Manson, *J. Elec. Spec. Rel. Phen.*, 8, 389(1976).

91. J. H. Scofield, *J. Elec. Spec. Rel. Phen.*, 8, 129(1976).

92. C. D. Wagner et al., *Surf. Interface Anal.*, 3, 211(1981).

93. C. E. Kuyatt, "*Methods of Experimental Physics*", *vol.7A*, L.Marton,ed., Academic Press, New York(1968),p.16

94. A. Barrie, in "*Handbook of X-ray and Ultraviolet Photoelectron Spectroscopy*", D. Briggs,ed., Heyden London(1977), p79.

95. A. E. Hughes and C. C. Pillips, *Surf. Interface Anal.*, 4(5)(1982).

96. S. Fadley, "*Progress in Solid State Chemistry*", *vol.11*, G. Somorjai and J. McCaldin, eds., Pergamon Press, Oxford(1976), p265.

97. D. T. Clark et al., *J. Elec. Spec. Rel. Phen.*, 14, 247(1978).

98. R. W. Paynter, *Surf. Interface Anal.*, 3, 186(1981).

99. For example, (a) D. T. Clark, in *Reference 94*, p211, (b) A. Dilks, in "*Electron Spectroscopy : Theory, Techniques and Applications*", *Vol 4*, C. R. Brundle and A. D. Baker, eds., Academic Press, London,(1981), p277. (c) D. Briggs, in "*Surface Analysis and Pretreatment of Plastics and Metals*", D. M. Brewis, ed., Applied science, London(1982).

100. D. T. Clark, D. Kilcast, W. J. Feast, and W. K. R. Musgrave, *J. Polym. Sci. Polym. Chem. ed.*, 11, 389(1973).

101. D. W. Dwight and W. M. Riggs, *J. Coll. Interf. Sci.*, 4(3), 650(1974).

102. D. W. Dwight, J. E. McGrath, and J. P. Wightman, *J. Appl. Polym. Sci., Appl. Polym. Symp.*, 343, 35(1978).

103. H. R. Thomas, *Ph.D. Dissertation*, Univ. of Durham (1977).

104. D. T. Clark and H. R. Thomas, *J. Polym.Sci. Polym. Chem.*, 14, 1671(1976).

105. D. T. Clark and H. R. Thomas, *J. Polym. Sci. Polym. Chem.*, 16, 791(1978).

106. D. T. Clark in "*Electron Emission Spectroscopy*", W. Dekeyser and D. Reidel, eds., Reidel Dordrecht(1973).

107. T. A. Koopmans, *Physica*, 1, 104(1933).

108. D. T. Clark, B. J. Cromarty and A. Dilks, *J. Polym. Sci. Polym. Chem.*, 16, 3173(1978).

109. D. T. Clark and A. Harrison, *J. Polym. Sci. Polym. Chem.*, 19, 1945(1981).

110. D. S. Everhart and C. N. Reilley, *Surf. Interface Anal.*, 3, 126(1981).

111. D. T. Clark, H. R. Thomas and D. Shuttleworth, *J.Polym. Sci. Polym. Lett. Ed.*, 16, 465(1978).

112. P. Cadman, G. Gossedge and J. D. Scott, *J. Elec. Spec. Rel. Phen.*, 13, 1(1978).

113. S. Evans, *Discuss. Faraday Soc.*, 60, 198(1975).

114. R. G. Steinhardt, J. Hudis and M. C. Perlman, *Phys. Rev. B 5*, 1016(1972).

115. D. T. Clark et al., *J. Polym. Sci. Polym. Chem. ed.*, 13, 857(1975).

116. D. T. Clark, M. M. Abu-Shbak, and W. J. Brennan, *J. Elec. Spec. Rel. Phen.*, 28, 11(1982).

117. R. F. Roberts, D. L. Allara, C. A. Pryde, D. N. E. Buchanan, and N. D. Hobbin, *Surf. Interface. Anal.*, 2, 5(1980).

118. D. C. Webster, *PhD Dissertation*, VPI&SU(1984).

119. J. E. McGrath, J. L. Hedrick, D. C. Webster, B. C. Johnson, D. K. Mohanty, and I. Yilgor, *NASA Final Report*, VPI&SU, June 1983.

120. J. E. McGrath et al., *SAMPE Proceedings, Reno, April 1984.*

121. J. E. McGrath et al., *Polym. Prepr., Div. Polym. Chem., Am. Chem. Soc.*, 24(1), 161(1983).

122. I. Yilgor et al., *Polymer(London)*, in press(1984).

123. B. C. Johnson, *PhD Dissertation*, VPI&SU(1984).

124. J. E. McGrath et al., *Polym. Prepr., Div. Polym. Chem., Am. Chem.*, 24(2), 78(1983).

125. W. D. Harkins, "*The Physical Chemistry of Surface Films*", Reinhold, New York(1952), p175.

126. G. L. Gaines, Jr., *Polym. Eng. Sci.*, 12, 1(1972).

127. S. Wu, *J. Macromol. Sci.-Revs., Macromol. Chem.*, C10(1), 1(1974).

APPENDIX A

CALCULATION OF THE SILOXANE CONTENT AT THE SURFACE

The procedure for converting the XPS C_{1s} and Si_{2s} peak intensities into carbon to silicon atomic ratio has been outlined in the section 4.3. The representative calculations for further obtaining the weight percentage siloxane at the surface from this ratio are shown in brief here.

Let M_2 and C_2 be the molecular weight of and the number of carbon atoms per a repeating unit of the block other than the siloxane block in a given two-component system. The corresponding values for the siloxane blocks are 74 and 2 respectively. Let C be the number of carbon atoms and Si be the number of silicon atoms detected by XPS in any given situation. Then, 2Si carbon atoms are associated to the siloxane blocks and C-2Si carbon atoms are associated to the second component present in the analyzed volume. This gives:

weight of siloxane in the analyzed volume = $74Si = W_1$

and,

weight of the second component in the analyzed volume

$= (C - 2Si)(M_2/C_2) = W_2$

Hence,

weight percentage siloxane = $(100W_1)/(W_1 + W_2)$

This reduces to a general equation of the form:

$$\text{weight percentage siloxane} = 7400/\{A(C/Si) + B\} \quad .....(A.1)$$

where C/Si is the carbon to silicon atomic ratio provided by XPS; and A and B are constants dependent on the type of the second component.

The values of A and B for the systems studied here are:

Component	A	B
Sulfone	16.4	41.3
Ester	15.6	42.9
Urea	39.1	17.4

The above simple procedure is useful in cases of both a neat block copolymer and its blends with homopolymers corresponding to its components. Note that the same can not be used when the homopolymer is different in structure from both of the copolymer blocks- as in case of the polyurea/polysiloxane-polyurethane blends, or when the the block copolymer itself has a complex random structure- as in the case of polyimide/polysiloxane block copolymers here.

SECURITY CLASSIFICATION OF THIS PAGE *(When Data Entered)*

REPORT DOCUMENTATION PAGE

READ INSTRUCTIONS BEFORE COMPLETING FORM

1. REPORT NUMBER	2. GOVT ACCESSION NO. AD-A140 020
3. RECIPIENT'S CATALOG NUMBER	
4. TITLE *(and Subtitle)* "Surface and Bulk Phase Separations in Block Copolymers and Their Blends"	5. TYPE OF REPORT & PERIOD COVERED Interim, 9/30/82-12/30/83
	6. PERFORMING ORG. REPORT NUMBER
7. AUTHOR(s) Niranjan M. Patel and David W. Dwight	8. CONTRACT OR GRANT NUMBER(s) ONR N00014-82-K-0185 ARO DAAG29-80-K-0093
9. PERFORMING ORGANIZATION NAME AND ADDRESS Center for Adhesion Science and Departments of Chemical Engineering and Materials Engineering, VPI & SU, Blacksburg, VA 24061	10. PROGRAM ELEMENT, PROJECT, TASK AREA & WORK UNIT NUMBERS
11. CONTROLLING OFFICE NAME AND ADDRESS ONR, 800 N. Quincy St., Arlington, VA 22217 ARO, POB 12211, Research Triangle Park, NC 27709	12. REPORT DATE March 1984
	13. NUMBER OF PAGES 125
14. MONITORING AGENCY NAME & ADDRESS *(if different from Controlling Office)*	15. SECURITY CLASS. *(of this report)*
	15a. DECLASSIFICATION/DOWNGRADING SCHEDULE

16. DISTRIBUTION STATEMENT *(of this Report)*

Distribution Unlimited

17. DISTRIBUTION STATEMENT *(of the abstract entered in Block 20, if different from Report)*

18. SUPPLEMENTARY NOTES

19. KEY WORDS *(Continue on reverse side if necessary and identify by block number)*

Block Copolymers; Homopolymers; Multi-component; Multi-phase; Morphology; Micro-phase separation; Macro-phase Separation; Polymer Blends; Surface Properties; X-ray Photoelectron Spectroscopy (XPS); Electron Spectroscopy for Chemical Analysis (ESCA); Transmission Electron Microscopy (TEM).

20. ABSTRACT *(Continue on reverse side if necessary and identify by block number)*

Surface and bulk properties have been studied in terms of composition and morphology of siloxane containing block copolymers and their blends with homopolymers. X-ray Photoelectron Spectroscopy (XPS) has been used to obtain the compositional information from the top 60 angstroms or so at the surface. Transmission Electron Microscopy (TEM) was utilized to probe the bulk morphology. An attempt is made to compare the bulk and the surface and find possible mechanisms governing them. It is found that solvent-cast neat block copolymers have a uniform layer at the surface that is rich in siloxane whereas their bulk has a microphase-

(Over)

DD FORM 1 JAN 73 1473 EDITION OF 1 NOV 65 IS OBSOLETE

SECURITY CLASSIFICATION OF THIS PAGE *(When Data Entered)*

Block 20 (continued)
separated domain structure. In the case of blends, siloxane enrichment is quite pronounced even at bulk concentrations as low as 0.05% w/w siloxane. Amount of surface siloxane as a function of bulk content is studied with the help of XPS. At the same time, the bulk morphology of these blends is studied by TEM. The changes occuring in the surface and the bulk are found to have similar patterns. It is shown that the observed surface behavior may be related to the bulk morphology. Molecular weight of the blocks in the copolymers is found to be a very important parameter governing both the surface and the bulk properties in the neat copolymers as well as their blends.